Development of an optimised integrated underbalanced drilling strategy for cuttings transport in gas-liquid flow through wellbore annuli.

MAHON, R.

2022

Development of an Optimised Integrated Underbalanced Drilling Strategy for Cuttings Transport in Gas-Liquid Flow through Wellbore Annuli

Ruissein Mahon

PhD **2022**

Development of an Optimised Integrated Underbalanced Drilling Strategy for Cuttings Transport in Gas-Liquid Flow through Wellbore Annuli

Ruissein Mahon

A thesis submitted in partial fulfilment of the requirements of Robert Gordon University for the degree of Doctor of Philosophy

June 2022

Abstract

Although understanding the relationship between gas-liquid two-phase fluid flows and the effects of the major drilling variables is critical to optimising underbalanced drilling (UBD) operations, to date, this has been an area of limited research and knowledge. This study contributes to the limited knowledge base by: 1) determining the key operational drilling parameters which shape the gas-liquid two-phase multiphase flow behaviour characteristics during UBD operations, 2) evaluating the most critical operational issues that have impacted the implementation of global UBD programmes, and 3) investigating the Newtonian and non-Newtonian gas-liquid two-phase flow patterns which affect the wellbore hydraulics and cuttings transport efficiency during UBD operations. Thus, this study developed a rigorous integrated strategy for maximising the efficiency of UBD for the transport of cuttings in gas-liquid two-phase flow through wellbore annuli.

An experimental approach was applied to analyse and evaluate the relationship between the gas-liquid two-phase flow patterns and the major operational drilling parameters (gas and liquid flowrates, fluid rheology, inner pipe rotation, pipe inclination angle, pipe eccentricity and solid particle size and density) and to investigate their influence and interaction on the fluid flow dynamics and solids transport mechanisms in horizontal and inclined annuli. Experimental results revealed that drilling fluid flowrate along with fluid flow pattern are the most prominent parameters that strongly influence the cuttings transport efficiency within wellbore annuli. Annuli cleaning requirements for a concentric annulus was found to be lower than that required for an eccentric annulus for both Newtonian and non-Newtonian fluids. Pipe inclination angle was shown to affect hole cleaning, with the degree of its effect being significantly influenced by the drilling fluid properties, prevailing gas-liquid fluid flow pattern and cuttings transport mechanism. Moreover, inner pipe rotation was observed to improve cuttings transport in both horizontal and inclined eccentric annuli to varying extents.

Experimental evidence was supplemented with a theoretical approach. Flow pattern dependent multi-layered mathematical models applicable for any level of pipe eccentricity were used for the different cuttings transport mechanisms existing in the different fluid flow patterns (dispersed bubble, bubble, and slug), offering a unique method to evaluate cuttings transport efficiency and wellbore hydraulics performance for UBD operations. A favourable comparison was observed between the experimental data and proposed flow pattern dependent multi-layered mathematical models with an error margin of ±15%.

This research has generated new knowledge and created value through mapping the factors influencing particle transport and by evaluating the fluid-particle dynamics (fluid forces, gas-liquid fluid flow patterns and particle transport mechanisms) for flow in wellbore annuli. It has further identified and evaluated the effect of gas-liquid two-phase fluid flow patterns on fluid-particle transport dynamics which results in areas of preferential flows and stagnation zones. It also proposed a systematic solution to the governing equations for the

simultaneous flow of gas-liquid two-phase fluids and solid particles in wellbore annuli. Overall, the mapping of the major operational drilling parameters and their influence and interdependencies on wellbore dynamics and cuttings transport efficiency in the context of gas-liquid fluid systems, provides a tool for the prediction of cuttings transport mechanism, determination of the stationary bed height, and calculation of the annuli pressure losses. Therefore, wellbore pressure evaluation and management and hole cleaning requirements for UBD operations can be addressed.

Keywords: Underbalanced drilling, Multiphase flow, Solids transport, Newtonian and non-Newtonian, Inner pipe rotation, Eccentricity, Experimental studies, Multi-layered models

Dedication

This thesis is lovingly dedicated to my mother, Elizabeth Jane Mahon, and my father, Dennis Auther Mahon (deceased), the greatest Professors in life that I know, and have known.

Acknowledgements

I am deeply indebted to my supervisors, Dr Gbenga Oluyemi, Professor Babs Oyeneyin, Dr Sheikh Islam, and Dr Amol Bali, for their tremendous and unwavering intellectual support, expert guidance, and encouragement throughout my PhD journey. Sirs, you will always have my gratitude and respect.

I am indebted to the School of Engineering administrative staff, Dr Rosslyn Shanks and Kirsty Stevenson for their help and direction in navigating RGU's administrative systems and processes. My sincere appreciation is also extended to the technical services team led by Alan McLean, namely, Alexander Laing, Martin Johnstone, David Smith, Allan MacPherson, Patrick Kane, and Ross Henderson. Gentlemen, thank you very much for your practical support in facilitating the experimental rig setup and maintenance throughout the years. I am also very thankful to Nick Anderson and Martin Simpson for their support on PhD related matters.

My gratitude goes to my lab partner and collaborator Dr Voke Salubi for your crucial contributions.

To my PhD brother Dr Yakubu Balugun, thank you for your friendship and stimulating technical discussions about my work.

Thank you Dr Ibiye Iyalla for believing in me, as well as, for your kind and steady support and advice.

To my colleagues and friends, Dr Oluwademilade Ogunsesan, Dr Haider Al-Mashhadanie, Paul Okpozo and Emmanuel Eke, thank you for your camaraderie which created an enjoyable working atmosphere.

Finally, I wish to express my deep appreciation for my family. Thank you for your love, patience, support and understanding throughout my PhD journey. When the going got tough, you were always there and for this, I truly appreciate each of you.

Table of Contents

List of Tables

List of Figures

List of Abbreviations

BHP	Bottomhole pressure
BNN	Backpropagation neural networks
BOP	Blowout preventer
BSL	Best straight line
CFD	Computational fluid dynamics
DT	Decision tree
ECD	Equivalent circulating density
FS	Full scale
HEM	Homogeneous flow model
IAC	Interfacial area concentration
IAT	Interfacial area transport
ID	Inner diameter
ML	Machine learning
MWD	Measurement while drilling
NN	Nearest Neighbour
OBD	Overbalanced drilling
OD	Outer diameter
PDF	Probability density function
QDA	Quadratic discriminant analysis
RGU	Robert Gordon University
RPM	Revolution per minute
UBD	Underbalanced drilling
UBHD	Underbalanced horizontal drilling

Nomenclature

(In consistent units)

A	Cross-sectional area
B_1, B_2, B_3	Empirical constants
C	Cutting concentration
C_D	Coefficient of drag
C_L	Coefficient of lift
$\partial P/\partial L$	Pressure gradient
d_c	Cuttings size
d_{dc}	Drill collar diameter
d_e	Distance between the centre of the outer pipe and the inner pipe
d_h	Borehole diameter
d_2	Inner diameter of casing or wellbore
d_1	Outer diameter of drillpipe
d_x	Distance between the drillpipe and the casing wall at the lowest side
e	Wellbore eccentricity
F_B	Buoyancy force
F_D	Drag force
F_G	Gravitational force
F_L	Lift force
f_s	Coefficient of friction
f	Friction factor
g	Acceleration due to gravity
h	Height
H	Hold up
K	Consistency coefficient of Power Law fluids
K'	Consistency coefficient of Herschel Bulkley fluids
K_a	Pipe diameter ratio
L	Length
n	Power-law flow behaviour index
n'	Flow behaviour index of Herschel Bulkley fluids
P_p	Pump pressure
P_r	Reservoir pressure
p_{wf}	Flowing bottomhole pressure
P_{wH}	Pressure at the heel of the horizontal borehole
PV	Pore volume
q	Flowrate
Q	Volumetric flowrate
R	Pressure gradient ratio
R_1	Radius of the inner cylinder
R_2	Radius of the outer cylinder
S	Wetted perimeter
V	Average velocity
v	Relative velocity
$X1, X2, X3$	Functions for cross-sectional area calculations
ΔP	Pressure drop

β	Inclination angle between the vertical and wellbore flow axis
ρ	Density
τ	Shear stress
τ_y	Yield point
τ_o	Yield stress
η	Ordinate in the complex plane
μ	Apparent viscosity
μ_p	Plastic viscosity
λ	No-slip hold up
γ	Shear rate
Δ	Centre-to-centre distance between cylinders
σ	Diameter ratio
Θ	Annulus inclination angle

Subscripts

a	Annulus
b	Stationary cuttings bed
c	Cuttings
1	Layer 1
2	Layer 2
3	Layer 3
f	Fluid
G	Gas
Gf	Gas in the liquid-film/gas pocket region
Gs	Gas in the slug body
L	Liquid
Lf	Liquid in the liquid-film/gas pocket region
$Lf0$	Starting position of the liquid film
LfA	Cuttings-fluid mixture in the liquid-film/gas pocket region
Lfc	Liquid-cuttings mixture in the liquid film
Ls	Liquid in the slug body
m	Gas-liquid mixture
MB	Moving bed
MR	Minimum for rolling bed
O	Oil
P	Drillpipe wall
S	Slug body
T	Translational
U	Slug unit
w	Annuli wall
x, y	Cartesian coordinate axes

Peer reviewed Papers and Presentations

Published PhD-related papers:

1. Salubi, V., **Mahon, R.**, Oluyemi, G., Oyeneyin, B., 2021. Effect of two-phase gas-liquid flow patterns on cuttings transport efficiency. J. Pet. Sci. Eng. https://doi.org/10.1016/j.petrol.2021.109281
2. Salubi, V., **Mahon, R.**, Oluyemi, G., 2021. The combined effect of fluid rheology, inner pipe rotation and eccentricity on the flow of Newtonian and non-Newtonian fluid through the annuli. J. Pet. Sci. Eng. https://doi.org/10.1016/j.petrol.2021.110018

PhD-related papers under review or in-preparation:

1. **Mahon, R.**, Salubi, V., Oluyemi, G., Oyeneyin, B., 2021. Towards the development of an optimised strategy for underbalanced drilling: A best evidence review of global field case studies. J. Pet. Sci. Eng. Under review
2. **Mahon, R.**, Salubi, V., Oluyemi, G., 2021. Experimental investigation of cuttings transport dynamics in two-phase gas-liquid fluids. In preparation
3. **Mahon, R.,** Salubi, V., Oluyemi, G., Oyeneyin, B., 2021. A systematic review of constraints and technical issues in underbalanced drilling. In preparation

Other published papers:

1. **Mahon, R.**, Oluyemi, G., Oyeneyin, B., Balogun, Y., 2021. Experimental investigation of the displacement flow mechanism and oil recovery in primary polymer flood operations. SN Appl. Sci. 3. https://doi.org/10.1007/s42452-021-04360-7
2. **Mahon, R.**, Balogun, Y., Oluyemi, G., Njuguna, J., 2020. Swelling performance of sodium polyacrylate and poly(acrylamide-co-acrylic acid) potassium salt. SN Appl. Sci. 2. https://doi.org/10.1007/s42452-019-1874-5
3. Balogun, Y., Iyi, D., Faisal, N., Oyeneyin, B., Oluyemi, G., **Mahon, R.**, 2021. Experimental investigation of the effect of temperature on two-phase oil-water relative permeability. J. Pet. Sci. Eng. 203. https://doi.org/10.1016/j.petrol.2021.108645

Other papers under review or in-preparation:

1. Balogun, Y., **Mahon, R.**, Oluyemi, G. 2021. Investigation of oil recovery and displacement efficiency of water and polymer-flooding in micromodel porous media using a CFD approach. Exp. Comput. Multiph. Flow. Under review
2. Iyi, D., Balogun, Y., Faisal, N., Oyeneyin, B., Oluyemi, G., **Mahon, R.**, 2022. Experimental Study of Oil-Water Relative Permeability in Porous Media: Effect of Injection Rate and Oil Viscosity. Petroleum Science and Technology. Under review

Presentations:

1. **Mahon, R.**, 2018. Underbalanced horizontal drilling: Concept, technical issues and integrated implementation strategy. International Student Petroleum Congress and Career Expo, Krakow, Poland, 10-12 April 2018
2. Salubi, V., **Mahon, R.**, Oluyemi, G., 2021. Solids transport in multiphase production systems / drilling operations. 9th SPE SMN Sand Management Euroforum, Maximising Value Using Innovative Sand Management Technology Efficiency, Innovation and Data Management, Aberdeen, UK, 4-5 November 2021

Chapter 1 : Introduction

1.1 Research context

Underbalanced drilling (UBD) involves a transient and complex multiphase flow phenomenon which is difficult to understand, describe, predict, and model (Mykytiw et al., 2004; Aladwani and Gray, 2012). This method of drilling requires proper downhole pressure management, between the toe and heel of the wellbore annulus, and efficient drilling fluid carrying capacity for the effective transport of drilled cuttings to the surface. However, this can be challenging within field operations since there are issues related to accurate gas-liquid drilling hydraulics and effective cuttings transport in wellbore annuli (Salubi et al., 2022). This is particularly the case with horizontal, deviated, high extended reach and multibranched wells. What is more, to date, the effect of major operational drilling parameters and their influence on wellbore dynamics and cuttings transport efficiency in the context of gas-liquid fluid systems within the wellbore annuli has received little research attention.

An in-depth understanding of the fluid-particle dynamics involved in gas-liquid multiphase fluids with cuttings in wellbore annuli, particularly regarding its physical and hydrodynamic nature, underpin the application of appropriate prediction techniques. For example, multiphase flow prediction techniques have been used to predict several parameters such as pressure drops (through the wellbore annuli), multiphase flow patterns, in-situ (local) velocities, liquid holdup, and cuttings transport efficiency. Thus, consideration must be given to factors such as (Oyeneyin, 2003, 2015; Fan et al., 2009; Salubi et al., 2022):

- Inflow performance relationship[1] (crossflow modelling);
- Fluid and solid phase properties (e.g., density, viscosity, size, and shape) and at a mixture compositional level;
- Mass transfer behaviour of fluids as it relates to temperature and pressure changes;
- Fluid flow pattern (gas-liquid), cuttings transport mechanisms and phase migration features; and
- Geometry and deviation of the wellbore.

Although the UBD technique has proven itself to be an enhanced drilling solution in various applications, its success relies on the maintenance of the underbalance condition throughout the drilling process, especially between the toe and heel section of the wellbore annulus. Therefore, it is crucial to model the effect of gas-liquid fluid flow patterns and major operational drilling parameters realistically and accurately (fluid flowrate and rheology, inner pipe rotation, inclination angle, pipe eccentricity and solid particle size and density) on wellbore hydraulics and cuttings transport efficiency in horizontal and inclined, concentric and eccentric annuli, in order to properly plan and execute UBD operations.

This research study attempts to overcome some of these technical issues encountered in the implementation and execution of UBD operations by performing laboratory experiments and theoretical analysis to investigate the

[1] Inflow performance relationship refers to a mathematical tool that is used to assess a production well's performance and is influenced by the reservoir fluid composition and behaviour of the fluid phases.

influence and interaction of fluid flow dynamics and solid transport mechanisms in horizontal and inclined, concentric, and eccentric annuli.

While some investigators have paid little attention to the effect of cuttings transport or assumed that cuttings have minimal effect on annuli hydraulics calculations (Haciislamoglu and Langlinais, 1990; Merlo et al., 1995; Sunthankar et al., 2003; Zhou et al., 2004a; Kelessidis et al., 2011; Erge et al., 2014; Saasen, 2014; Taghipour et al., 2014), other investigators have not considered the effect of the minimum transport velocity on the prevailing cuttings transport mechanism and its impact on annuli pressure gradient (Lage and Time, 2000; Guo and Ghalambor, 2004; Osgouei et al., 2013). In this study, solid transport mechanisms and efficiency are experimentally investigated as the interaction between the complex multiphase fluid flow and cuttings underpin the deeper understanding of the fluid dynamics within UBD operations.

For the above-mentioned reasons, this study focuses on the application of multi-layered multiphase flow models that can be used as a predictive optimisation tool for well dynamics and control in the design of UBD operations. Based upon the flow pattern dependent multi-layered mathematical framework, the models can predict the cuttings transport mechanism, determine the stationary bed height, and calculate the annuli pressure losses. The performance of the flow pattern dependent multi-layered models are evaluated through comparison with experimental data gathered as part of the research study.

Although research advances have been made in the area of multiphase flow modelling in annular geometries, to the author's knowledge there exist no integrated UBD strategy available in the literature. Thus, another core area of

this research study is the development of a rigorous optimisation strategy for maximising the efficiency of UBD operations for oil reservoir applications.

1.2 Research aim and objectives

The aim of this work is to develop a rigorous integrated strategy for maximising the efficiency of UBD for the transport of cuttings in gas-liquid two-phase flow through wellbore annuli.

The six key objectives of this work are:

1. To update the theoretical and practical UBD knowledge base through consolidation of the technical issues relating to UBD operations;
2. To aggregate and synthesise the most critical technical issues relating to UBD field operations promoting operational success and/or failure, as well as mitigation action;
3. To design and construct a multiphase flow loop in order to generate experimental data on the nature of the gas-liquid two-phase fluid flow structures (dispersed bubble, bubble, and slug) which dominate in UBD operations in horizontal and inclined, concentric and eccentric annuli for Newtonian and non-Newtonian flows with and without solid particles;
4. To investigate the effect of the major operational drilling parameters on the fluid flow dynamics and solids transport mechanisms;
5. To investigate the effect of cuttings transport mechanisms on annuli pressure gradient while identifying areas of preferential flows and stagnation zones; and
6. To develop and implement flow pattern dependent multiphase flow models that can evaluate the wellbore hydraulics performance and cuttings transport efficiency and compare with experimental data.

1.3 Conceptual framework and methodology

This investigation of UBD operations is anchored within a multi-disciplinary conceptual framework which draws on three key applied components: 1) key operational drilling parameters (e.g., gas and liquid flowrates, fluid rheology, inner pipe rotation, hole inclination angle, pipe eccentricity and solid particle size and density), 2) different cuttings transport mechanisms in wellbore annuli, and 3) annuli pressure gradient management.

The research programme used a multistage, mixed method strategy (Figure 1.1) combining theoretical and experimental techniques. It began with a comprehensive baseline examination of the scholarly literature to investigate and consolidate key UBD operational issues; as well as, to identify and describe elements of the research gap. The literature review detailed in Chapter 2 provides the basis for the development of an Alpha version of an integrated UBD strategy in oil reservoir applications. *Stage 1: Experimental Studies* detailed in Chapters 3 and 4 develops and applies the experimental methodology, and documents the experimental results, and findings. *Stage 2: Multi-layered Multiphase Flow Modelling* detailed in Chapter 5 develops flow pattern dependent multi-layered flow models; and conducts a comparative analysis between the experimental results emanating from Stage 2 with the flow model predictions.

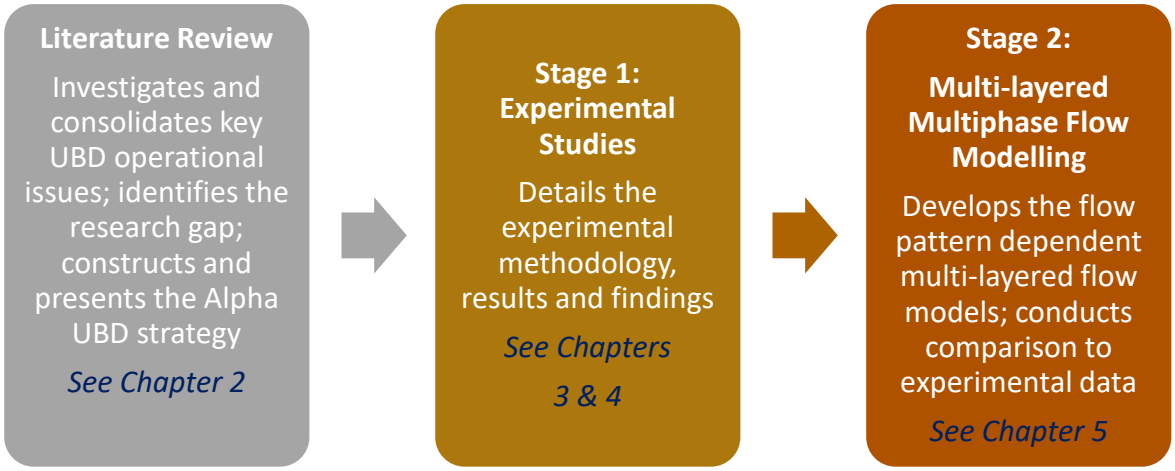

Figure 1.1 Multistage, mixed method methodological framework employed in this study

The conceptual framework is discussed fully in Chapter 2, while the methodological framework is discussed in full in Chapter 3. The alignment of the research aim, questions, objectives, and methods investigated and/or applied in this PhD thesis are summarised in Table 1.1.

Table 1.1 Research aim, objectives and methods investigated and/or applied in this research programme

AIM	OBJECTIVE(S)	METHOD(S)	REFERENCE CHAPTER
To develop a rigorous integrated strategy for maximising the efficiency of UBD for the transport of cuttings in gas-liquid two-phase flow through wellbore annuli	RO1: To update the theoretical and practical UBD knowledge base through consolidation of the technical issues relating to UBD operations	Literature review of over 130 papers which focused on: 1) the factors affecting multiphase flow during UBD operations, and 2) the influence of reservoir/formation properties on UBD operations	Chapter 2
	RO2: To aggregate and synthesise the most critical technical issues relating to UBD field operations promoting operational success and/or failure, as well as the mitigation action	Best-evidence review of field case studies on the operational phases of 25 past global UBD implementations – 18 successful and 7 which were operationally challenged	Chapter 2
	RO3: To design and construct a multiphase flow loop in order to generate experimental data on the nature of the gas-liquid two-phase fluid flow structures (dispersed bubble, bubble, and slug) which dominate in UBD operations in horizontal and inclined, concentric and eccentric annuli for Newtonian and non-Newtonian flows with and with solid particles	Design and construction of multiphase flow loop	Chapter 3
	RO4: To investigate the effect of the major drilling parameters on the fluid flow dynamics and solids transport mechanisms	Experimental tests: 1) gas-liquid two-phase fluid flow pattern visualisation, 2) annuli pressure data, 3) cuttings transport mechanisms, and 4) cuttings bed height	Chapter 4
	RO5: To investigate the effect of cuttings transport mechanisms on annuli pressure gradient while identifying areas of preferential flows and stagnation zones		
	RO6: To develop and apply a multiphase flow model to evaluate the wellbore hydraulics performance and cuttings transport efficiency and compare with experimental data	Flow pattern dependent multi-layered mathematical modelling	Chapter 5

1.4 Research scope

The major boundaries of this research are as follows:

1. The research deals with the concept of UBD operations as it specifically relates to fluid dynamics and cuttings transport efficiency. It does not fully explore the wellbore-reservoir interaction in terms of formation fluid influx beyond the limits of the presented literature review and as a feature within the developed Alpha UBD strategies;
2. Emphasis in the analysis is placed on the key drilling parameters to improve BHP control and cuttings transport mechanisms which must be considered to access the sweeping benefits of UBD operations. Although the effect of inner pipe rotation is experimentally investigated, the flow pattern dependent multi-layered flow models do not incorporate the effect of inner pipe rotation;
3. The research does not examine borehole instability issues caused by the BHP fluctuations during UBD operations beyond the limits of the developed Alpha UBD strategies; and
4. The complex effect of fluid temperature variations along the wellbore annulus on annular pressure losses was not investigated as part of this study.

1.5 Contribution to knowledge

The study is driven by the need to optimise hydrocarbon productivity and recovery by using an enhanced drilling solution (UBD). It creates value through knowledge generation and the development of a rigorous integrated strategy for maximising the efficiency of UBD in oil reservoir applications. In so doing, this study makes three core contributions:

1. **Mapped the factors influencing particle transport and presented a qualitative and quantitative evaluation of the fluid-particle dynamics (fluid forces, gas-liquid fluid flow patterns and particle transport mechanisms) for flow in wellbore annuli.** An extensive phenomenological understanding of the complex mechanism, the hydraulics, and the characteristics of the two-phase flow in concentric and eccentric, horizontal and inclined annuli is presented as part of this research study.
2. **Identified and evaluated the effect of gas-liquid two-phase fluid flow patterns on fluid-particle transport dynamics which results in areas of preferential flows and stagnation zones.** These fluid-particle interactions directly affect the flow of drilling fluid in real well drilling situations and underpins the drilled cuttings settling tendencies and the conditions under which this would or would not occur. Particle transport dynamics in different gas-liquid two-phase fluid flow patterns were quantitatively and qualitatively demonstrated as part of this research study.
3. **Presented a systematic solution to the governing equations for the simultaneous flow of gas-liquid two-phase fluids and solid particles.** The fit-for-purpose flow pattern dependent multi-layered multiphase flow models balances between complexity and fidelity, by applying a systematic approach, combining experimental, theoretical, and numerical techniques to develop a package that fits drilling operations. This results in an extension of flow modelling techniques through the testing and validation of its performance against experimental data gathered as part of this research study.

The body of work presented in this thesis provides an in-depth understanding of wellbore dynamics in terms of the complex multiphase flow behaviour of the drilling fluids in UBD operations and its effect on cuttings transport efficiency. Finally, the findings provide a tool that can be applied for wellbore pressure management and the evaluation of hole cleaning requirements for UBD operations. The output from this study can be used to optimise the flow behaviour of the various fluid content within a drilling wellbore annulus. It is expected that the findings obtained as part of this research work will serve as a guide to drilling and mud engineers during the planning and design phase of a UBD operation, helping to facilitate effective hole cleaning and the maintenance of the underbalanced pressure window between the toe and heel of the wellbore annuli. This research also has the potential of helping in real-time prediction of downhole conditions in drilling operations.

1.6 Thesis outline

This thesis has 6 chapters.

Chapter 1: *Introduction* gives an overview of the PhD research programme; technical issues – gap identification, research aim and objectives, conceptual framework and methodology, research scope, and the contribution to knowledge.

Chapter 2: *Review of Underbalanced Horizontal Drilling Operations p*rovides an overview of the mechanics behind UBD operations. It also consolidates issues related to the key operational drilling parameters which must be considered for successful UBD operations and a provides a curated background and summary of studies on cuttings transport in UBD mud flow systems. An assessment of 25

global UBD field case studies in their operational phase and their associated outcomes is also presented.

Chapter 3: *Experimental Methodology* describes the research methodology employed in this study to achieve the research objectives. It presents details about the experimental unit, fluid system and solid particles used for the experimental tests, outlining the applied experimental procedure.

Chapter 4: *Experimental Results and Discussion* presents the results captured from experimental tests performed using the multiphase flow loop. This is a critical aspect in the development of the UBD strategy as it provides the raw data regarding the multiphase flow behaviour of Newtonian and non-Newtonian gas-liquid two-phase system with and without solid particles under different experimental conditions.

Chapter 5: *Multiphase Flow Modelling* presents the flow pattern dependent multi-layered flow models and provides a comparison against experimental data.

Chapter 6: *Conclusions and Recommendations* outlines the research study's conclusions, and suggestions for future work based upon the research framework directed toward the application of the UBD method.

Chapter 2 : Review of Underbalanced Horizontal Drilling Operations

2.1 Introduction

This chapter reviews the extensive multi-disciplinary literature on key multi-faceted components that lay the foundation for the conceptual framework that guides the investigation of the research aim. The chapter is divided into ten sections. The chapter begins by providing an overview of the concept and mechanics behind UBD and its derivative underbalanced horizontal drilling (UBHD) is discussed, followed by an extensive review of the literature on some of the factors which affect the complex multiphase flow phenomenon within UBD operations, with details on some of the hydraulic and multi-layered flow models being presented. The chapter also covers the assessment of 25 global UBD field case studies in their operational phase and their associated outcomes. The chapter concludes by highlighting the study's key research elements and discusses the need for a comprehensive UBD strategy which becomes the driving framework for investigating the research problem.

2.2 Underbalanced drilling operations

2.2.1 Mechanics of underbalanced drilling

The mechanics of UBD operations involve a complex fluid system of drilling and produced fluids along with drilled cuttings. Figure 2.1 illustrates the pressures involved in UBD operations.

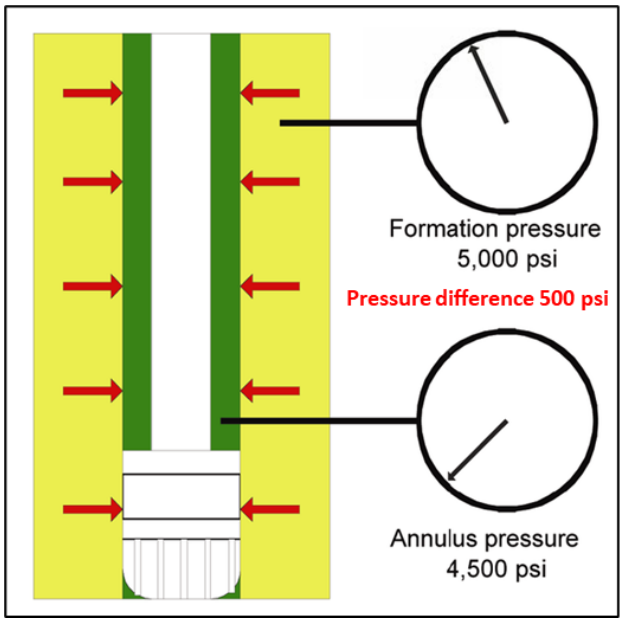

Figure 2.1 Pressures in underbalanced drilling (adapted from Davarpanah et al., 2020)

During UBD operations the formation pressure is always greater than the annulus pressure encouraging the formation fluid to flow into the wellbore annulus as the drilling operation is undertaken. Thus, UBD operations are based upon flow control principles to ensure that the pressure within the wellbore annulus is maintained 100% in the underbalanced condition during the entire operation although there is an influx from the formation.

Three mechanisms provide primary well control during UBD operations:

1. Hydrostatic pressure of the multiphase fluid in the wellbore (drilling mud, injection gas, drilled cuttings and formation fluid/s);
2. Frictional pressure from the movement of the multiphase fluid due to the circulating friction of the drilling fluid; and
3. Choke pressure at the surface generates a positive pressure as the pipe is sealed at surface.

During UBD operations, the fluids in the wellbore annulus (drilling and produced) are returned to a closed system at the surface. A blowout preventer (BOP)

system is also used to provide secondary well control and is kept closed as the well is flowing.

2.2.2 Technological advantages and limitations of underbalanced drilling operations

UBD operations which are effectively planned and properly executed provide a suite of reservoir and mechanical benefits to oil reservoir applications. Table 2.1 highlights some of the many technological advantages of UBD operations and demonstrates that these advantages significantly outweigh its inherent limitations.

Table 2.1 Benefits and limitations of underbalanced drilling operations (Qutob and Ferreira, 2005; Woodrow et al., 2008; Sun, 2016)

Benefits	Limitations
• Earlier and increased reservoir production • Reduced formation damage • Drilling fluid losses eliminated • Minimised drilling problems e.g., loss circulation and differential sticking eliminated • Improved well safety, dynamics, and control • Fewer wells needed to drain the reservoir • Reduced overall capital and operational costs • Reduced future reservoir stimulation • Improved rate of penetration (ROP) • Extended drill bit life • Decreased drilling time	• Additional engineering and operational considerations required • Potential wellbore stability issues • Increased operational risks • Specialised equipment required • Potentially higher daily operational costs • Increased drilling costs depending on the system used • Possible wellbore cleaning issue

UBD can significantly minimise the key issue of formation damage which can yield increased hydrocarbon production. This method of drilling facilitates increased ROP, which reduces the drilling time required, positively impacting the overall cost of a field development programme. Major operational limitations linked to OBD such as differential sticking and loss circulation issues may be fully resolved. UBD also enables a deeper understanding of the reservoir

characteristics which may be evaluated in real-time – an immediate and direct benefit to operators with far-reaching implications.

Figure 2.2 shows how a UBD operation can facilitate a significantly higher rate of production over time as compared to conventional OBD. This is the main operational motivation behind the implementation of this method of drilling in oil reservoirs which maybe be susceptible to formation damage and inherently difficult to exploit and produce at economic rates.

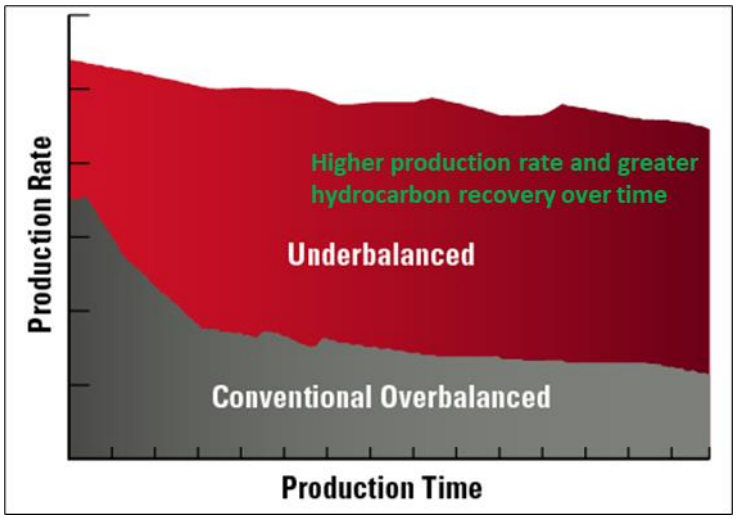

Figure 2.2 Underbalanced drilling alternative for better production (adapter after Halliburton, 2019)

2.2.3 Underbalanced horizontal drilling – A derivative of UBD operations

Underbalanced horizontal drilling (UBHD) is a synthesis of drilling a horizontal well in an underbalance condition and has expanded the range of engineering solution options by offering (Bahrami, 2012; Abdulrahman, 2013; Sun, 2016):

- Accelerated drilling rates;
- Decreased leakage issues related to pressure-depleted reservoirs;
- Early detection and identification of productive zones through interpretation of reservoir inflow profile;
- Increased well production rates;

- Improved reservoir drainage; and
- The ability to exploit multiple reservoirs within a hydrocarbon-bearing formation due to directional capabilities.

In the application of UBHD operations, the two main goals are:

1. The discovery and protection of potential oil and gas reservoirs; and
2. The optimisation and advancement of drilling and its associated production efficiencies.

2.3 Technical improvements for underbalanced drilling operations

The operational success of UBD operations depends upon the complement between the geomechanical and geophysical properties of the reservoirs and the technological aspects of the applied drilling method. Different technological strategies can be implemented to maximise hydrocarbon recovery while minimising operational drilling related issues. These technological improvements can be grouped into three broad headings:

1. Multiphase flow modelling;
2. Crossflow modelling; and
3. Non-damaging drilling fluids.

2.3.1 Multiphase flow modelling

Computation of accurate well control parameters for UBD hydraulics requires the development of fit-for-purpose multiphase flow models for specific wellbore conditions. The objective of hydraulic modelling is to achieve and maintain an underbalanced condition between the toe and heel of the open-hole wellbore section which offers the maximum reservoir and drilling benefits (Oyeneyin, 2003) (a further discussion is presented in Section 2.4).

2.3.2 Crossflow modelling (wellbore-reservoir interaction)

During UBD operations, the level of the underbalanced condition experienced within the wellbore annulus determines its production capacity (level of reservoir influx) , which may be variable between the toe and heel (Guo and Shi, 2007). This is due to the transient nature of the multiphase flow phenomena within the wellbore annulus leading to a differential drawdown, pressure difference between the reservoir and wellbore. A difference in drawdown will result in a different inflow rate which results in a different inflow pattern along a well (Oyeneyin, 2003). Typically, there are three types of wellbore-reservoir inflow patterns as a result of wellbore-reservoir interaction during UBHD operations (Figure 2.3):

1. Rectangular (uniform) inflow pattern;
2. Triangular inflow pattern; and
3. Trapezoidal inflow pattern.

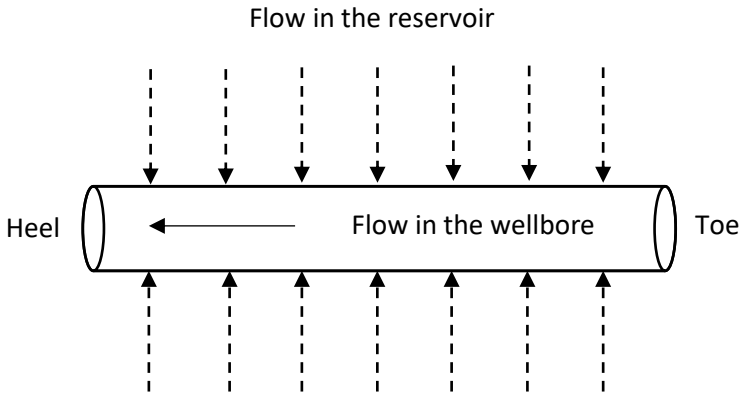

(a)

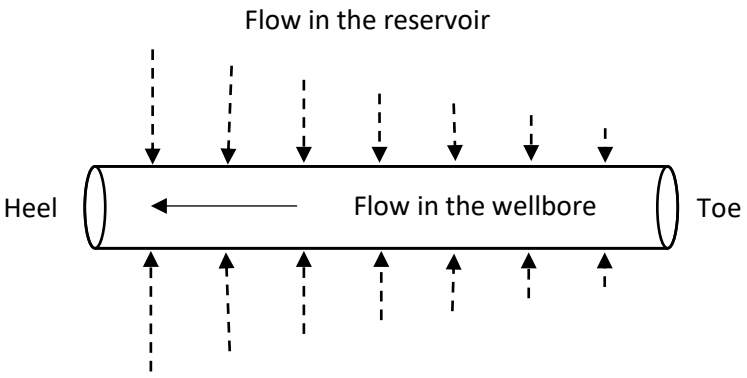

(b)

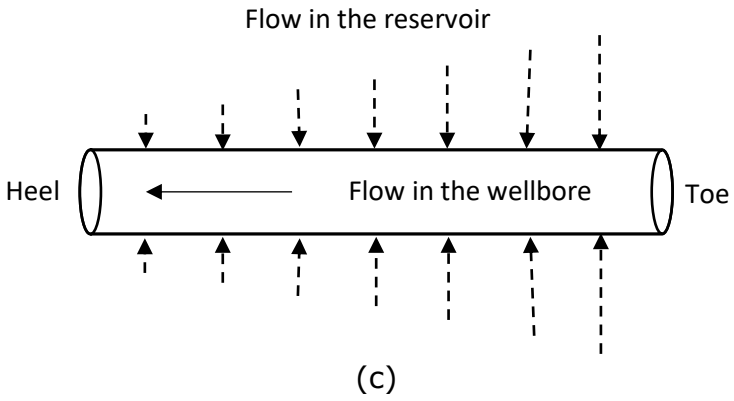

Figure 2.3 Wellbore-reservoir interaction showing inflow patterns (a) rectangular (uniform) pattern, (b) triangular pattern (c) trapezoidal pattern

During UBD operations, the rectangular (uniform) inflow pattern is the desired wellbore-reservoir interaction. However, due to the transient nature of the underbalance pressure window, the triangular or trapezoidal inflow patterns may occur, resulting in a variable inflow of reservoir fluids along the wellbore annulus. This in turn may lead to the pressure gradient within the wellbore annulus between the toe and heel increasing significantly. In practice, this means that drilling with a moderate underbalance condition may result in a significant amount of reservoir fluid influx, which would generate a significantly higher pressure at the toe (i.e., bit) to compensate for the annular frictional pressure. As such, there are operational limitations on the length of lateral sections which can be drilled underbalanced (Oyeneyin, 2003).

Therefore, the formation inflow must be modelled and a method to predict reservoir fluid inflow rate and volume specifically from oil reservoir applications during UBD operations is required to help maintain the pressure integrity of the underbalanced condition between the toe and heel section of the wellbore annulus. Specific relationships need to be developed that couples wellbore hydraulics and reservoir productivity for different inflow patterns (Guo and Shi, 2007; Guo et al., 2008).

2.3.3 "Non-damaging" drilling fluids

The selection of drilling fluids is based upon its "non-damaging" properties. Fluid-fluid and rock-fluid incompatibility are associated with permeability impairment risk and near wellbore formation damage. Thus, careful consideration must be given to this aspect in the design and planning phase of the UBD programme (Guimerans et al., 2001; Lim et al., 2015).

To ensure the use of a "non-damaging" drilling fluid content, during the design and development of the UBD well fluid, consideration is given to the (i) compatibility of the drilling fluid content with the formation lithology and fluids, (ii) hole cleaning issues, (iii) temperature effects, (iv) corrosion, (v) downhole tools, (vi) health and safety issues, (vii) environmental and disposal issues, and (viii) logistical issues concerned with the acquisition of the drilling fluid content. The drilling fluid design significantly impact other operational and borehole parameters such as the formation damage, ECD, wellbore stability, underbalance pressure, surface equipment configuration and waste management facilities (Guimerans et al., 2001).

Drilling muds can be grouped according to their base fluid type as gas, or liquid-based fluids. A variety of multiphase drilling fluids are available that can produce sub hydrostatic BHP and a balance can be found between the most suitable fluid system and the candidate reservoir (Lim et al., 2015). Poor fluid selection can lead to inefficient cuttings transport, increased drag and torque, differential sticking, lost circulation, formation damage and increased drilling non-productive time (NPT).

Drilling fluid sweeps are developed by adjusting the properties of the base fluid through the incorporation of additives to aid the cuttings removal capability and

efficiency which is controlled by tuning properties. While other drilling parameters such as drillpipe rotation and fluid flowrate can aid in lifting and suspending drilled cuttings, efficient drilling fluid management techniques are crucial in the success of UBD operations. To fully understand the working mechanism of the mud system, its downhole stability and flow properties under operating conditions and its compatibility with other drilling system components needs to be comprehensively analysed as a wholly functional system. Optimising the design of the sweep fluid can significantly reduce the cost of the drilling programme by decreasing the number of wiper trips and reducing the NPT (H. Mahmoud et al., 2020).

2.4 Multiphase flow modelling

Multiphase flow behaviour is a prolific research subject area due to its varied industrial applications – oil and gas, chemical, civil, and nuclear (Bello et al., 2007; Jahanandish et al., 2011; Al-Hadhrami et al., 2014; Tariq et al., 2020). Multiphase flow describes how liquid and gas phases and even solid components interact inside flow systems which can be wellbores annuli or production pipelines. This interaction is governed by complex physics. As such, models are commonly used to predict multiphase flow behaviour and are a combination of computational science and fluid dynamics. Model calculations can be made for fluid flowrates and velocities, volume fraction of each phase, and downhole temperature and pressure (Jacobs, 2015). Fundamentally, multiphase flow behaviour is governed by the conservation of mass, momentum, and energy, thermodynamics and heat transfer principles (Jacobs, 2015).

2.4.1 Fluid rheological characteristics

Typically, drilling muds exhibit non-Newtonian rheological characteristics (Rashidi et al., 2021). Within UBD operations, the drilling mud can be aerated with various gases (air, nitrogen and natural gas) to keep the pressure in the wellbore annulus less than the formation pressure. The drilling mud helps to maintain an acceptable level of underbalanced, lubricates the drill bit and facilitates the removal of cuttings and debris from the wellbore annulus. The underbalanced condition can be achieved by adjusting the density, viscosity, and the flowrate of the drilling fluid content (drilling mud and injected gas). These three drilling process parameters require continuous monitoring for optimal process performance.

Within, the UBD wellbore environment, a non-Newtonian fluid mixture exists of the drilling mud, injection gas, formation fluid/s (oil, water, gas) and drilled cuttings. Therefore, it is important to determine the most appropriate non-Newtonian rheological model applicable – Bingham Plastic, Power Law or Herschel Bulkley. Laboratory viscometer measurements can be performed to describe the rheological behaviour of the fluids involved within the UBD operations. The three most common non-Newtonian rheological models are outlined below:

Bingham Plastic shear stress model

$$\tau = \tau_y + \mu_p \gamma \quad \text{Eq. 2.1}$$

Power Law shear stress model

$$\tau = K\gamma^n \quad \text{Eq. 2.2}$$

Herschel Bulkley shear stress model

$$\tau = \tau_o + K'\gamma^{n'} \quad \text{Eq. 2.3}$$

Where τ represents the shear stress, τ_y represents the yield point, τ_o represents the yield stress, μ_p represents the plastic viscosity, γ represents the shear rate, K represents the consistency coefficient of Power Law fluids, n represents the power-law index, K' represents the consistency coefficient of Herschel Bulkley fluids, n' represents the flow behaviour index of Herschel Bulkley fluids.

Figure 2.4 illustrates the flow curves of the different rheological models. Fluids at rest have their flow curves emanating from the origin as any applied stress will generate a corresponding shear rate, Newtonian. Yield stress fluids have their flow curves intercepting the stress axis at a value greater than zero signifying that a shear rate can only be generated when an initial yield stress has been exceeded. A fluid which has yield stress but shows Newtonian characteristics after yielding is known as a Bingham Plastic fluid, exhibiting idealised behaviour, and is not commonly encountered. Most fluids, however, have apparent yield stress and show non-Newtonian behaviour after yielding, generalised as plastic behaviour.

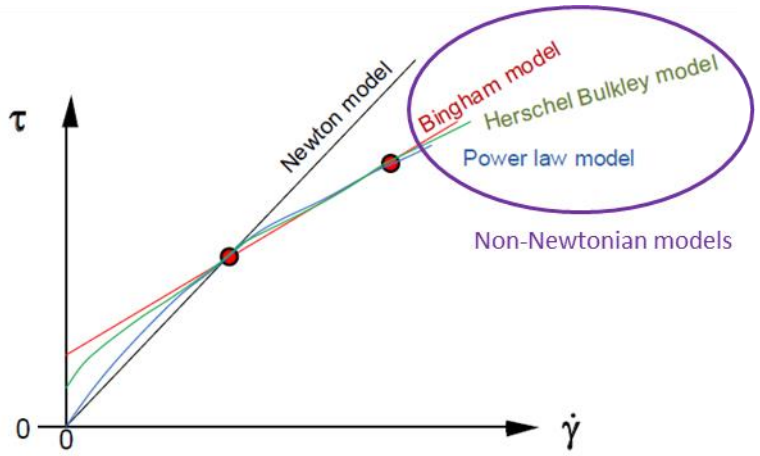

Figure 2.4 Flow curve of different rheological models (adapted from Skalle, 2011)

2.4.2 Multiphase flow patterns

The flow of two or more phases of fluids simultaneously in a closed system is referred to as multiphase flow. Its associated term, flow pattern, describes the geometric structure of the fluid flow and its distinct features based upon the gas-liquid interface. The behaviour and shape of the interfaces between phases are the result of competing forces and the balance between these forces determines the flow pattern. Researchers (Lage and Time, 2002; Falcone et al., 2009; Jacobs, 2015) have found that the flow pattern of multiphase flow in a conduit (inclusive of drilling annuli) is governed by factors such as:

1. Fluid phase properties, fractions, and velocities;
2. Operating temperature and pressure;
3. Conduit diameter, geometry, length, shape, inclination angle and roughness;
4. Flow type – steady-state, pseudo steady-state or transient; and
5. Upstream or downstream pipework.

Factors governing the flow patterns and interfacial distribution within a gas-liquid flow are inertia, buoyancy, turbulence, wetting, dispersion, surface tension, coalescence, body forces and heat flux effects. The flow pattern that dominates depends on the relative magnitude of these factors and changes with fluid flowrates, wellbore geometry, inclination and the fluid properties of each phase. A brief description of flow patterns typically encountered are identified and described in Table 2.2.

Table 2.2 Description of various flow patterns (Oyeneyin, 2015)

Flow pattern	Description
Stratified smooth	Occurs when gravitational separation is complete and the liquid flows along the bottom of the conduit and the gas along the top.
Stratified wavy	As gas velocity is increased, waves are formed on the gas-liquid interface producing the wavy flow pattern.
Annular	Liquid flows on the wall of the conduit as a film and the gas flows in the core of the conduit.
Churn	Characterised by slug flow bubbles which have broken down to give oscillating disordered flow.
Slug	Characterised by gas flowing in large bubbles known as "Taylor bubbles" while the liquid carries distributed bubbles.
Bubble	Phase composed of gas distributed as small discrete bubbles within a continuous liquid phase. Bubbles (spherical or cap-shaped) tend to accumulate in the upper part of the conduit due to buoyancy forces.
Dispersed bubble	Gas-phase is distributed as discrete bubbles in an axially continuous liquid phase. No bubble accumulation occurs, and bubbles are uniformly spread in liquid phase without any slippage between the phases.
Plug	Bullet-shaped bubbles which tend to flow along the top of the conduit because of buoyancy forces.

Gas-liquid two-phase flow patterns in annuli

Within gas-liquid two-phase flow, each flow structure has distinctive characteristics and is categorised according to the direction of the fluid flow relative to gravitational acceleration. Based on the description of the various

gas-liquid flow patterns, investigators have determined through experimental observation and/or theoretical analysis, the region where each gas-liquid flow pattern exist. When these regions are established, they are typically represented in a two-dimensional plot as a function of superficial phase velocities, called a flow pattern map. Figure 2.5 presents commonly accepted flow pattern maps for upward two-phase flow in annuli.

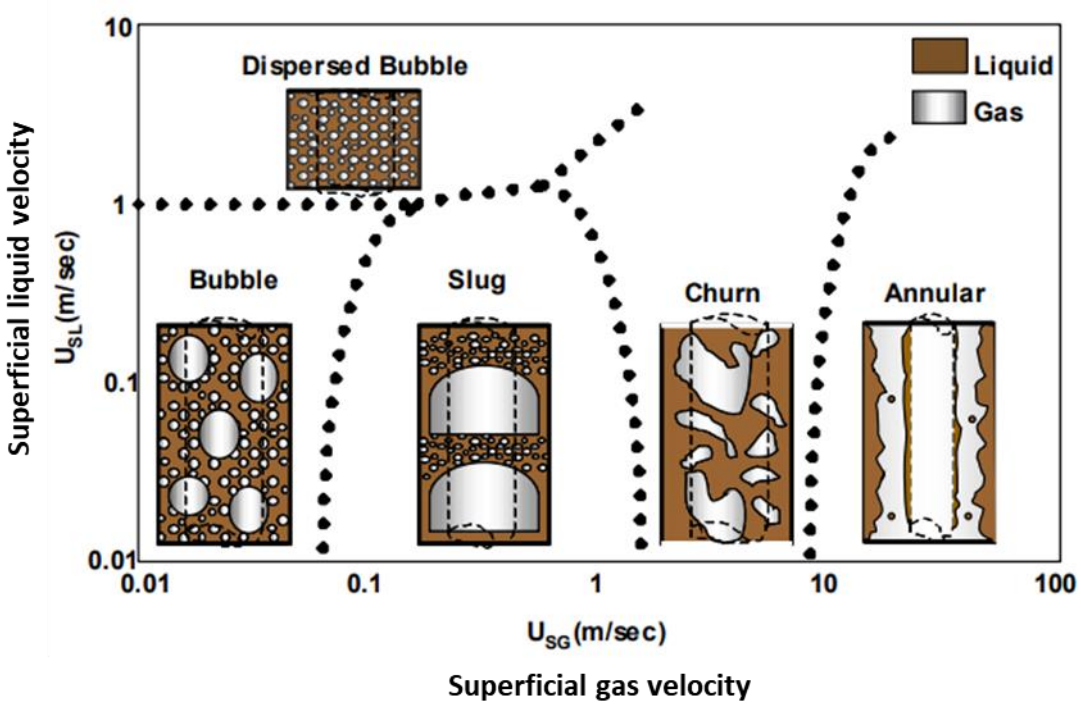

Figure 2.5 Flow pattern map for upward gas-liquid two-phase flow in annuli (adapted from Lage and Time, 2000; Perez-Tellez, 2003)

During UBD operations, well control and safe surface fluid (drilled and produced) handling are of paramount concern. Thus, if high gas superficial velocities are anticipated at the surface, the return line will be choked to increase the pressure to substantially limit the gas velocity. Additionally, considering the pressure and temperature profile changes along the UBD wellbore path, churn flow is only likely to occur at flow conditions close to the surface. However, at downhole conditions dispersed bubble, bubble, and slug flows are more likely to dominate

within the wellbore annulus. As the possibility of churn flow occurring is quite small coupled with the fact that there is no generalised or well-defined churn flow model available in literature, it is typically treated as slug flow. As such, dispersed bubble, bubble, and slug flow are the dominant two-phase upward flow patterns in annular geometries during UBD operations (Perez-Tellez, 2003; Sunthankar et al., 2003). Using the drillpipe (standpipe) gas injection method, gas and liquid are simultaneously injected through the drillstring at high injection pressure. This high pressure produces turbulent forces and compressible effects high enough to ensure that the gas phase remains dispersed in the continuous liquid phase, significantly limiting the occurrence of annular flow.

Various investigators have studied gas-liquid two-phase flow patterns in annuli using analytical, experimental, and data-driven methods (Table 2.3). These studies have considered different annuli geometries, diameter ratios, inclination angles, inner pipe eccentricities, fluid properties and flow velocities (Kelessidis and Dukler, 1989; Hasan and Kabir, 1992; Wongwises and Pipathattakul, 2006; Jeong et al., 2008; Nossen et al., 2017). Different approaches have been used to characterise the various two-phase flow patterns in annuli including digital image processing, visual observation, and conductance probe – 4 sensor and parallel plate (Das et al., 1999; Wongwises and Pipathattakul, 2006; Jeong et al., 2008; Ozbayoglu and Yuksel, 2012). Collectively, these studies reveal the differences in the distribution of the gas and liquid phases which characterise the different gas-liquid flow patterns in annuli geometries.

Table 2.3 Summary of studies on gas-liquid two-phase flow patterns in annuli

Investigator	Method(s)	Annulus geometry	Test fluids	Measurement	Main findings
Nossen et al. (2017)	Experimental	θ = 0° and 4° e = 0	SF6 gas – water and SF6 gas – Exxsol D60 oil	Flow pattern map, liquid holdup and pressure drop	Conducted two-phase flow experiments in horizontal and inclined annuli. Flow patterns observed were slug, large waves, very low frequency slugs and transitional flow. Data analysis showed subtle differences in flow patterns compared to pipe flow.
Ozbayoglu and Yuksel (2012)	Experimental and artificial intelligence	θ = 0° e = 1	Air-water	Flow pattern map and liquid holdup	Analysed the flow behaviour of air-water in a horizontal annulus and used the experimental data to develop artificial intelligence models. Using digital image processing techniques, obtained liquid holdup values, and identified flow pattern types and boundaries. Three different artificial intelligence techniques: 1) Nearest Neighbour (NN), 2) Decision Tree (DT) and 3) Backpropagation Neural Networks (BNN) were used as estimation models. The results indicated that the BNN technique performed the best (over 90%) in estimating the correct flow pattern while the NN technique estimated the liquid holdup value within an accuracy range of 17% average absolute error.
Jeong et al. (2008)	Experimental	θ = 90° e = 0	Air-water	Void fraction, interfacial area concentration (IAC) and bubble interface velocity	Experimentally studied interfacial area transport (IAT) of upward, vertical, two-phase flow under cap–slug, bubbly, and churn–turbulent flow conditions. Made measurements of the local flow parameters void fraction, bubble interface velocity and IAC. The axial and radial developments of the local flow structures were analysed using bubble coalescence and bubble breakup.
Ozar et al. (2008)	Analytical and experimental	θ = 90° e = 0	Air-water	Flow pattern map, void fraction, interfacial velocity, and area concentration	Investigated the IAT of upward, vertical, two-phase flow in an annulus for inlet flow conditions covering cap-slug, bubbly, and churn-turbulent flows. Flow patterns for each flow condition were identified based on visual observations and compared with several flow regime maps. Made measurements of local flow parameters void fraction, bubble interface velocity and IAC. Used these parameters to calculate the distribution parameter, Co, in the drift-flux model. Based upon the experimentally obtained Co values, proposed a new

Investigator	Method(s)	Annulus geometry	Test fluids	Measurement	Main findings
					correlation, showing that the distribution parameter in an annulus should be smaller than that in a tube.
Metin and Ozbayoglu (2007)	Analytical and experimental	$\theta = 0^o$ e = 1	Air-water	Flow pattern map and pressure drop	Performed air-water experiments in a fully eccentric horizontal annulus and developed a mechanistic model to determine flow patterns and to calculate the frictional pressure losses. A new diameter term was developed to characterise the fully eccentric annulus.
Wongwises and Pipathattakul (2006)	Experimental	$\theta = 0^o$, 30^o and 60^o e = 0	Air-water	Flow regime map, void fraction and pressure drop	Experimentally investigated upward two-phase flow patterns, pressure drop and void fraction in mini-gap annular channels. Observed and recorded plug, slug, annular, annular/slug, bubbly/plug, bubbly/slug–plug, churn, dispersed bubbly and slug/bubbly flow and their transition boundaries. Found that inclination angle significantly affects void fraction, flow pattern transitions and pressure drop. For horizontal flow, the homogeneous flow model (HEM) provided a good match with the measured pressure drop data while the void fraction data was reasonable correlated with the CISE correlation.
Sun et al. (2004)	Analytical, experimental, and neural network	$\theta = 90^o$ e = 0	Air-water	Flow regime map, void fraction, and transition boundary	Investigated using impedance void meters and a self-organizing neural network the cap bubbly-to-slug flow pattern transition in a vertical annular flow channel. The statistical parameters from the impedance signals were used as the inputs for the neural network for pattern categorisation. The flow visualisation patterns agreed with the classified patterns. An analytical model to predict the transition from cap bubbly to slug flow was also developed.
Zhou et al. (2004b)	Analytical and experimental	$\theta = 0^o$ e = 0	Air-water	Liquid holdup, transition boundaries, and pressure drop	Developed a mechanistic model for air-water hydraulics based on conservation equations and existing two-phase pipe flow correlations. Presented a sensitivity analysis to quantify the influence of flow parameters on the frictional pressure loss. Observed several flow patterns including stratified smooth, stratified wavy, slug, stratified to slug, slug to dispersed bubble and slug to annular. The theoretical basis for flow pattern transitions was also developed.
Lage and Time (2000)	Analytical and experimental	$\theta = 90^o$ e = 0	Nitrogen-water	Flow pattern map, gas	Proposed a mechanistic model to predict the behaviour of upward two-phase flow in vertical concentric annuli. The model is comprised

Investigator	Method(s)	Annulus geometry	Test fluids	Measurement	Main findings
				fraction, and pressure drop	of a procedure to predict the flow patterns and a set of independent mechanistic models to calculate the gas fraction and pressure drop in dispersed bubble, bubble, annular and slug flow.
Das et al. (Das et al., 1999)	Experimental	$\theta = 90^o$ e = 0	Air-water	Flow pattern map and phase distribution	Studied upward two-phase flow through concentric annuli to identify the phase distributions in bubbly, churn, and slug flow. Probability density function analysis was performed for a robust appraisal of the flow situation especially for the asymmetric phase distribution in the slug flow pattern. Developed mechanistic models for the transition boundaries between the bubbly-slug and the slug-churn flow patterns based upon the physical mechanism underlying the transitions between different flow patterns.
Das et al. (Das et al., 1999)	Analytical	$\theta = 90^o$ e = 0	Air-water	Phase distribution and transition boundaries	Theoretically predicted the transition boundaries between bubbly, churn, and slug flow for upward two-phase flow. Developed mechanistic models for flow pattern boundaries as functions of annulus dimensions, physical properties of the two-phase and their velocities, using the dataset of Das et al., 1999a. At a limiting void fraction of 0.2, the bubbly-slug transition occurred while the slug-churn transition occurred due to the flooding of the liquid films by Taylor bubbles.
Ansari et al. (1994)	Analytical and field	$\theta = 90^{o**}$ e = 0	Gas-oil	Liquid holdup and pressure drop	Proposed a mechanistic model to predict the flow behaviour of upward two-phase flow by predicting the existing flow pattern and then calculating the flow variables. Liquid holdup and pressure drop were predicted for bubble, annular and slug flow patterns. Evaluation of the model was done by using a well data bank comprising of 1,712 well field cases.
Caetano et al. (1992a)	Analytical	$\theta = 90^o$ e = 0 and 1	Air-water and air-kerosene	Flow pattern map, friction factor and Taylor bubble velocity	Experimentally investigated flow patterns in upward, vertical, gas-liquid flow in concentric and fully eccentric annuli. Made measurements of volumetric average liquid holdup and average total pressure gradient for each flow pattern. Obtained data on single-phase friction factor and Taylor bubble rise velocities. Found that the friction factor is significantly affected by diameter ratio, inner pipe eccentricity and Reynolds number. Developed a semi-empirical model for turbulent flow by incorporating the analytical results obtained under laminar flow conditions. The Taylor bubble rise velocity in an

Investigator	Method(s)	Annulus geometry	Test fluids	Measurement	Main findings
					annulus increase in comparison to full pipe flow due to the insertion of the tubing through the bubble, which results in a change of bubble cap shape. Also, the bubble rise velocity increases with a decrease in the hydraulic diameter.
Caetano et al. (1992b)	Analytical and experimental	$\theta = 90^o$ e = 0 and 1	Air-water and air-kerosene	Pressure drop	Developed mechanistic models for two-phase flow in annuli for dispersed bubble, bubble, annular and slug flow patterns. Models incorporate annulus dimensions and the effect of inner pipe eccentricity with a new predictive method for friction factor and Taylor bubble rise velocity based upon the work of Caetano et al. (1992a). The developed models were used to predict the flow behaviour, average volumetric liquid holdup, and the average total pressure gradient for each of the flow patterns.
Hasan and Kabir (1992)	Experimental	$\theta = 58^o$, 66^o, 74^o, 82^o and 90^o e = 0	Air-water	Void fraction and bubble rise velocity	Using the relative motion between the gas and liquid phases, caused by the density difference between the phases, presented a flow pattern approach to predicting the void fraction in bubbly, churn and slug flow patterns in annuli. The flow parameters Co and C1, in bubbly, churn and slug, do not appear to be affected by annular dimensions. Recommended that the values of C_o and C_1 must be chosen appropriately for circular annuli channels.
Nakoryakov et al. (1992)	Analytical and experimental	$\theta = 90^o$ e=0	Air-water	Flow pattern map	Experimentally studied upward two-phase flow in a narrow annular channel. Proposed a mathematical model based on the physical mechanisms suggested for different flow patterns, to predict the friction factor in a narrow annular channel. A method to calculate the friction factor based on the obtained empirical correlation of the mean gas-to-liquid velocity ratio was also proposed.
Papadimitriou and Shoham (1991)	Analytical	$\theta = 90^o$ e=0 and 1	Air-water Air-kerosene	Pressure drop	A mechanistic model was developed for the prediction of pressure gradients in pumping wells. The proposed model is based upon the concept of zero net liquid flow and incorporates the flow and system parameters such as casing pressure, gas flowrate and the annulus degree of eccentricity to predict the BHP. Models were developed for bubble and slug flow under zero net liquid flow conditions. These models, combined with a transition criterion between the flow patterns, constitute the overall model.

Investigator	Method(s)	Annulus geometry	Test fluids	Measurement	Main findings
Kelessidis and Dukler (1989)	Experimental	θ = 90° e = 0 and 0.5	Air-water	Flow pattern map	Proposed mathematical models to predict flow pattern transitions for both concentric and eccentric annuli, bubble-slug flow transition, slug-churn flow transition and churn-annular flow transition. Using probability density function (PDF) analysis classified the different flow patterns. Found flow pattern transition boundaries were insignificantly affected by inner pipe eccentricity.
Sadatomi et al. (1982)	Experimental	θ = 90° e = 0	Air-water	Flow pattern map, void fraction and pressure drop	Experimentally investigated vertical two-phase flow through several noncircular channels. Made measurements of cross-sectional distribution of void fraction, mean void fraction, rise velocity of gas bubbles and pressure drop. A correlation method to calculate frictional pressure drop was presented for single-phase turbulent flow. The friction factor for fully developed turbulent single-phase flow was correlated with Reynolds number using the turbulent geometry factor. Channel geometry had no significant influence on the flow pattern transitions both from bubble to slug flow and from slug to annular flow when Dh was greater than about 10 mm.

2.4.3 Effect of pipe eccentricity

Eccentricity is used to describe the degree to which a pipe is off-centre within another pipe or the openhole. The eccentricity, e, of an annulus can be expressed mathematically as:

$$e = \frac{\delta}{R_2 - R_1} = \frac{2\delta}{D_2 - D_1} \quad \text{Eq. 2.4}$$

where eccentricity can range from a value of zero to unity, with $e = 0$ corresponding to a concentric annulus and $e = 1$ corresponding to a fully eccentric annulus.

It significantly affects the velocities within the wellbore annulus and the prevailing gas-liquid two-phase flow patterns and its associated transition boundaries. This can lead to issues with wellbore cleaning and pressure regimes within the wellbore annulus (Oyeneyin et al., 2009).

Erge et al. (2015) employed analytical, experimental, and numerical approaches to study the effect of inner pipe eccentricity on annuli pressure losses using non-Newtonian fluids. Experimental results showed that pipe eccentricity can cause more than a 50% reduction in annuli pressure losses in fully eccentric annuli. Thus, the researchers emphasised the need to account for drillpipe eccentricity during the hydraulic planning for horizontal and extended reach wells. They also found that the flow patterns within eccentric annuli significantly differ from that of concentric annuli and this difference affects the flowrate at which the laminar-turbulent transition occurs, and the resultant pressure drop.

Ignoring the effect of pipe eccentricity on equivalent circulating density (ECD) and frictional pressure drop, serious problems relating to formation fracture, wellbore stability and/or well control, may arise. As such, within UBD operations,

pipe eccentricity must be taken into account to accurately predict the wellbore pressure profile, to achieve and maintain a good level of underbalance.

Traditionally, a nonlinear regression equation is applied to determine the frictional pressure gradient, R, in an eccentric annulus to that of a concentric annulus. Highlighted below are two models by Haciislamoglu and Langlinais (1990) and Patel (2006).

Haciislamoglu and Langlinais (1990) correlation is given as:

$$R = 1 - 0.072\left(\frac{e_{avg}}{n}\right)\sigma^{0.8454} - 1.5{e_{avg}}^{2}\sqrt{n}\sigma^{0.1852} + 0.96{e_{avg}}^{3}\sqrt{n}\sigma^{0.2527} \quad \text{Eq. 2.5}$$

Correlation is valid for the parameter ranges of $0.3 \leq \sigma \leq 0.9$, $0 \leq e \leq 0.95$ and $0.4 \leq n \leq 1.0$

with,

$$\Delta P_{EA} = \Delta P_{CA}\frac{\left(\frac{\Delta P}{\Delta L}\right)_{EA}}{\left(\frac{\Delta P}{\Delta L}\right)_{CA}} \quad \text{Eq. 2.6}$$

$$R = \frac{\left(\frac{\Delta P}{\Delta L}\right)_{EA}}{\left(\frac{\Delta P}{\Delta L}\right)_{CA}} \quad \text{Eq. 2.7}$$

where ΔP_{EA} is the pressure profile for eccentric annulus, ΔP_{CA} is the pressure profile for concentric annulus, $\left(\frac{\Delta P}{\Delta L}\right)_{EA}$ is the pressure gradient in an eccentric annulus, $\left(\frac{\Delta P}{\Delta L}\right)_{CA}$ is the pressure gradient in a concentric annulus, R is the pressure gradient ratio, e_{avg} is the average drillstring eccentricity, δ is the centre-to-centre distance between cylinders, R_1 is the radius of the inner cylinder, R_2 is the radius of the outer cylinder, D_1 is the outside diameter of the inner cylinder,

D_2 is the inside diameter of the inner cylinder, n is the Power-law flow behaviour index, σ is the diameter ratio and e is eccentricity.

$$\sigma = \frac{D_1}{D_2} \quad \text{Eq. 2.8}$$

Patel (2006) correlation is given as:

$$R = 1 - 0.1019 e_{avg} n \sigma^{-0.4675} - 1.6152 {e_{avg}}^2 n^{0.085} \sigma^{0.7875} + 1.1434 {e_{avg}}^3 n^{0.0547} \sigma^{1.1655} \quad \text{Eq. 2.9}$$

Correlation is valid for the parameter ranges of $0.2 \leq \sigma \leq 0.8$, $0 \leq e \leq 0.98$ and $0.2 \leq n \leq 1.0$.

Patel (2006) method is sometimes preferred over the Haciislamoglu and Langlinais (1990) correlation as it offers a wider range of operating parameters and overcomes some of its inherent limitations such as $R \to -\infty$ as $n \to 0$.

2.4.4 Effect of inner pipe rotation

Several studies on the effect of drillstring rotation have shown contradictory results of whether BHP and ECD are positively or negatively altered (Delwiche et al., 1992; Hansen and Sterri, 1995; McCann et al., 1995; Charlez et al., 1998; Ward and Andreassen, 1998). These observations have been recorded for single-phase (liquid) flow in annuli.

Inner pipe rotation in laminar flow can result in an additional shear velocity component. Typically, drilling fluids are shear thinning and inner pipe rotation increases the total shear stress, decreasing viscosity, with a resultant decrease in pressure drop. For Newtonian fluids, fully developed laminar flow, viscosity is independent of shear rate, and the described effects could not take place. At

low rotational speeds, below the critical Reynolds and Taylor number, the laminar flow can be described as a helical type of flow (Skalle, 2011).

While most drilling operations do experience an increased pressure drop with drillstring rotation, this may be explained as being the result of instabilities developed within the wellbore (Skalle, 2011). Drillstring rotation can generate centripetal forces pushing the fluid close to the pipe, leaving a void within the wellbore (Marken et al., 1992). These voids are filled with fluid from the outer part of the wellbore annulus. Thus, secondary flow called Taylor vortices develop. Inner pipe rotation allows for the development of these vortices and can promote axial-radial mixing, and this can have the same effect on momentum transport with turbulent mixing (Skalle, 2011).

Fluid flow with drillstring vibration coupled with the motion of the drillpipe during drilling operations can change the flow regime. Rotational and lateral motion, along with axial vibration and motion, contribute to the 'turbulent-like' flow (Marken et al., 1992).

Table 2.4 presents the limited published studies on the effect of pipe rotation on gas-liquid two-phase flow in annuli conducted using experimental and data-driven methods.

Table 2.4 Summary of studies on the effect of pipe rotation on gas-liquid two-phase flow in annuli

Investigator	Method(s)	Operational parameters	Test fluids	Measurement	Main findings
Baghernejad et al. (2019)	Experimental	θ = 0° and 10° RPM = 0, 50, 100, 200, 300 and 400	Air-water	Flow pattern map and pressure drop	Experimentally studied the effect of pipe rotation on two-phase flow and found that flow patterns, their transition boundaries and pressure drop are significantly affected by pipe rotation. In horizontal pipe, as the pipe rotation increases the stratified smooth flow pattern flow region decreases and no longer exist at high rotational speeds with the annular flow pattern region widening with increased rotational speed. For a 10° inclined pipe, as rotational speed increases the stratified wavy flow pattern region appears. In both horizontal and inclined pipes, as rotational speed increases, pressure drop also significantly increases.
Raeiszadeh et al. (2016)	Experimental	θ = 90° RPM = 0, 60, 120, 180, 240, 300, 400 and 500	Air-water	Flow pattern map	Using image processing techniques, studied the effect of pipe rotation on downward two-phase flow. Found that pipe rotation had a significant influence on the flow pattern maps and changed the transition boundaries between flow patterns. In bubbly flow, pipe rotation resulted in bubbles accumulating around the pipe axis, increasing the probability of their coalescence. Based upon the air and water flowrates, the pipe rotation changed the flow patterns from slug to froth, bubbly to slug, and at higher rotational speeds, from slug to annular. Thus, increasing pipe rotation shifts transition boundary between bubble and slug flow to lower V_{SG}, with annular flow also appearing at lower V_{SG}. As pipe rotation increases, the turbulence intensity decreases, and the froth zone decreases in size and at some rotational speeds the froth zone ceases to exist between slug and annular flow.
Ozbayoglu and Ozbayoglu (2007)	Neural networks	θ = 0° RPM not specified	Air-water	Pressure drop	Studied flow patterns and frictional pressure loss in two-phase flow through a horizontal annulus with inner pipe rotation using ANN. Compared results with experimental data and showed that the ANN could estimate flow patterns with high accuracy (the error is less than ±5%). No information concerning the dataset was presented in the study.
Shiomi et al. (1993)	Experimental	θ = 90°	Air-water	Flow pattern map	Investigated two-phase flow in the bubbly flow region in a concentric annulus with a rotating inner cylinder. Flow patterns observed were dispersed bubbly, triple-spiral, double-spiral single spiral, ring-form

Investigator	Method(s)	Operational parameters	Test fluids	Measurement	Main findings
		RPM = 100, 400, 500, 650 and 800			flow and their transition region. Results showed that at moderately low rotational speed, the flow field is dominated by the buoyancy effect of bubbles, forming dispersed bubbly flow. However, at relatively high rotational speed, the flow field was dominated by the vortex motion, forming ring-form and spiral flows.

2.4.5 Combined effect of pipe eccentricity and rotation

The combined effect of drillstring eccentricity and rotation has been studied by different investigators – using analytical, experimental, numerical, and field methods – with different conclusions being drawn (Table 2.5). These studies, however, have been limited to single-phase flow in annular geometries.

Ooms and Kampman-Reinhartz (2000) performed analytical and numerical studies to examine the effects of drillpipe rotation and eccentricity on the pressure drop of a borehole during drilling operations. Concluded that for laminar flow, drillpipe rotation and eccentricity result in increased axial pressure drop. Escudier et al. (2002) experimentally and numerically studied the effect of inner pipe rotation on frictional pressure loss in concentric and eccentric annuli using Newtonian and non-Newtonian fluids. Results showed that inner pipe rotation increases the axial pressure gradient for Newtonian fluid flows in eccentric annuli which they attributed to increased inertial effects. It was shown that in a slightly eccentric annulus, the shear-thinning effects can be dominant and surpass the inertial effects. However, in a highly eccentric annulus, the inertial effects can be dominant for non-Newtonian fluids. Erge et al. (2014) studied the effect of torsional motion on frictional pressure losses with various compression loads acting on the drillstring. They found that annular frictional pressure losses can increase or decrease with increasing drillstring rotation. Wan et al. (2000) numerically studied the effects of inner pipe rotation and eccentricity on frictional pressure losses in concentric and eccentric annuli using Newtonian and non-Newtonian fluids. They found that inertial and shear-thinning effects define the magnitude of annuli frictional pressure losses with inner pipe rotation. The axial pressure gradient increases in eccentric annuli with inner pipe rotation since the inertial effects dominate shear-thinning effects. For

slightly eccentric and concentric annulus, the frictional pressure loss decreases as the inner pipe rotates since shear-thinning effects can counteract inertial effects. Neto et al. (2014), experimentally and numerically investigated the effects of inner pipe rotation in concentric and eccentric annuli using non-Newtonian fluids. They found that an increase in rotary speed increased the pressure drop along the axial direction and axial flow in the narrowest gap of the eccentric annulus, which is beneficial to the hole cleaning process, reducing the flow stagnation in this region.

Notable disparities in published literature are reflective of a lack of scholarly consensus of our evolving understanding regarding the effect of pipe rotation and eccentricity and their combined effect on annular pressure gradient (Ahmed and Miska, 2008; Ahmed et al., 2010). Progress in this area is particularly constrained by the difficulty and limitation to simulate complex real annular flow. The significant variation across experimental, numerical, and field observations may be attributed to drillpipe wobbling or instability, irregular wellbore geometry, tool joint effect, operating with multiple dimension scales, simple fluid systems in the laboratory or a combination of these factors (Saasen, 2014).

Table 2.5 Summary of studies conducted on the effect of pipe rotation and eccentricity on annular pressure loss for single-phase flows

Investigator	Method(s)	Geometry	Rotation	Fluid type	Main findings
Ferroudji et al. (2019)	Numerical	Concentric and eccentric	Yes	Non-Newtonian	For laminar flow regime, the rotation of the inner pipe causes a reduction in pressure drop in concentric annuli; negligible effect is observed for eccentric annuli; no significant effect of the inner pipe rotation on the pressure drop gradient in turbulent flow regime.
Erge et al. (2014)	Experimental	Eccentric	Yes	Non-Newtonian	Annular frictional pressure losses can increase or decrease with increasing drillstring rotation.
Neto et al. (2014)	Experimental and numerical	Concentric and eccentric	Yes	Non-Newtonian	Pipe rotation increases the pressure drop along the axial direction and the axial flow in the narrowest gap.
Sorgun et al. (2010)	Experimental and numerical	Concentric and eccentric	No	Newtonian	Pipe eccentricity significantly increases the average tangential velocity inside the annulus for turbulent flow; as pipe eccentricity increases frictional pressure drop decreases.
Ahmed et al. (2010)	Analytical and field	Eccentric	Yes	Non-Newtonian	Higher annular velocity tends to increase the pressure loss ratio and amplify the effect of pipe rotation on the BHP.
Ozbayoglu and Sorgun (2010)	Analytical and experimental	Concentric	Yes	Non-Newtonian	Increased frictional pressure losses with increasing rotational speed significant at lower flowrates, while the effect of pipe rotation disappearing at high axial flows.
Ahmed and Miska (Ahmed and Miska, 2008)	Analytical and experimental	Concentric and eccentric	Yes	Non-Newtonian	Annular pressure loss can increase or decrease with increasing rotation speed.
Hemphill et al. (2007)	Field	Concentric and eccentric	Yes	Non-Newtonian	Sharp increase in annular pressure loss at the low rotational speeds and smaller increase at higher rotational speeds.

Investigator	Method(s)	Geometry	Rotation	Fluid type	Main findings
Escudier et al. (2002)	Experimental and numerical	Concentric and eccentric	Yes	Newtonian and non-Newtonian	Inner pipe rotation increases axial pressure gradient in eccentric annuli; in slightly eccentric and concentric annuli, frictional pressure loss decreases with pipe rotation; in highly eccentric annuli, inertial effects can be dominant for non-Newtonian fluids.
Wan et al. (2000)	Numerical	Concentric and eccentric	Yes	Newtonian and non-Newtonian	Pipe rotation caused an increase in the magnitude of the axial pressure gradient during the flow of a Newtonian fluid in eccentric annuli; for non-Newtonian fluid, in slightly eccentric annuli, inertial effects are counteracted by shear-thinning effects which dominate the phenomena, whereas inertial effects are dominant in highly eccentric annuli.
Escudier et al. (2000)	Experimental and numerical	Eccentric	Yes	Newtonian	High pipe rotation along with eccentricity leads to axial velocity distribution with the development of a second peak and friction factor increase.
Isambourg et al. (1999)	Field	Eccentric	Yes	Non-Newtonian	At rotational speeds below 60 rpm, pressure loss slightly increases. Above 60 rpm, the pressure loss increases linearly with the rotation speed.
Nouri and Whitelaw (1997)	Experimental	Eccentric	Yes	Newtonian and non-Newtonian	Pipe rotation exhibits similar effects for both Newtonian and non-Newtonian fluids with uniform axial flow developing across the annulus along with the maximum tangential velocities at the narrowest gap.
Wei et al. (1997)	Experimental	Concentric and eccentric	Yes	Non-Newtonian	Pressure loss can increase or decrease as pipe rotation increases.

Investigator	Method(s)	Geometry	Rotation	Fluid type	Main findings
Hansen and Sterri (1995)	Experimental and numerical	Concentric and eccentric	Yes	Newtonian and non-Newtonian	Pressure loss can increase or decrease as pipe rotation increases.
McCann et al. (1995)	Experimental and field	Concentric and eccentric	Yes	Non-Newtonian	Increase in pressure drop with pipe rotation in turbulent flow and decrease in laminar flow. With increasing pipe eccentricity, found a significant decrease in the frictional pressure loss for power law fluids.
Delwiche et al. (1992)	Field	Eccentric	Yes	Non-Newtonian	Increase in pressure loss with the increase of pipe rotation.
Haciislamoglu and Langlinais (1990)	Analytical	Concentric and eccentric	Yes	Non-Newtonian	Frictional pressure loss reduces with eccentricity; rotation produces a wobbling motion and eccentricity fluctuations that create complicated flow patterns.

It should be noted that only a limited number of studies have been conducted on gas-liquid two-phase flow with the effect of inner pipe rotation being investigated (Table 2.4). Nevertheless, to date, there exists no study that has investigated the combined effect of inner pipe rotation and eccentricity on two-phase non-Newtonian flow in concentric and eccentric annuli.

Past studies on the combined effect of pipe rotation and eccentricity for single-phase (Newtonian and non-Newtonian) flow in concentric and eccentric annuli (Table 2.5) and the limited studies on the combined effect of inner pipe rotation and eccentricity for gas-liquid two-phase in annular geometries underpin the importance of performing selective experimental studies on the combined effect of inner pipe rotation eccentricity on non-Newtonian flow for UBD hydraulic analysis.

2.5 Hydraulic modelling

The underbalanced hydraulic circulating system is typically characterised by a complex multiphase flow of a gas, liquid and solid phase (Aladwani and Gray, 2012). Proper management of the complex multiphase system out of the well and the BHP is critical to the maintenance of the underbalanced condition along the entire lateral section of the well. During UBD operations, the downhole pressure management (between the toe to heel) is governed by the gas-liquid flowrates, reservoir inflow performance and operational procedures (such as unloading the well and tripping operations) (Lage et al., 2003). These drilling features are subjected to fluctuations resulting in transient responses to the circulation system and can only be minimised, making the multiphase flow process dynamic in nature. Therefore, hydraulic modelling is innately used for determining basic parameters of the multiphase flow system.

Several methods have been adopted throughout the last few decades to hydraulically model the multiphase flow dynamics in a UBD wellbore annulus. Initially, steady-state simulators were used which ignored the slip between the gas and liquid phases by using the assumption of homogeneity of the aerated mud. This led to inaccuracies in predicting wellbore annuli pressure and two-phase flow parameters for UBD hydraulic systems where there is slip between the phases. Thereafter, there was a shift toward the use of empirical correlations to develop UBD commercial computer programs to predict flow patterns and liquid holdup. However, these simulators are typically not robust and cannot describe the real nature of the two-phase flow system, inefficient tool to determine the feasibility and optimal parameters for UBD operations. As such, the possibilities of their use are restricted to conditions without well-defined borders. For example, the Beggs and Brill (1973) correlation which applies a homogeneous approach (no-slip) has been commonly used in commercial UBD simulators despite its well-known limitations. This method uses the Froude number to determine the flow pattern and then, dependent on the flow pattern, the liquid holdup and pressure drop are estimated. This empirical correlation has been shown to overpredict BHPs for both vertical and horizontal UBD operations as it was developed from experimental datasets, thereby making extrapolation unreliable (Pérez-Téllez et al., 2003).

However, two-phase mechanistic models are preferred as they able to phenomenologically differentiate between the different gas-liquid flow configurations (flow patterns) to predict with much greater accuracy the wellbore annuli pressure. Additionally, the results of mechanistic models can be extended to conditions different from those used for their development. In particular, mechanistic approaches, using OLGA and Ansari, have been used for

pressure drop predictions for flow in wellbore annuli during UBD pilot tests even though they have not been specially developed or modified for UBD operations. As a result, they are not generally used for designing UBD operations (Bendlksen et al., 1991; Ansari et al., 1994; Pérez-Téllez et al., 2003).

As stated earlier in Section 2.4.2, different multiphase flow patterns may exist within the wellbore annulus during UBD operations. These patterns result in different wellbore annuli pressures due to the dynamic component of the wellbore annuli pressure; the frictional pressure drop varies with each gas-liquid two-phase flow pattern.

Several studies have been performed which considered the gas–liquid two-phase flow in annular geometries with various correlations and mechanistic models being developed (see Table 2.3). These studies highlight the importance and disparity within various research works as regards two-phase flow characteristics in annular geometries. In addition, although there is considerable amount of literature related to the behaviour and properties of gas-liquid two-phase flow in annular configurations, only a few studies have examined flow patterns in annuli with an inner rotating tube/pipe. Therefore, one of the core objectives of this research study is to better understand the hydraulics and characteristics of the gas-liquid two-phase flow in horizontal and inclined, concentric and eccentric annuli with and without inner pipe rotation, which will in turn aid in accurately predicting bottomhole pressures.

2.6 Cuttings transport

As the drillstring progresses through the wellbore, it slides through the well, generating cuttings at the drill bit which mixes with the drilling fluid content and flow as part of the multiphase system within wellbore annulus. Cuttings

transport is a complex and challenging issue when drilling horizontal, inclined, high angle and extended reach wells. Fluid rheology and density, hole size, drillpipe size, fluid flowrate, pipe inclination angle, wellbore geometry, ROP and drillstring rotation and eccentricity are parameters which influence the distribution of drilled cuttings during drilling operations (Shiddiq et al., 2017; Al Rubaii, 2018; Yeu et al., 2019; Mahmoud et al., 2020; Busch and Johansen, 2020). Experimental observations have shown that a mixture of solid/liquid flow in horizontal annuli can exhibit generally four types of solids transport mechanisms (Figure 2.6).

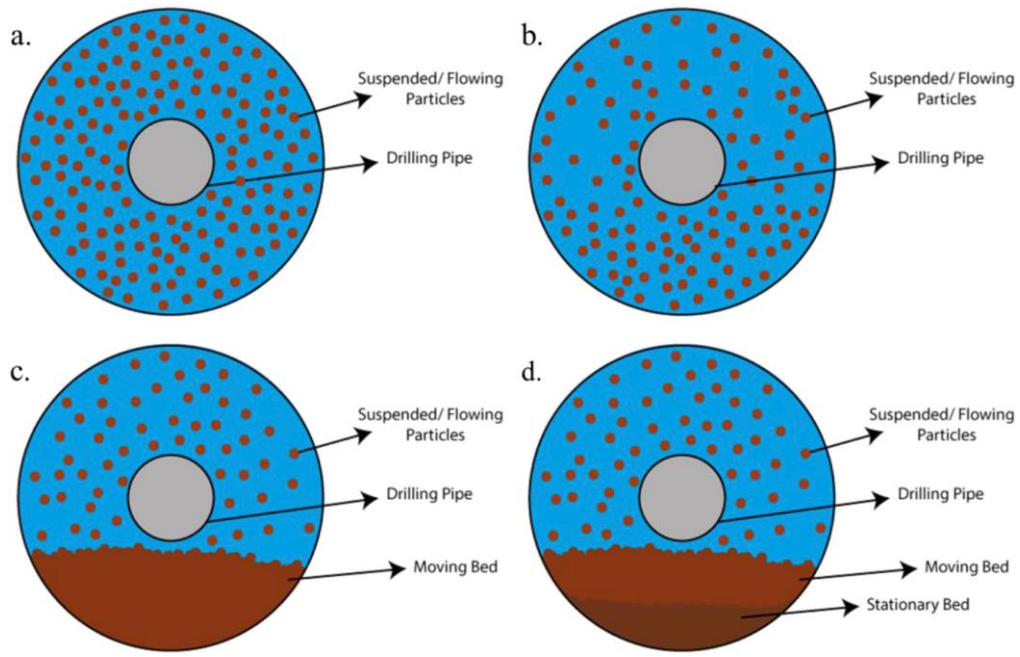

Figure 2.6 Solids transport mechanisms (a) fully suspended symmetric (b) fully suspended asymmetric (c) moving bed (d) stationary moving bed (Mahmoud et al., 2020)

Solids transport mechanisms that have been observed in laboratory experiments are, 1) fully suspended symmetric, 2) fully suspended asymmetric, 3) moving bed and 4) stationary moving beds (Kelessidis and Bandelis, 2004; Yeu et al., 2019). At high fluid velocities with fine solid particles (particle diameter of less than 1 mm), the fully suspended symmetric transport mechanism occurs when the solid particles become fully and uniformly

distributed in the liquid due to strong turbulent mixing, not allowing the solid particles to settle. This transport mechanism is not typically encountered during drilling operations. An asymmetric transport mechanism occurs when the fluid flow velocity is reduced, with the solid particles having a propensity to flow near the lower side of the wellbore but remain fully suspended which produces an asymmetric solids concentration. At low fluid flowrates, the moving bed transport mechanism is observed which results in the deposition of solid particles at the lower side of the wellbore, forming a moving solid bed and suspension layer on top of the bed with an irregular distribution of solid particles. The critical or suspension velocity refers to the minimum bed moving velocity. A reduction in the velocity lower than the critical velocity leads to the formation of three layers. The three layers are made up of a stationary bed at the bottom, moving bed in the middle, and suspension layer above (a heterogeneous solid-liquid mixture) (V. C. Kelessidis and Bandelis, 2004; H. Mahmoud et al., 2020).

Cuttings transport is influenced by several drilling parameters which impact hole cleaning in specific ways, but their effects differ depending on whether the well is horizontal, vertical, or inclined. Figure 2.7 shows some of the critical factors that affect hole cleaning.

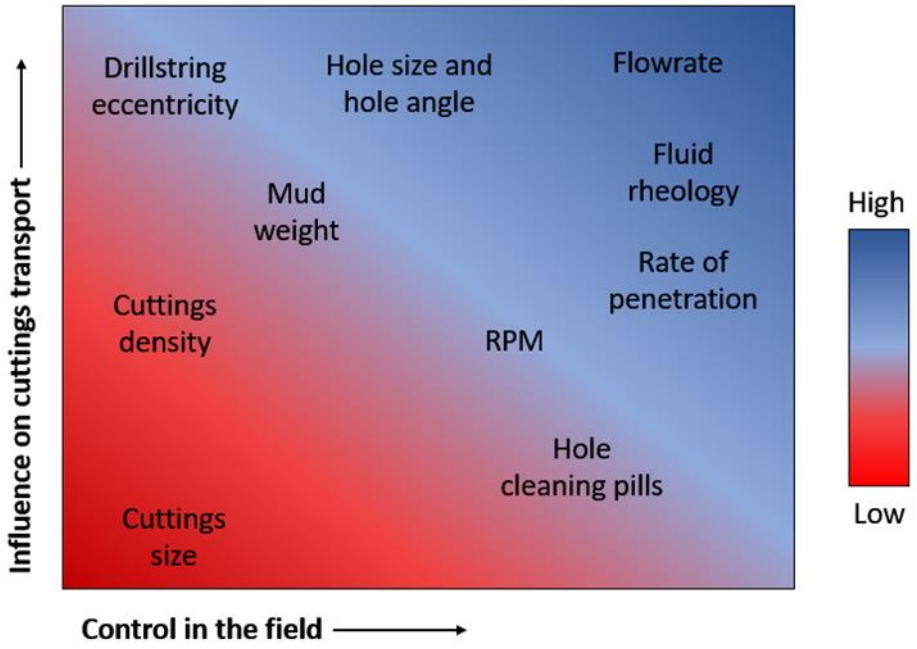

Figure 2.7 Factors affecting cuttings transport performance (adapted from Adari et al. (2000))

Flowrate, hole size, hole angle, fluid rheology and ROP have a strong influence on cuttings transport performance. Nevertheless, fluid rheology and flowrate are the preferred controllable parameters in field operations.

A valuable method which can be applied to prevent cuttings transport issues is for the designed system to operate above the critical condition to maintain favourable drilled cuttings movement. This critical condition is often referred to as the critical velocity or the minimum transport velocity (MTV) required to ensure that the drilled cuttings are mobile in the wellbore annulus and is a function of several drilling parameters. These parameters have been investigated and mapped out by various researchers and field reports over the years to be strong influencers of the cuttings transport mechanism during drilling (Gao and Young, 1995; Sun et al., 2014; Akhshik et al., 2015). The models for the MTV to ensure that the drilled cuttings are either transported in suspension or rolling as a bed at the bottom of the wellbore annulus are

expressed as a function of drilling parameters that govern the dynamics and movement of the cuttings entrained in the drilling fluid (Salubi et al., 2022):

In the case of moving bed:

$$V_{MR} = f(\rho_f, \rho_c, d_c, d_x, \mu_f, g(\rho_c - \rho_f)[f_s \sin\beta + \cos\beta]) \quad \text{Eq. 2.10}$$

In the case of suspension:

$$V_{MS} = f\left(\rho_f, \rho_c, d_c, d_x, \mu_f, g(\rho_c - \rho_f)\sin\beta\right) \quad \text{Eq. 2.11}$$

where ρ_f is the drilling fluid density, ρ_c is the drilled cuttings density, d_c is the cuttings sizes, μ_f is the drilling fluid viscosity, f_s is the coefficient of static friction between the drilled cuttings and the wellbore annulus wall, d_x is the distance between the drillpipe and wellbore annulus wall at the lowest position, g is the acceleration due to gravity and β is the wellbore inclination angle.

These models have been generated from a fundamental knowledge of physics but refined with CFD datasets and validated with experimental studies and field acquired data. Unlike the conventional drilling methods, the gas-liquid drilling fluid properties and the prevailing gas-liquid flow pattern in the wellbore annulus are additional parameters that strongly influence the cuttings transport efficiency during UBD operations. The complexities induced by multiphase flow in the wellbore annulus affects the forces that are responsible for the movement of the drilled cuttings and these hydrodynamic forces differ with different flow patterns. This means that the critical condition required to ensure an effective cuttings transport system for UBD environments must be modelled and developed by considering the gas-liquid flow pattern that is likely to be present in the wellbore annulus.

Several research studies have been performed to investigate cuttings transport in vertical, horizontal and inclined annular geometries using various approaches, analytical experimental, numerical and neural networks (Xu et al., 2013; Suradi et al., 2015; Rooki and Rakhshkhorshid, 2017; Prasun and Ghalambor, 2018; Huaizhong et al., 2019). Some studies have examined cuttings transport considering the effect of pipe rotation cutting transport, concluding that drillpipe rotation speed with specific limits enhances cuttings transport within the wellbore annulus (Duan et al., 2010; Sorgun, 2013; Wei et al., 2013; Xu et al., 2013; Suradi et al., 2015). While several studies have analysed cuttings transport phenomena in terms of the cuttings concentration and pressure drop, which can be physically measured, only a few studies have analysed the velocities of solid particles (Garcia-Hernandez et al., 2007; Epelle and Gerogiorgis, 2018). However, negative eccentricity increases the accumulation of drilled cuttings on the lower side of the wellbore annulus, resulting in a cuttings bed due to the narrower gap which produces a local reduction in drilling fluid velocity (Heydari et al., 2017; Busch and Johansen, 2020). Table 2.6 provides a summary of studies on cuttings transport in UBD operations and their main findings.

Table 2.6 Summary of studies on cuttings transport in underbalanced drilling operations

Investigator	Method(s)	Hole inclination	Rotation and eccentricity	Fluid type	Particle size and density	Study	Main findings
Huaizhong et al. (2019)	Experimental and numerical simulation	$\theta=90^0$	RPM=0, 30, 60, 90, 120 and 150; e=0	Single-phase	8 mm; 2610 kg/m^3	Analysed the laws of cuttings transport in a narrow annulus with a focus on the technique of coiled tubing partial underbalanced drilling (CT-PUBD).	As drillpipe rotation increases particle velocity declines but increases with an increase in flow ate; with an increased flowrate particles become concentrated and limits the particles in a small area; particle distribution undergoes a process of concentration, dispersion, and concentration as drillpipe rotation increases; particles deviate from the high fluid velocity area due to high rotational speed causing low particle velocity; and collision phenomenon of particles, sinking and rising of particles, and variation of particle velocity were observed in experiments.
Epelle and Gerogiorgis (2018)	Numerical simulation	$\theta=0^0$, 45^0 and 90^0	RPM=100 and 400; e=0 and 0.6	Single-phase; non-Newtonian	1, 5 and 10 mm; 2610 kg/m^3	Studied the dispersion of cuttings, in relation to their axial, tangential and slip velocity profiles in a wellbore annulus under steady and transient conditions.	Particle slip velocities are the lowest at the centre of the wellbore annulus whereas the effect of asymmetry caused by drillpipe rotation is distinctively noticeable along the longitudinal plane; a change of turbulence properties of the continuous phase is strongly influenced by particle diameter results; the occurrence of ejections

Investigator	Method(s)	Hole inclination	Rotation and eccentricity	Fluid type	Particle size and density	Study	Main findings
							of coherent structures at the walls of the flow domain was captured by the cuttings trajectory analysis.
Prasun and Ghalambor (2018)	Numerical simulation	$\theta=90^0$	RPM=0; E=0.5	Foam quality =70%, 80% and 90%	3.81 mm; 1896 kg/m^3	Studied the relationship between drilling parameters on cuttings concentration and bed height and proposed a transient wellbore hydraulic and cuttings transport model.	Bed height and cuttings concentration are sensitive to changes in surface foam injection rates and back-pressure and can be optimised by suitable adjustment of the input parameters; and strong link made between hole-cleaning and inclination with bed height increasing with an increase in inclination angle until a critical angle of 90°-φ (φ is the angle of repose) after which, it reduces.
Akhshik and Rajabi (2018)	Numerical simulation	$\theta=0^0$ and 30^0	RPM=0; e=0	Aerated water and mud; Newtonian and non-Newtonian	3.66 mm; 2400 kg/m^3	Used computational fluid dynamics–discrete element method (CFD-DEM) to simulate cuttings transport in an aerated mud and investigate the hydraulics of aerated mud flow for cuttings transport performance under downhole conditions.	Cuttings transport efficiency predominantly affected by liquid flowrate but also gas-liquid ratio, ambient temperature and injection pressure; reduction of cuttings volume concentration with increasing gas injection rate; formation of isolated dunes occurs at inclination angles of 45° or less; low inclination angles coupled with the effect of elevated pressure has a negligible effect on cuttings volume concentration; as

Investigator	Method(s)	Hole inclination	Rotation and eccentricity	Fluid type	Particle size and density	Study	Main findings
							temperature increases cuttings transport efficiency decreases, however cuttings transport efficiency significantly decreases as the injection of gas increases, this means that gas injection can compensate for temperature effects.
Heydari et al. (2017)	Numerical simulation	$\theta=0^0$	RPM=0, 50, 100 and 150; e=0, 0.125, 0.25, 0.375, 0.5, 0.625 and 0.75	Foam and single-phase; non-Newtonian	6.35 mm; 2650 kg/m^3	Used the finite volume model (FVM) to study the effects of drillpipe rotation, different rates of penetration, drilling fluid flowrate and drillpipe eccentricity on cuttings accumulation and to predict cutting's bed height.	Effect of pipe rotation is minor in concentric annuli compared with eccentric annuli; pipe rotation has a pronounced effect within eccentric annuli; high rotational speed leads to lower cuttings concentration in the wellbore annulus; in horizontal sections of a well, drillpipe rotation role redistributes the accumulation of drilled cuttings in the wellbore annulus; drillpipe eccentricity results in cutting's accumulation, reducing the flow path available for the drilled cuttings to move through; drilled cutting accumulation can be correlated with the ratio of ROP to fluid flowrate, higher ROPs require higher fluid rates to prevent further accumulations; tangential velocity of the drillpipe rotation helps drilled

Investigator	Method(s)	Hole inclination	Rotation and eccentricity	Fluid type	Particle size and density	Study	Main findings
							cutting to occupy a greater cross-sectional area of the annulus, giving them a larger flow area through which in turn increases the average axial velocity of drilled cuttings.
Rooki and Rakhshkhorshid (2017)	Neural network	$\theta=0^0$	RPM=0, 40, 80 and 120; e=0 and 0.78	Foam quality=60%, 70%, 80% and 90%	3 mm; 2610 kg/m^3	Applied a radial basis function network (RBFN) model with three layers to estimate cuttings concentration in foam drilling using foam velocity, foam quality, temperature, and pressure, drillpipe rotation and eccentricity.	The ability of the RBFN model in the training phase produced an average absolute percent relative error (AAPE) of 2.0e-13% and a correlation coefficient of 1 while the testing phase resulted in an AAPE of 5.93% and a correlation coefficient of 0.922.
Suradi et al. (2015)	Experimental	$\theta=0^0$ to 60^0	RPM=0-120; e=0, 0.25 and 0.5	Foam	0.25, 0.5, 1, and 2 mm	Evaluated the effectiveness of polymer beads in foam-based mud as a stabiliser and lubricant agent by observing the half-life of the foam, performing rheological and lubricity testing and	Increasing foam velocity decreases cutting concentration; cuttings concentration consistently decreases with pipe rotation; frictional pressure drop decreases with pipe rotation due to a reduction in cuttings concentration in the wellbore annulus, this results in a smaller cuttings bed cross-sectional area, leading to a larger fluid flow area, decreasing the

Investigator	Method(s)	Hole inclination	Rotation and eccentricity	Fluid type	Particle size and density	Study	Main findings
						assessing the performance of the stabilised foam as drilling fluid in cuttings lifting operations.	pressure losses and flow resistance.
Rooki et al. (2014)	Numerical simulation	$\theta=0^0$, 15^0, 30^0, 45^0 75^0 and 90^0	RPM=0, 80 and 120; e=0 and 0.78	Foam quality =80% and 90%	3 mm; 2610 kg/m^3	Studied cuttings transport with foam using a 3D computational fluid dynamics (CFD) simulation for liquid-solid mixture flow through both concentric and eccentric annuli and varied foam qualities, foam velocities, drillpipe rotations and inclination angles.	Increasing foam quality, foam quality and drillpipe rotation increases drilled cuttings transport; with an angle of inclination between 0° to 45° cuttings transport ratio decreases, but the ratio varies only slightly between 45° and 90°.
Wei et al. (2013)	Experimental	$\theta=0^0$	Yes	Aerated	6 mm	Developed a physical model for drilling fluid carrying capacity and wellbore cleaning in horizontal wells. Proposed a mathematical model for critical transport.	In horizontal wellbore sections, the drilling fluid cannot carry large, drilled cutting and remain on the lower side of the wall waiting for the drilling tool to roll helping to form smaller particles which can be transported by fluid downstream; cuttings transport depends on the gas-liquid velocity and the drilling

Investigator	Method(s)	Hole inclination	Rotation and eccentricity	Fluid type	Particle size and density	Study	Main findings
							fluid viscosity in horizontal wellbore sections and the drillpipe rotation aids cuttings transport; carrying cuttings smoothly.
Xu et al. (2013)	Analytical and experimental	$\theta=70^0$, 80^0 and 90^0	RPM=0, 40 and 80, e=0.78	Foam quality=70%, 80% and 90%	–	Studied cuttings transport with foam enhanced with polymers in highly inclined wells under elevated pressure and elevated temperature (EPET) conditions, along with the effect of pipe rotation.	Change of inclination angle from 90^o to 70^o has a minor effect on both cuttings concentration and frictional pressure loss under EPET conditions; cuttings concentration is strongly influenced by foam superficial velocity, cuttings concentration reduces with an increase in foam superficial velocity; under EPET conditions, high-quality foam results in slightly lower cuttings concentration; cuttings concentration and frictional pressure loss reduces with drillpipe rotation in low-quality foams at low flowrates.
Piroozian et al. (2012)	Experimental	$\theta=60^0$, 70^0, 80^0 and 90^0	RPM=0; e=0	Single-phase; non-Newtonian	1.74 mm	Studied the effect of hole inclination, fluid viscosity and velocity on cuttings transport performance (CTP).	For all angles of inclination, the turbulent regime is the best for cuttings removal, followed by transition then laminar regime; as an annulus' inclination angle increases the removal of cuttings from the wellbore is also increased; an increase of mud plastic viscosity results in an increase of recovered

Investigator	Method(s)	Hole inclination	Rotation and eccentricity	Fluid type	Particle size and density	Study	Main findings
							cuttings; stationary bed removal is positively impacted by velocity; increased wellbore inclination angle and higher fluid viscosities results in an incremental increase in annular velocity with higher cuttings transport performance.
Duan et al. (2010)	Experimental	$\theta=0^0$	RPM=0, 40, 80 and 120; e=0.78	Foam quality=60%, 70%, 80% and 90%	3 mm	Studied cuttings transport using foam with pipe rotation.	Pipe rotation enhanced drilled cuttings removal in low-quality foam; in horizontal wellbores increasing foam quality and rotational speed improves hole cleaning and decreases the frictional pressure loss; higher foam velocity improves hole cleaning but increases pressure losses. Developed simulator can predict bed height, cuttings concentration and pressure drop for horizontal foam drilling operations with input parameters such as drillpipe rotation and eccentricity, foam quality and velocity under different pressure and temperature conditions.
Chen et al. (2007)	Experimental	$\theta=0^0$	RPM=0; e=0	Foam quality=90%	3 mm; 2610 kg/m^3	Studied the effects of foam quality, different polymer concentrations,	Fully suspended flow and stationary cuttings bed were observed during the cuttings transport experiments; an increase

Investigator	Method(s)	Hole inclination	Rotation and eccentricity	Fluid type	Particle size and density	Study	Main findings
						annular velocity, temperature, and pressure on foam cuttings transport in a horizontal annulus.	in annular velocity decreases the cuttings concentration in the wellbore annulus; volume of cuttings accumulated in the annulus is not sensitive to flow velocity increase until a critical velocity is reached, and the borehole is cleaned; critical velocity depends on foam quality, polymer concentration, inclination angle, pressure and temperature; low quality foams require higher velocity than high quality foams; adding viscosifiers, to foam system decreases cuttings concentration and increases frictional pressure loss; temperature can affect the cuttings-transport efficiency and frictional-pressure drop; increasing pressure causes a slight decrease in the cuttings concentration; frictional-pressure losses in the annulus increase when cuttings are injected along with foams.
Capo et al. (2006)	Experimental	$\theta=45^0$, 55^0 and 65^0	RPM=0; e=0	Foam quality= 70% and 80%	–	Investigated the effects of foam quality, foam velocity, ROP and inclination angle on cuttings transport.	Low-quality foam provides enhanced cuttings transport performance, in relation to cuttings concentration; increasing ROP for a given inclination angle and similar foam-flow conditions can result in

Investigator	Method(s)	Hole inclination	Rotation and eccentricity	Fluid type	Particle size and density	Study	Main findings
						Based upon the volume-equalized power-law model, developed a simulator to predict flow velocity, pressure, foam quality and specific volume-expansion ratio throughout the wellbore annulus.	an increase in the in-situ cuttings concentration. Used Archimedes number, Reynolds number, Froude number, density ratio and inclination angle to develop a correlation for the ratio of the cuttings-bed area to the cross-sectional area of the wellbore annulus.
Li and Kuru (2003)	Analytical and numerical	$\theta=0^0$	RPM=0; e=1	Foam quality=60%	12.7 mm; 2500 kg/m^3	Developed a two-layer model to study factors affecting cuttings transport with foam in horizontal wells.	An increase in drillpipe eccentricity and ROP increases the cuttings bed height.; increasing foam quality and total flowrate effectively decrease cuttings bed height; improved cuttings transport efficiency with increasing total foam flowrate suggests that if the equivalent circulating foam density stays below the required limit for underbalance, maximum possible gas-liquid injection rates should be used for effective borehole cleaning; influx of formation fluid has a positive effect on cuttings transport efficiency as indicated by reduced cuttings bed height, but with formation fluid influx, foam stability becomes a critical issue

Investigator	Method(s)	Hole inclination	Rotation and eccentricity	Fluid type	Particle size and density	Study	Main findings
							and its impact needs to be properly evaluated.
Martins et al. (2001)	Experimental	$\theta=45^0$, 75^0 and 90^0	RPM=0; e=1	Foam quality =60 to 95%	6 mm; 2600 kg/m^3	Studied cuttings transport performance of foamed systems in horizontal and inclined wells and performed curve-fitting functions to explain the flow- and cuttings-transport behaviour observed.	High-quality foams have the capability to erode cuttings beds with liquid flowrates influencing this phenomenon to a higher degree in lower-foam-quality tests; and proposed methodology for predicting bed heights as a function of foam quality and liquid flowrates accurately reflects the phenomena involved in the cuttings-bed removal process.

The computation of the cuttings transportation process in gas-liquid UBD mud flow systems (Wei et al., 2013; Akhshik and Rajabi, 2018) is more complicated than the single-phase fluid case (Sorgun, 2013; Epelle and Gerogiorgis, 2018). Furthermore, in the case of drilling directional and horizontal wells, the prediction modelling process is more complex and intensive as these reservoirs may be more susceptible to the impact of pipe inclination angle and the contact/collision emergence of solid particles and their deposition phenomenon (Piroozian et al., 2012; Prasun and Ghalambor, 2018). Also, both the hydraulic behaviour and the mechanism of the cuttings transport performance within the UBD flow system is not fully understood due to uncertainties relating to the selection of most appropriate fluid flow properties of the gas-liquid two-phase composition (Akhshik and Rajabi, 2018). Thereby, inhibiting the prediction of the optimal flowrates (both pump and injection) for the UBD operations (Li and Kuru, 2003).

2.7 Multi-layered modelling

Cuttings transport is a three-dimensional, unsteady problem (Kamp and Rivero, 1999). Within literature, researchers have developed different cuttings transport models to describe the series of processes involved in cuttings transportation and deposition. These physical models have been used as a predictive tool for cuttings transport as empirical models typically are rigid and are difficult to extend over wide range of operational drilling scenarios. These models can be either two-layered or three-layered. The two-layer model comprises of a heterogeneous suspension layer at the top side of the annulus, and a layer of solids on the bottom of the outer pipe that may be moving, even-though at a very low velocity. This modelling approach uses the different cuttings transport mechanisms and results in a system of four algebraic equations and one integral equation which describes the turbulent diffusion of solids. Solutions to the system provides the solids bed

height and its resulting pressure drop. Figure 2.8 illustrates of the two-layer model.

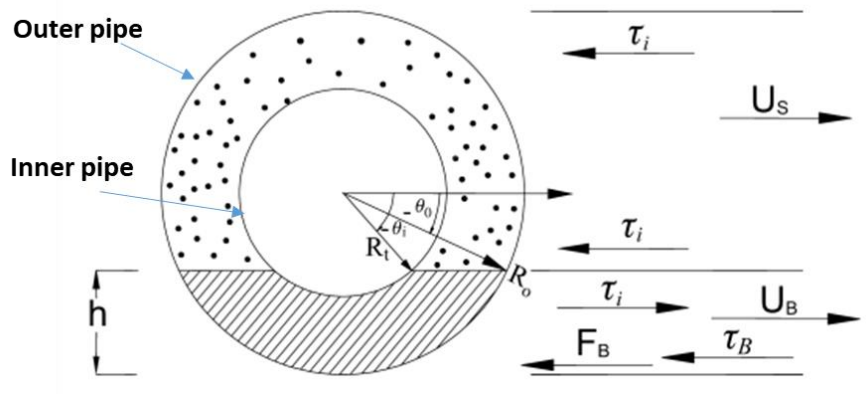

Figure 2.8 Schematic diagram of a two-layer model for a concentric horizontal annuli (adapted from Kelessidis and Bandelis, 2004)

Prediction deficiencies (accuracy) from two-layer models has led to its extension, three-layer models. Its theoretical development follows that of the two-layer model approach, with the inclusion of a stationary bed below the moving bed. As such, a three-layer model comprises of a stationary bed of drilled cuttings at the bottom, a moving-bed layer above it, and a heterogeneous suspension layer at the top. Figure 2.9 depicts a three-layer model in a fully eccentric horizontal annulus.

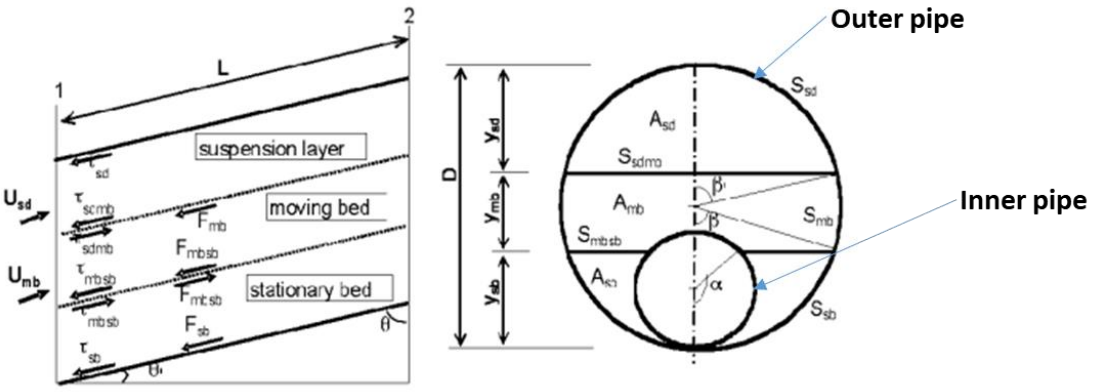

Figure 2.9 Schematic diagram of a three-layer model for a fully eccentric horizontal annuli (adapted from Cho et al., 2002)

Clark and Bickham (1994) developed a two-layer cuttings transport model which utilises fluid mechanical relationships developed for different particle transport mechanisms, as a means of evaluating cuttings transport as a function of fluid flowrate, ROP, mud rheology, wellbore configuration and cuttings properties. Model predictions were in good agreement with experimental data from literature for flowrates below critical conditions. However, model predictions at flowrates for critical transport (no bed formation), were underpredicted compared to experimental results.

Nguyen and Rahman (1998) presented a three-layer mathematical model to predict the effect of various parameters and operational conditions (mud flowrate and rheology, annular geometry, and cuttings size) on bed thickness, annular cuttings concentration and pressure gradient in highly deviated to horizontal annuli based upon different cuttings transport mechanisms. Model predictions showed favourable agreement with experimental results.

Kamp and Rivero (1999) developed a two-layer model to carry out numerical simulations in an effort to predict cuttings bed height, pressure drop, and transport velocities at different ROPs and mud flowrates. Numerical results were compared to correlation-based model predictions. These comparisons showed that the two-layered model generally performed better than the correlation-based models, apart from the model overpredicting cuttings transport at given mud flowrates.

Cho et al. (2000) presented a three-layer mathematical model to predict cuttings transport mechanism in horizontal wellbore annuli. The model is developed through force analysis of the different cuttings transport mechanisms and the effects of drilling fluid pump rate and rheology, cuttings properties and

concentration, wellbore geometry, and eccentricity upon it. The simulation results showed favourable agreement with experimental data published in literature.

Masuda et al. (2000) performed an experimental investigation on cuttings transport in inclined annuli to establish the critical cuttings transport velocity. Thereafter, they developed a transient cuttings transport numerical model using a two-layer modelling approach. A comparison of their experimental and numerical results showed a reasonably good match with the calculated and measured cuttings velocity agreeing well.

Naganawa and Nomura (2006) developed a transient cuttings transport simulator using a two-layer model to evaluate hole cleaning in extended reach wells. Simulation results demonstrated the transient distributions of cuttings bed height and annuli pressure over the whole wellbore trajectory.

Wang et al. (2010) presented a dynamic three-layered cuttings transport model which takes into account the cuttings movement between the layers, slip between the solid and liquid phase, and drillpipe rotation to predict the dynamic thickness of cuttings bed using measured ECD to be used in cuttings bed monitoring and control for extended reach well drilling. The model was successfully used in an oilfield in the South China Sea.

As noted in the literature, some researchers have utilised the two-layered modelling approach while others have adopted a three-layered modelling approach to evaluate the effectiveness of major drilling parameters on cuttings transport (Gavignet and Sobey, 1989; Martins and Santana, 1992; Nguyen and Rahman, 1998; Kamp and Rivero, 1999; Cho et al., 2000; Wang et al., 2010). However, none of these studies, to the author's knowledge, have developed

cuttings transport models applicable to gas-liquid two-phase flows in wellbore annuli. Nevertheless, not accounting for the effect of the transient fluid flow patterns that occur in gas-liquid two-phase flow in annular geometries would lead to inaccurate model predictions when compared with experimental results, and unreliable predictions when modelling over a wide range of operational conditions during drilling operations, having significant inconsistencies with field data. The physical phenomena of the gas-liquid two-phase flow pattern is required for wellbore hyraulics and cuttings transport modelling for gas-liquid UBD operations and it must be flow pattern dependent.

2.8 Field case studies

With drilling cost considered one of the key determinant factors of drilling operations, achieving an improved ROP and reduced drilling problems are generally considered as effective ways by which drilling costs can be reduced (Fattah et al., 2011). It is within this overarching paradigm that UBD has been applied as an enhanced drilling solution globally in a variety of geological settings such India (Motghare et al., 2019), Libya (Safar et al., 2007), Russia (Berg et al., 2020), Venezuela (Villasmil et al., 2003; Beltran et al., 2006), Norway (Eck-Olsen et al., 2004), Algeria (Moore et al., 2004), Oman (Eissa and Al-Harthi, 2003; Al-Saadi et al., 2006) and the United Kingdom (Davison et al., 2004).

The objective of each UBD operation varies according to the drilling context. Specific objectives include (i) enhance well control, increase ROP, reduce NPT and increase well productivity (Fattah et al., 2011), (ii) minimise drilling-induced formation damage and improve drilling performance (Fattah et al., 2011), (iii) reduce/prevent fluid losses to speed up well clean-up (Ashraf et al., 2020), (iv)

real-time capture of surface flow and pressure data (Motghare et al., 2019), (v) minimise the footprint of surface equipment (Eck-Olsen et al., 2004).

To assess the operational phase and associated outcomes of global UBD operations, 25 global UBD field case studies – 18 successful and 7 which were operationally challenged, were evaluated. Table 2.7 presents field case studies of historical applications of UBD operations providing evidence that UBD is an enhanced drilling solution. In the sampled case studies, use of an aerated mud system with nitrogen as the injection gas was the most common scenario (Davison et al., 2004; Beltran et al., 2006; Shadravan et al., 2009; Marbun et al., 2013; Ashraf et al., 2020). The operational justification for each UBD application varied from (i) geologic complications as a result of several fractures (Berg et al., 2020), (ii) highly depleted, low reservoir pressure and high bottomhole temperature (Marbun et al., 2013), (iii) extremely hard to drill, abrasive sandstone (Moore et al., 2004), (iv) environmental considerations requiring no release of hydrocarbons into the atmosphere or flaring during the operation (Eck-Olsen et al., 2004), and (v) high water cut (Eissa and Al-Harthi, 2003). Remarkable results have been achieved by operators implementing UBD as the preferred drilling operation, such as (i) drilling time cut by half and formation kept in "virgin" state at all stages, delivering an unprecedented production rate from the subject well (Ashraf et al., 2020), (ii) increased initial oil production, 1.5 to 1.8 times more oil with lower water cut than comparative wells (Motghare et al., 2019), (iii) well drilled to target total depth, with no circulation losses and added value from early oil production (Shadravan et al., 2009), (iv) faster drilling times, 12.36 days compared with 19.94 days with OBD (Beltran et al., 2006), and (v) NPT per well reduced from 302 hours to less than 1 hour and cost per well reduced (Davison et al., 2004).

Table 2.7 Field case studies of successful underbalanced drilling operations

Investigator	Field/location	Target formation	Working fluids	Operational justification	Result(s)
Ashraf et al. (2020)	Qadirpur, Pakistan	Sui Main Limestone formation – limestone reservoir	Nitrogen and liquid mud	Severe circulation losses resulted in excessive drilling time with substantial loss circulation material (LCM) pumped into the wellbore to reduce losses; extensive clean-up operation along with acidizing to reduce the damage caused to the formation; and extensive formation damage during drilling led to no production.	Drilling time cut by half and formation kept in "virgin" state at all stages delivering an unprecedented production rate from the subject well; no reservoir damage recorded hence zero skin; production enhancement significant, moving from production of similar offset wells from 1-2 MMSCFD to 20 MMSCFD; sweet spots were identified with production of almost 1 MMSCFD; no loss circulation observed; continuous cuttings transport to surface enabled the operator to mark the well targets accurately; electromagnetic measurement while drilling (EM-MWD) guided the well to reach the target.
Berg et al. (2020)	Archinskoe, Russia	Carbonate reservoir	Nitrogen and water /crude oil mud systems	Difficult to drill due to zero pressure window; and geologic complications as a result of several fractures	Controlled drawdown during drilling operations from the fractures, significantly longer wells drilled, and maximised fractures discovered per well.
Motghare et al. (2019)	Heera and Mumbai High, India	Bassein formation (Heera field) – carbonate reservoir L-III formation (Mumbai High field) – carbonate reservoir	Nitrogen and base oil	Depleted/under-pressured reservoir; severe mud losses recorded in adjacent wells leading to formation damage; inability to reach target depths resulting in premature total depth; drilling issues like differential sticking and ROP reduction; and improve productivity index by reducing skin damage.	Increased initial oil production, 1.5 to 1.8 times more oil with lower water cut than comparative wells; zero damage to formation recorded; real-time assessment, characterisation, and evaluation of formation; real-time production and completion performed in underbalance condition; and project executed within the scheduled time frame and cost.
Miszewski et al. (2018)	Appalachian Basin, USA		Nitrogen and produced water	Depleted reservoir having low permeability, susceptible to fines invasion from drilling fluid; avoid formation damage; increase cash flow	Drilling programme revealed two significantly productive fractures; significant understanding of the reservoir's characteristics gained through testing while

Investigator	Field/location	Target formation	Working fluids	Operational justification	Result(s)
		–		from the well by accessing more of the reservoir using a horizontal wellbore to intercept natural fractures and increase production from the well and increase ROP shortening the required drilling time.	drilling and reservoir characterisation programme with modelled results found to be within 8% of the actual measured result; and real-time drilling information informed the decision-making process to reduce the risk of hitting a water zone and shorten the side-track length. Multi-disciplinary approach and drilling engineering models were noted as the reasons for the successful delivery of the drilling programme.
Arliyando et al. (2013)	Field A, Indonesia	Vugular limestone reservoir	Nitrified mud	Highly depleted, low reservoir pressure and high bottomhole temperature.	Delivered maximum productivity improvement; reduction of formation damage; cost-saving; increased ROP; reduced drilling problems.
Shatwan et al. (2011)	Field AA, Libya	XX formation – sandstone reservoir	Nitrogen and native crude oil	Minimising formation damage; improving production rate and enhancing recovery; minimising lost circulation issues, differential pipe sticking and NPT; evaluating and characterising the reservoir while drilling and increasing the ROP.	UBD improved ROP, reduced rig time, and provided reservoir evaluation while drilling. No major problems were encountered during the drilling phase and the 3 wells were drilled and completed successfully.
Fattah et al. (2011)	Belayim, Gulf of Suez, Egypt	Belayim formation – sandstone reservoir	Nitrified mud – nitrogen and diesel	Increase ROP; enhance well control; reduce the occurrence of lost time incidents; and increase well productivity.	ROP was drastically enhanced in sand layers up to 50 m/h, and in anhydrite between 8–10 m/h.
Shadravan et al. (2009)	Parsi, Iran	Asmari formation Limestone reservoir with intercalations of dolomite and clay roasts into shale layers	Nitrogen and native crude	Depleted reservoir pressure; increased possibility of blowouts or damage to the reservoir; to increase reservoir productivity by decreasing formation damage that results from drilling fluid losses.	Well drilled to target total depth; no circulation losses; value-added with early oil production.

Investigator	Field/location	Target formation	Working fluids	Operational justification	Result(s)
Uribeta et al. (Urbieta et al., 2009)	Samaria, Mexico	Carbonate and dolomite reservoir	Nitrogen and oil-based mud	Highly depleted reservoir resulting in loss circulation and differential sticking problems.	UBD technique allowed the build-up and correction of the well trajectory, achieving the proposed targets; higher production rates achieved; and higher ROP resulting from improved hole cleaning coupled with only one-bit run led to shorter time to complete the section.
Safar et al. (2007)	Fidaa, Libya	Facha formation – dolomite reservoir	Nitrified diesel	Severe lost circulation and differential sticking issues; invasion of foreign fluids and cuttings into the reservoir led to formation damage accounting for low production rates.	Enhanced production; no quality, health, safety and environmental (QHSE) incidents reported; and allowed real-time reservoir analysis.
Beltran et al. (2006)	San Joaquin, Venezuela	Merecure formation – sandstone reservoir San Juan formation – sandstone reservoir	Nitrified mineral oil-based mud	Complex reservoir characteristics and natural decrease in virgin pressure; OBD induced significant operational problems and formation damage coupled with recurrent loss circulation issues.	Obtained savings during drilling activity and improved production; faster drilling times (12.36 days compared with 19.94 days with OBD); lost circulation control and reduced formation damage.
Al-Saadi et al. (2006)	Northern Oman Carbonate, Oman	Carbonate reservoir	–	Need for real-time reservoir characterisation; improvement to productivity index through the elimination of skin effect; and improvement in the initial and ultimate recovery.	Absence of skin doubled the productivity index of most wells drilled with oil being produced at a lower drawdown and coning problems significantly reduced; better well placement while drilling and optimised well completion design due to real-time reservoir characterisation; better understanding of reservoir pressure, water production intervals and facies characterisation.
Moore et al. (2004)	Hassi Messaoud, Algeria	Ra formation – sandstone reservoir	Nitrogen and crude oil	Extremely hard, abrasive sandstone, hard to drill.	Better ROP; production while drilling benefits and improved well quality with increased production rates; required less time overall to drill compared to OBD.

Investigator	Field/location	Target formation	Working fluids	Operational justification	Result(s)
		R2 formation – sandstone reservoir Ri formation – sandstone reservoir R3 formation – sandstone reservoir			
Eck-Olsen et al. (2004)	Gullfaks, Norway	Sandstone reservoir	–	Existing pressure control problems due to high pore pressure; environmental considerations, no release of hydrocarbons into the atmosphere or flaring during the operation.	Recovery of substantial additional volumes of oil; extension of the producing life of the field; and no operational failure and HSE incident.
Davison et al. (2004)	Brent, United Kingdom	Brent and Statfjords formations – sandstone reservoirs with interbedded shales	–	Lost circulation problems; depleted reservoir pressure; sub-seismic shales, difficult to detect make infill drilling problematic due to uncertainty in pressure estimation and impact on fracture pressure estimation.	Reached total depth without losses; NPT per well reduced from 302 hours to less than 1 hour; cost per well reduced.
Villasmil et al. (2003)	Lake Maracaibo (Tia Juana, Lagunillas and Bachaquero areas), Venezuela	LL-05 formation (Tia Juana Area) – sandstone reservoir B-6-X formation (Tia Juana Area) – sandstone reservoir Bachaquero-01 formation (Lagunillas	–	Significantly depleted reservoir with drilling issues relating to hole instability, loss circulation and extensive formation damage.	58.7% reduction in drilling times; reduced investment drilling cost by 3.6%; increased production by 4%; lowered drilling investment cost per barrel by 12%; and NPT reduced to 2.6% from 24.1%.

Investigator	Field/location	Target formation	Working fluids	Operational justification	Result(s)
		Area) – sandstone reservoir Bach-02 formation (Bachaquero Area) – sandstone reservoir			
Eissa and Al-Harthi (2003)	Nimr and Saih Rawl, Oman	Carbonate reservoirs	–	Reservoir impairment due to high levels of overbalance; high water cut.	Significant productivity improvements due to no skin damage or mud filter cake over wellbore; valuable reservoir data has been gathered during the drilling operations; drilling performance improvements; identification of unsealed fractures and their connectivity to water sources quickly proved, allowing for timely water shutoff.
Cunha et al. (2001)	Estreito, Brazil	Sandstone reservoir	Nitrified mud – nitrogen and water base drilling fluid	Depleted production zones; demonstrate the technical and economic feasibility of the UBD method to increase oil production; field-test new equipment and operational procedures.	UBD found to be a feasible technique even in an unconsolidated formation; preliminary results show an increase in well productivity compared to conventionally drilled wells.

It is expected that a well drilled underbalanced will lead to significantly reduced formation damage, but the implementation of inappropriate operational techniques or poor BHP management can result in periods of overbalance which may lead to severe formation damage. In some cases, an overbalance event could permanently impair production from a well by as much as 75% (Pérez-Téllez et al., 2004). Also, if the screening method for selecting the appropriate candidate reservoir for UBD operations is not correctly applied (e.g., over pressurised shale and highly tectonic stress areas), the probability of the UBD operation failing is high due to wellbore stability and proper BHP management issues.

Table 2.8 presents field case studies which have faced operational challenges during UBD operations. These UBD programmes experienced issues relating to (i) downhole equipment failure due to high temperature (Fattah et al., 2011), (ii) logistical issues with injection gas (Vonthethoff et al., 2009), (iii) environmental release of highly toxic gas (H_2S vented to the atmosphere) (Muqeem et al., 2008), (iv) BHP fluctuations (due to bumping of drillstring float to establish the accurate standpipe pressure) (Muqeem et al., 2008), (v) steering problems (Veeken et al., 2007), (vi) longer drilling times and significantly reduced ROPs (Hoekstra et al., 2000), and (vii) economic losses due to formation damage (Kimery and McCaffrey, 2004; Kimery and Van Der Werken, 2004).

Some reasons for the challenges encountered include: (i) absence of highly productive natural fractures resulted in no significant productivity gains for the UBD offshore programme (Veeken et al., 2007), (ii) inappropriate candidate reservoir selection for UBHD, (iii) comparatively hydraulic fracturing, operationally and economically more competitive than as-drilled horizontal well design (iv) poor

BHP management and inefficient hole cleaning resulting in various instances of BHP exceeding the pore pressure (Kimery and Van Der Werken, 2004).

Although the UBD projects discussed in Table 2.8 encountered different operational challenges, some projects still managed to achieve various key performance indicators, including (i) maximum sustainable capacity (MSC) target by adding 5,000 BOPD to gas-oil separation plants (GOSP) (Muqeem et al., 2008), (ii) four of five wells produced with increased rates (Vonthethoff et al., 2009), (iii) successful development and application of a new technique for installing solids control in an underbalance condition (Veeken et al., 2007), and (iv) drilling an underbalance, ultra-slim well on coiled tubing up to a world-record horizontal length of 1457 m (Hoekstra et al., 2000).

Table 2.8 Field case studies of operational challenges during underbalanced drilling operations

Investigator	Field/location	Formation	Working fluids	Operational justification	Operational challenge(s)
Fattah et al. (2011)	Western desert, Egypt	Mesozoic Lower Safa – sandstone reservoir	Water and nitrogen	Prevent reservoir damage	After drilling 200 m of drilling, operations had to be stopped due to failure of downhole equipment by high temperature.
Vonthethoff et al. (2009)	Moomba, Australia	Late Permain T and Early Permain D formations – sandstone reservoir	Mist – nitrogen and KCl brine	Achieve a zero-skin wellbore and lower the abandonment pressure to potentially add incremental reserves.	Technical challenges encountered as a result of high-pressure depletion (reservoir pressures in the range of 600 psia from an initial pressure of 3400 psia), complex geology of the reservoir (interbedded sands, shales and coals), hostile drilling environment (high bottomhole temperature) and remote location (BHA and surface separation package logistical issues). Four of the five wells drilled, produced with increased rates. The variance in well results demonstrated that well location was a key element to project success. Identified areas for improvement were 1) BHA reliability due to downtime associated with electrical components of the BHA, attributed to the harsh (high downhole temperature) drilling environment, 2) motor and bit reliability due to the lack of fluid associated with mist drilling, there were heat and erosion related failures of the PDM motors and bits and 3) issues relating to the delivery of nitrogen as a result of close drilling times of wells and wet weather delays which highlighted the need for more storage of nitrogen to be available closer to well sites.
Muqeem et al. (2008)	Ghawar, Saudi Arabia	Arab D formation – carbonate reservoir	Diesel/native crude oil	Demonstrate that a closed/semi-closed system can be utilised properly and safely to undertake UBD operations. Minimisation of formation damage, fluid losses and reduction of NPT were key well design objectives.	Some of the operational challenges encountered included 1) higher concentrations of H_2S than the chemical programme was designed to handle, 2) gas venting as a result of too many vent points, resulting in the release of gas at various positions when fluid influx volume was highest, 3) bumping of drillstring float to establish the accurate standpipe pressure led to pressure spikes, and 4)

Investigator	Field/location	Formation	Working fluids	Operational justification	Operational challenge(s)
					failure of mechanically operated isolation valve (twice). Despite these challenges, key performance indicators were achieved, 1) oil producer lateral drilled underbalance to the targeted zones, 2) improved ROP, and 3) achieved the MSC target.
Veeken et al (2007)	Southern North Sea, Netherlands	Rotliegend formation – sandstone reservoir	Potassium carbonate, potassium formate brine and oil-based fluid with a $CaBr_2$ brine	Boost well capacity and increase ultimate recovery of tight gas wells.	Poor well performance was attributed to various factors including, 1) significant washouts of the openhole which compromised the perforation performance which triggered surface equipment erosion problems and early total depth (TD), 2) requirement to maintain underbalance conditions complicated the running of sand screens and contributed to the screen installation failure, 3) foaming issues at surface prevented the target drain-hole length not being achieved, and 4) steering problems. Highly productive natural fractures were key to the success of the UBD offshore programme but were not encountered and the productivity improvement factor (PIF) associated with the reduction of drilling fluid impairment remained difficult to quantify. Successfully developed and applied a new technique for installing solids control underbalanced.
Kimery and McCaffrey (2004)	Ansell and Chickadee, Canada	Cardium formation (Ansell field) – fine-grained marine sandstone reservoir Gethind D Pool (Chickadee field) –	–	*Ansell field:* Suffered from stuck drillstring issues and downhole and surface equipment problems necessitating side-tracking of some of the wells. *Chickadee field:* Complex geology (heterogeneous, fluvial-incised valley fill deposit).	*Ansell field:* Vertical wells initial production was 27% higher than UBHD wells. Production forecast predicted recovery from the vertical wells to be approximately 37% more gas within a 10-yr period. Analysis indicates that the conventional wells are better performers than the UBHD wells. Possible reasons for failure are 1) the Ansell region is not an appropriate candidate for UBHD due to very low-low in-situ permeability (not economically viable), and 2) the UBHD well designs not competitive with hydraulic fracturing and were not optimally designed to minimise formation damage.

Investigator	Field/location	Formation	Working fluids	Operational justification	Operational challenge(s)
		sandstone reservoir			*Chickadee field:* Vertical wells initial production was 44% higher than UBHD wells. Projected recovery from the vertical wells is approximately 22% more gas within a 10-yr period. Analysing the UBD operational data reveals that the programme had a negative effect on ultimate productivity. Poor BHP transient management and inefficient hole cleaning yielded several instances of the BHP exceeding the pore pressure adjacent to the wellbore, leading to formation damage.
Kimery and van der Werken (2004)	North-eastern, British Columbia, Canada	Jean Marie formation – limestone reservoir with intercrystalli ne/intergran ular dolomites and calcarebties	–	Depleted, low permeability, fractured carbonate with low initial water saturation making it susceptible to formation damage using conventional drilling fluids.	*Case study 1:* Underbalanced lateral that was severely damaged resulting in 75% reduction in productivity index (PI). Economic analyses performed on production forecast to abandonment for the as drilled and the theoretical undamaged horizontal scenarios predicted that an undamaged well will recover approximately 1.5% more gas and realise an 11.5% improvement in net present value (NPV). An internal rate of return (IRR) by 300% for the undamaged horizontal is expected. *Case study 2:* The second case study concerns a horizontal well that incurred damage in the early stages of the underbalanced lateral. The PI curve indicates a 38% reduction in productivity. Economic analyses performed on production forecasts to abandonment for the as drilled and undamaged well scenarios predicted that the undamaged well will recover 0.8% more gas than the damaged well and that the NPV is increased by 14%. The IRR is significantly higher for the undamaged lateral, increasing from 86% to 120%. It was concluded that inappropriate operational techniques or poor BHP management can lead to overbalance events. These overbalance events can be severely damaging, often reducing well productivity. Traditional pressure transient analysis in very heterogeneous or fractured reservoirs often cannot give any indication of the extent or impact

Investigator	Field/location	Formation	Working fluids	Operational justification	Operational challenge(s)
					of this damage. Using transient PI data collected while drilling, the damaging events can be easily identified and the magnitude of the impact of the damage can be determined.
Hoekstra et al. (2000)	Yibal, Oman	Carbonate reservoir	Native crude oil, dehydration water (DHW)	Minimisation of high water cut and drilling of side-tracks and extensions from existing wells to improve hydrocarbon recovery.	Technical challenges encountered during the UBD coiled tubing operations included: 1) identified targets were inaccessible from near-by wells which increased the required reach to beyond the typical ultra-slim hole (USH) side-track length, 2) non-soluble friction reduction agent dispersed in the water-based mud led to several surface problems in the tank system due to the formation of emulsions, 3) some drilling sections took longer than planned with significantly slower ROPs in the range of 2 to 10 m/hr as opposed to 40 to 50 m/hr experienced on previous wells, and 4) during the initial stages of some side-tracks, significant water production was encountered, requiring further supplies of crude by road, with the drilling continuing with DHW. Despite these challenges, underbalance, ultra-slim wells were drilled on coiled tubing up to a world-record horizontal length of 1457 m which was a technical achievement that pushed the technological boundaries associated with coiled tubing drilling. It was recommended that to fully realise the benefits of the underbalance system, the wells should be lined and cemented without treating the loss zones.

2.9 Key research elements

The key research elements based upon the identified technological gaps are outlined in Figure 2.10.

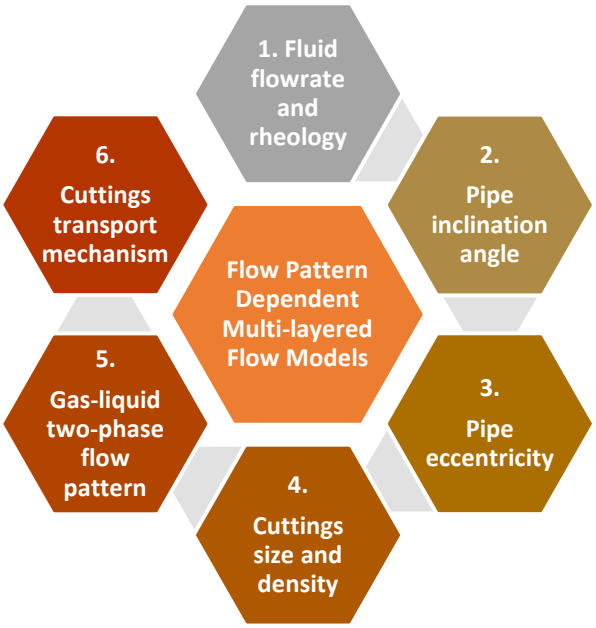

Figure 2.10 Key research elements

Each research element identified has been shown to be a key operational issue associated with current multiphase flow models that facilitate UBD operations, critical to achieving a stable unbalanced condition downhole.

2.10 Summary

Relationships are not available that consider the combined interactions of non-Newtonian gas-liquid two-phase fluids, fluid flowrates, pipe eccentricity, hole inclination angle and cuttings transport mechanisms. Thus, the technical challenges which face the application of UBD in various oil reservoirs are:

1. Phenomenological behaviour of Newtonian and non-Newtonian gas-liquid two-phase flow in horizontal and inclined, concentric and eccentric annuli, uncertainties in the flow behaviour characteristics;

2. Cuttings transport mechanisms which facilitate effective hole cleaning; and
3. Effect of the gas-liquid two-phase fluid flow pattern and cuttings transport mechanisms on wellbore hydraulics and cuttings transport efficiency.

To help overcome the outlined challenges, experimental tests and theoretical modelling will be performed to develop a strategy for UBD hydraulics and cuttings transport efficiency for various reservoirs application. To accomplish this, a unique experimental rig will be designed and fabricated to provide information on the cuttings transport mechanisms found in Newtonian and non-Newtonian gas-liquid two-phase flow in horizontal and inclined, concentric and eccentric annuli and to gather reliable annuli pressure gradient and stationery bed height data. The experimental setup will allow for a detailed parametric study and generation of dataset(s) for theoretical model development.

The hydrodynamic processes governing the gas-liquid two-phase with and without solid particles flow will be explored to:

1. Understand the Newtonian and non-Newtonian gas-liquid two-phase flow and cuttings interaction in the gas-liquid UBD flow system given the associated effects of operating and geometric conditions;
2. Gather reliable data from controlled experimental tests and use for theoretical model testing and validation; and
3. Validate some of the experimental and theoretical conclusions made by previous studies related to multiphase flow and cuttings transport mechanisms and to extend the body of work in this area.

This chapter presented a review of the literature. Three main research areas focusing on multiphase flow modelling and cuttings transport have emerged as requiring research attention and, on this basis, several methods and models

have been identified, evaluated, and interlinked to form the overarching conceptual and methodological framework for investigating the research problem.

The technological framework for implementing successful UBD operations in oil and gas reservoirs which meets the wellbore stability criteria has been outlined. The groundwork for setting up the design considerations and operational parameters critical to maintaining the underbalance condition has been explored. Evaluation of the reservoir and well dynamics variables used to improve the BHP control mechanism of the complex multiphase flow within the wellbore annulus have been delineated. These considerations will ensure that the underbalance pressure window is maintained during the entire UBD operation and that the desired benefits whether reservoir, drilling or a combination of both will be derived. Figure 2.11 illustrates the structure of the Alpha UBD strategy outlining the considerations discussed in this section.

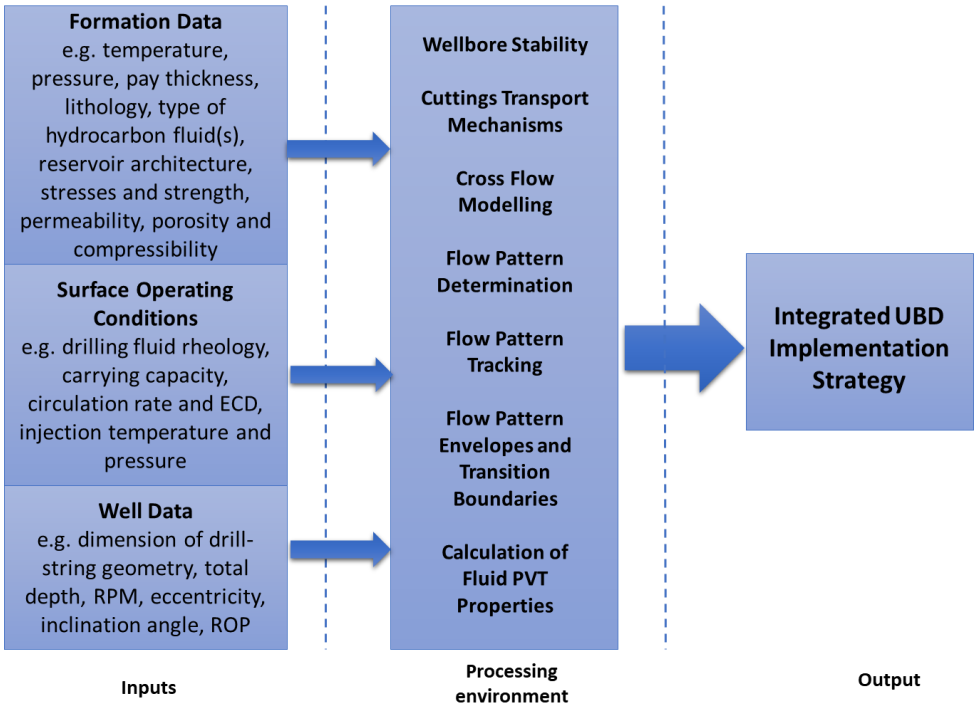

Figure 2.11 Alpha underbalanced drilling strategy

The research questions, objectives and contributions addressed and/or made in Chapter 2 are summarised in Table 2.9. Chapter 3 will discuss the methodology for data generation and analysis.

Table 2.9 Research objectives, and outputs addressed and/or made in Chapter 2

AIM	OBJECTIVES	METHODS	OUTPUT(S)
To develop a rigorous integrated strategy for maximising the efficiency of UBD for the transport of cuttings in gas-liquid two-phase flow through wellbore annuli	RO1: To update the theoretical and practical UBD knowledge base through consolidation of the technical issues relating to UBD operations	Literature review of over 130 papers which focused on: 1) the factors affecting multiphase flow during UBD operations, and 2) the influence of reservoir/formation properties on UBD operations	Objective analysis of the body of work on UBD and the identification of open challenges and research gaps in its technological advancement
	RO2: To aggregate and synthesise the most critical technical issues relating to UBD field operations promoting operational success and/or failure, as well as the mitigation action	Best-evidence review of field case studies on the operational phases of 25 past global UBD implementations – 18 successful and 7 which were operationally challenged	Synthesis of the technical issues encapsulating the operational method of UBD coupled with the field case study findings – assessing the operational phase and associated outcomes from 25 global underbalanced drilling field case studies – 18 successful and 7 which were operationally challenged.

Chapter 3 : Methodology

3.1 Introduction

This chapter presents the research methodology employed within this study to answer the study's research questions and achieve the research objectives outlined in Chapter 1. More specifically, it describes the multistage, mixed method strategy anchored within a multi-disciplinary conceptual framework for UBD applications. This section introduces the chapter. Section 3.2 presents a discussion of the research methodology and methods. Sections 3.3 to 3.5 describes the different research stages and elements applied in this research programme. Section 3.6 summarises the chapter.

3.2 Research methodology and methods

The research programme is characterised by a series of distinct yet inter-related research stages and elements that address the study's aim, and six research objectives outlined in Chapter 1 (Figure 3.1).

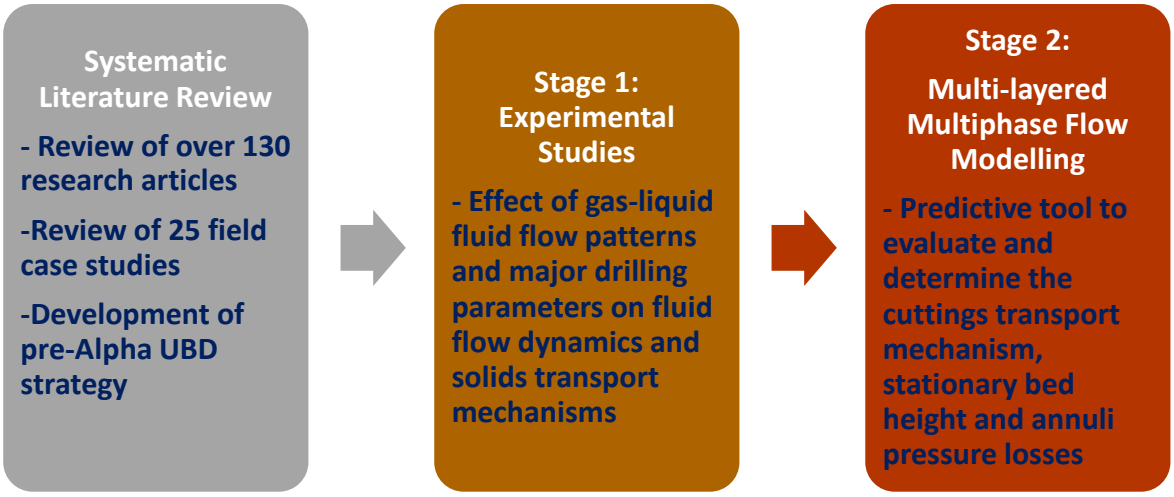

Figure 3.1 Stages and elements of research programme

Stage 1 is characterised by the experimental work programme. In this stage, experimental tests were performed using the multiphase flow loop rig at the Robert Gordon University (RGU) with the purpose of experimentally investigating the effect of Newtonian and non-Newtonian gas-liquid two-phase and major operational drilling parameters on UBD hydraulics and cuttings transport mechanisms in horizontal and inclined, concentric and eccentric annuli. These experimental tests were used for qualitative and quantitative evaluation of the fluid-particle dynamics (fluid forces, gas-liquid two-phase flow patterns and particle transport mechanisms) for flow in wellbore annuli (see Chapter 4). The experimental unit is capable of real-time data acquisition and allows for the visualisation and recording of the nature and structure of different gas-liquid two-phase flow patterns and particle transport mechanisms. In Stage 2, a new theoretical approach proposed by Salubi et al. (2022) for use in UBD operations which applies a flow pattern dependent multi-layered flow modelling technique was applied. These models can predict the cuttings transport mechanism, calculate the stationary bed height, and compute the annuli pressure losses along with other relevant information for Newtonian and non-Newtonian gas-liquid two-phase fluids for any level of eccentricity and horizontal and inclined annuli (see Chapter 5).

3.3 Stage 1: Experimental methodology

During UBD operations, the flow of the drilling fluid content in the wellbore annulus is accompanied by cuttings making the nature of the gas-liquid two-phase flow and cuttings transport mechanism a complex and transient flow problem. It involves different phenomenological and hydrodynamics behaviours which are influenced by all aspects of the design and construction of the underbalance well with reservoir uncertainty being the primary culprit to flow

modelling problems. To date, relationships are not available in published literature which consider the combined effect of fluid flow patterns for non-Newtonian fluid flow behaviour and the major operational drilling parameters which involves different cutting transport mechanisms, either theoretically or experimentally. This study aims to experimentally investigate the phenomenological and hydrodynamics behaviour of this complex multiphase flow scenario with solid particles using a multiphase flow loop experimental rig to simulate horizontal and inclined, concentric and eccentric wellbore annuli.

Specifically, an experimental approach was chosen to allow for the visualisations and determination of the experimental parameters which influenced the variations in fluid flow structures and cuttings transport mechanism which are important to the developmental design and application of the fit-for-purpose flow pattern dependent multi-layered mathematical models. The gas-liquid two-phase fluid flow pattern and solids transport mechanisms are influenced by a complexity of factors, which makes it difficult to theoretically analyse without a visual interpretation of the flow dynamics at work.

3.3.1 Multiphase flow loop experimental rig

The RGU multiphase flow loop facility was designed and constructed as a laboratory testing facility to simulate horizontal and inclined, concentric and eccentric wellbore annuli with the effect of inner pipe rotation being considered. The new experimental rig allows measurements and visual observations of the gas-liquid two-phase fluid flow with and without solid particles. Figure 3.2 provides a schematic diagram of the experimental unit setup.

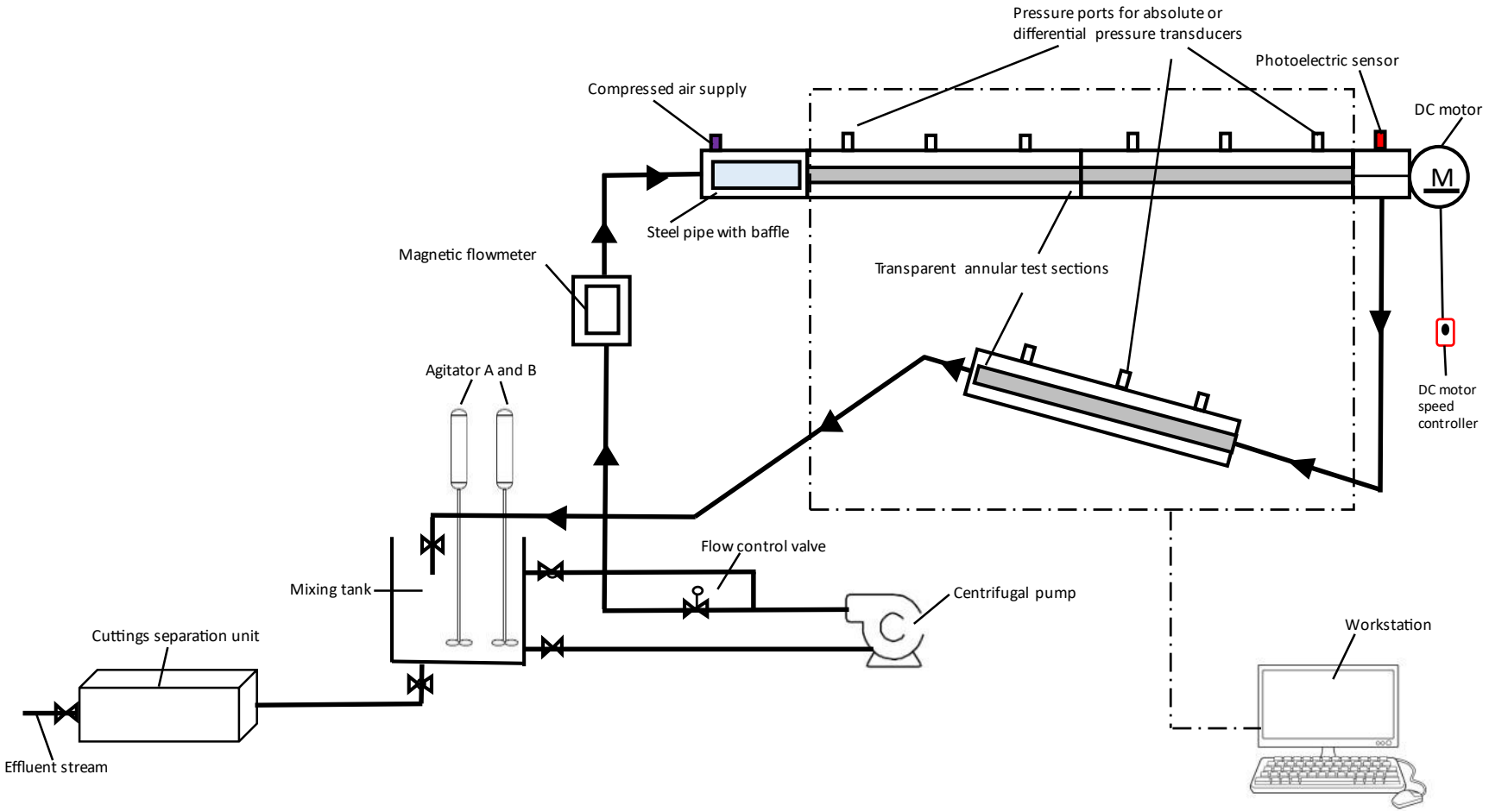

Figure 3.2 Schematic diagram of the experimental unit setup

The experimental unit includes an upper horizontal 4 m annular test section and lower 2 m test section which can be elevated to inclination angles between 10^0 to 30^o. These test sections have an outer pipe ID of 0.144 m and inner pipe OD is 0.088 m. The fluids used in experimental tests were water or polymer (xanthan gum solution) as the liquid phase and air as the gas phase. Solid particles were added to liquid phase for particle transport experiments. The experimental unit was designed to implement flow control using a pump speed controller and gas regulator, making it possible to perform investigations on the phenomenological behaviour of multiphase flow with and without solid particle transport. Clear acrylic annular test sections permitted visualisation, recognition and capturing of different fluid flow patterns and cuttings transport mechanisms as the operating conditions in the flow loop were changed.

Multiphase flow loop experimental rig setup

The multiphase flow loop experimental rig was used to conduct a series of experimental test involving single- and two-phase Newtonian and non-Newtonian fluid flow with and without solid particles under controlled experimental conditions. Figure 3.3 shows a photo of the experimental unit setup used for all experimental tests.

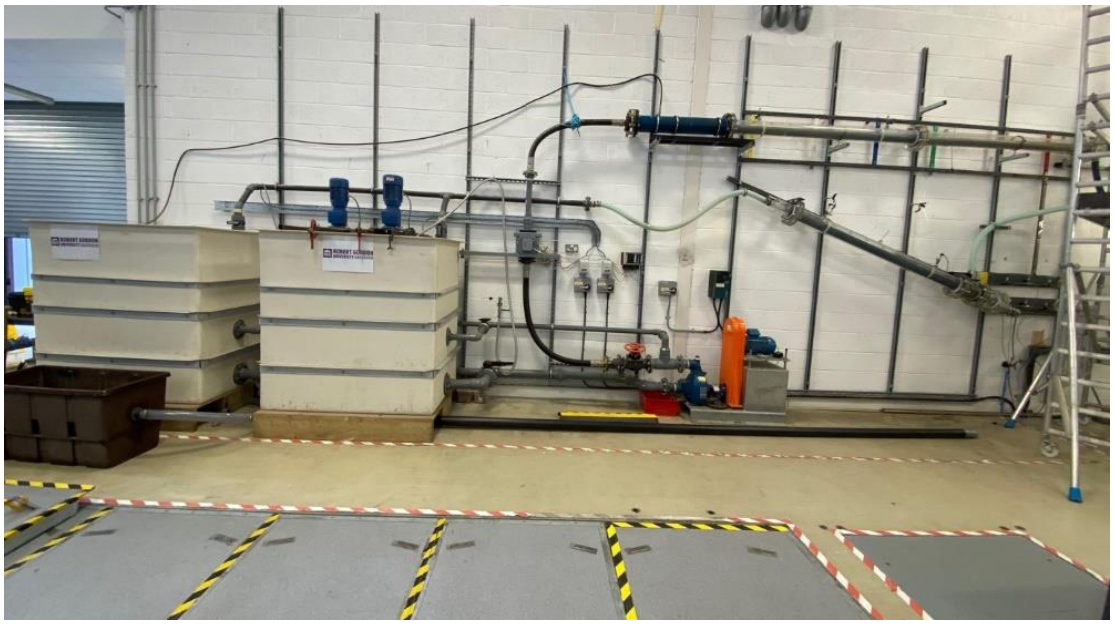

Figure 3.3 Photo of the experimental unit setup

The experimental unit consisted of several major pieces of equipment. Figure 3.4 to Figure 3.11 detail the major components of the experimental unit.

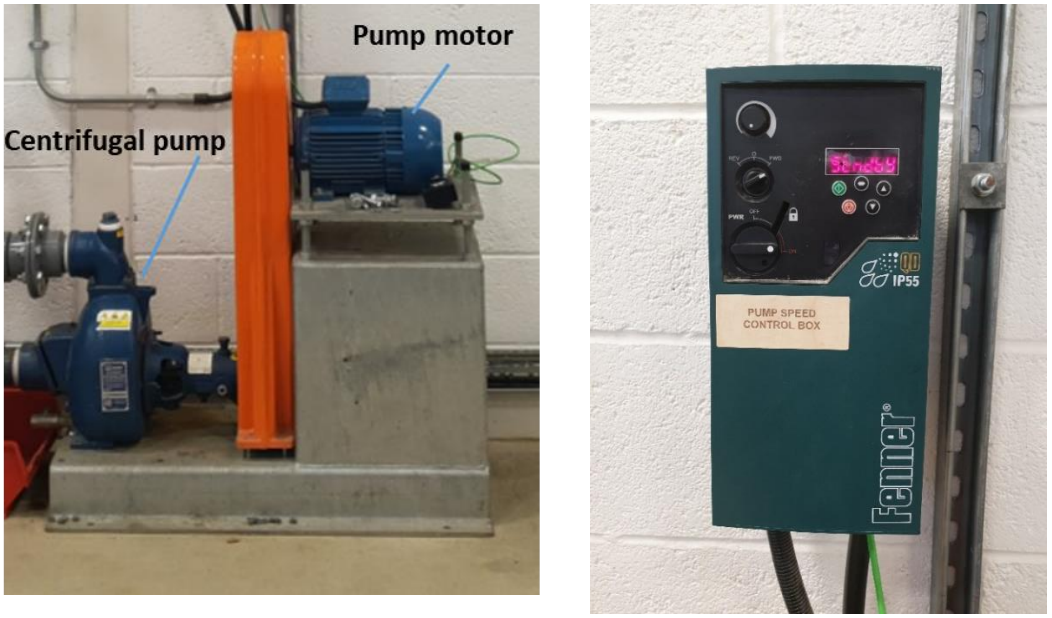

(a) (b)

Figure 3.4 Photo of (a) self-priming centrifugal pump and pump motor and (b) frequency inverter

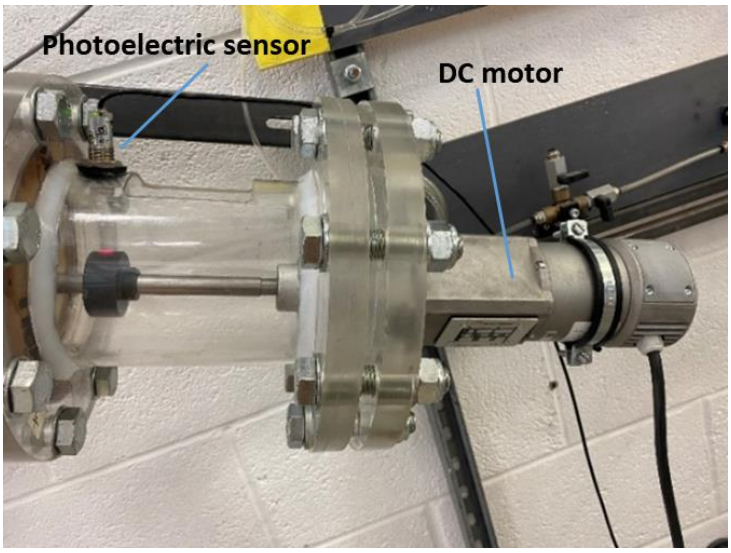

(a)

(b)

Figure 3.5 Photo of (a) DC motor and (b) DC motor speed controller

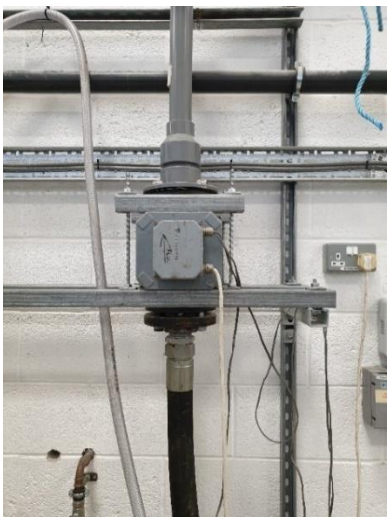

(a)

(b)

Figure 3.6 Photo of (a) magnetic volumetric flowmeter and (b) flowrate indicator

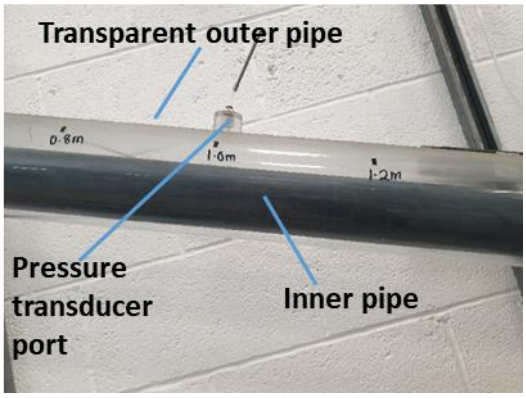

Figure 3.7 Photo example of an inclined eccentric annulus test section

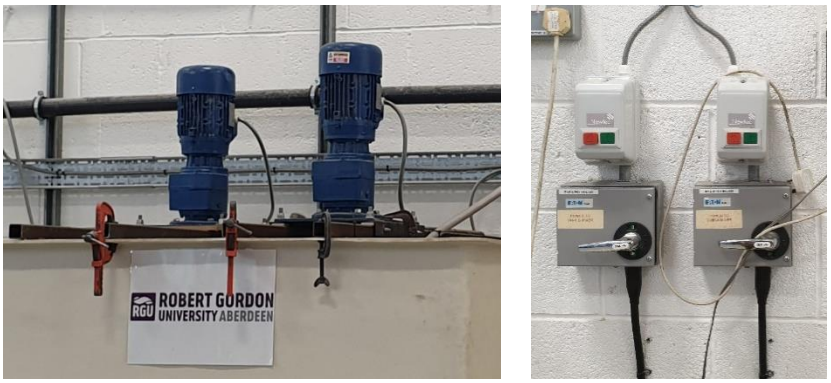

(a) (b)

Figure 3.8 Photo of (a) mechanical agitators and (b) power supply for mechanical agitator

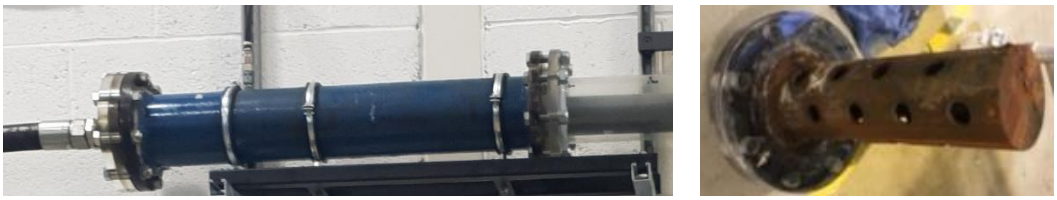

(a) (b)

Figure 3.9 Photo of (a) accumulator, steel pipe with baffle inside (b) baffle

Figure 3.10 Photo of the air flowrate regulator

Figure 3.11 Photo of solids separation tank with the solid particles which have sifferent sizes and densities

Experimental tests were conducted in horizontal and inclined, concentric and eccentric wellbore annuli using Newtonian and non-Newtonian fluids, with and without inner pipe rotation. Table 3.1 presents the operational ranges of the test conditions used in the multiphase flow loop are presented in.

Table 3.1 Operational ranges for multiphase flow loop experiments

Parameters	**Value Range**
Inclination angle	0 to 30^0
Eccentricity	0 and 0.7
Rotation	0 to 150 rpm
Air flowrate	0 to 28 m^3/hr
Liquid flowrate	0 to 35 m^3/hr

3.3.2 Experimental tests materials

To simulate gas-liquid two-phase flow in annuli, water and 0.1% xanthan gum polymer solutions were used to represent the liquid phase in the gas-liquid mixture. Figure 3.12 shows the chemical structure of xanthan gum used which had a purity of 98%.

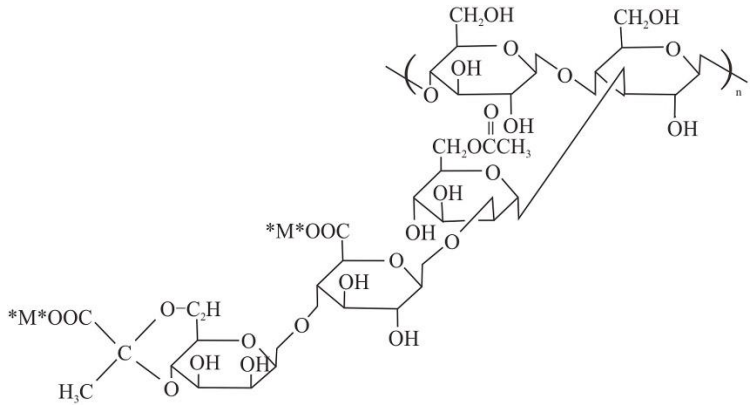

Figure 3.12 Structure of xanthan gum (Firozjaii & Hamid, 2019)

The polymer solutions were prepared by slowly adding the xanthan powder to distilled water at a temperature of about 35 ^{0}C and thereafter thoroughly mixed to ensure that a homogeneous solution is formed and to prevent "fish-eyes" during the mixing process. After an adequate hydration period, shear stress-shear rate measurements were obtained using a 12-speed fann 35SA viscometer at a temperature of about 22 ^{0}C. Figure 3.13 shows the shear stress and viscosity flow curves of the polymer solution. Appendix C presents the fluid properties measurement procedure.

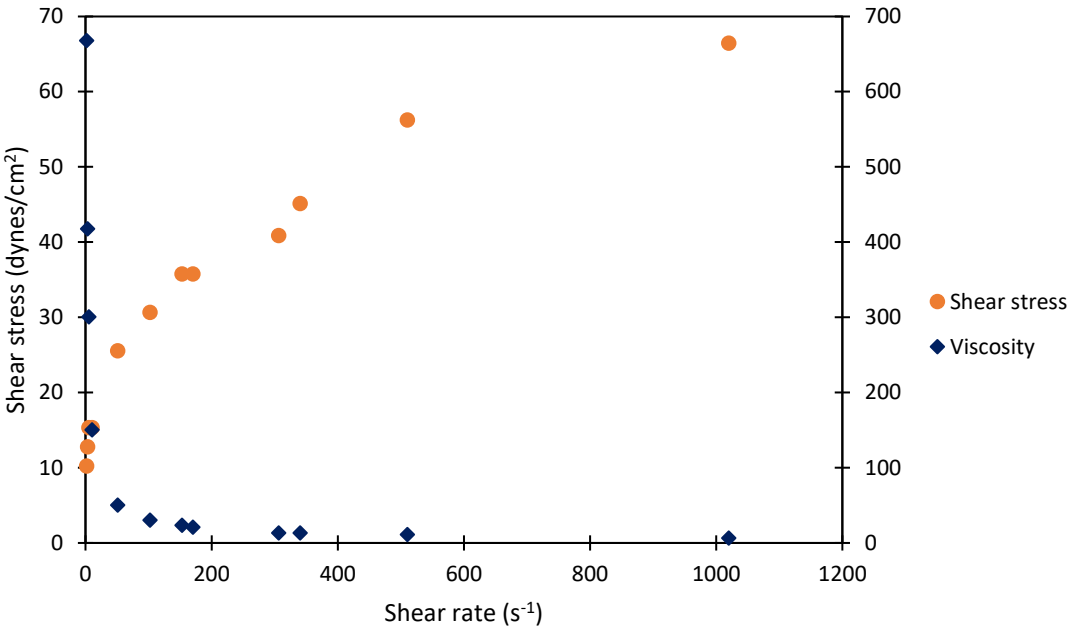

Figure 3.13 Shear stress and viscosity flow curves of polymer solution used in experimental tests (complete dataset in Appendix D)

Using nonlinear regression on the rheological data, the polymer solution was found to best characterise the Herschel Bulkley rheological model with its rheological parameters being $K' = 0.094$, $n' = 0.68$, and $\tau_o = 0.001$.

In this research study, glass and plastic bead particles (Figure 3.14) were used to represent cuttings in an effort to analyse and evaluate the cuttings transport efficiency in Newtonian and non-Newtonian gas-liquid two-flow in horizontal and inclined, concentric and eccentric annuli.

Figure 3.14 Photo of the different solid particles used in flow experiments

Each type of solid particle had a specific size and colour which enhanced visualisation of the cuttings transport mechanism at play for the various experimental tests performed. Glass and plastic beads were used in experimental tests as they are inert and do not react with the liquid phase (water or polymer) and can also be reused within the system. Table 3.2 provides the details of each particle type used in experimental test with the solid particles having a size range of 1.25 to 4.0 mm and a density range of 900 to 2000 kg/m^3.

Table 3.2 Solid particles used in experimental tests

Particle type	Colour	Size, mm	Density, kg/m^3
1	White	1.25	900
2	Transparent	2.00	950
3	Red	4.00	1000
4	Blue	1.65	1500
5	Green	2.40	2000

3.3.3 Measurement strategy and error

The steel pipe (approximately 1.5 m in length) is an accumulator which contains a baffle to provide better fluid flow distribution and minimise perturbation ensuring that the fluid flow (or gas-liquid flow pattern) is fully developed. Thus, it helps to avoid entrance effects on the downstream pressure measurements.

An electromagnetic flowmeter is used to measure the liquid flowrate (water or polymer solution) and is located upstream of the test section. It measure the liquid flowrate out of the centrifugal pump before it enters the annuli test section. The outlet of the air flowrate regulator is used to keep the pressure of the compressed air at a constant level before entering the test section.

The pressure measurements are taken from the specially designed ports on each test section with there being six (6) absolute and three (3) differential pressure

transducers available to measure frictional pressure losses and the average pressure inside the loop at given test points. Each test section is capable of have a maximum of three (3) absolute pressure transducers or one (1) differential transducer and one (1) absolute transducer. These pressure transmitters are supposed to indicate the system pressure for either single- or two-phase (air-water or air-polymer mixtures) at different locations along the test section. The differential pressure is measured between the first and the third, pressure tapping of each test section.

The instrumentation measurement errors associated with the multiphase flow loop are summarised in Table 3.3.

Table 3.3 Measurement errors

Measured parameter	**Measurement error**	**Instrument**
Absolute and differential pressure	Absolute accuracy: ±0.25% FS BSL (linearity, hysteresis, and repeatability) Differential accuracy: +/- 0.40% FS BSL (linearity, hysteresis, and repeatability)	Omega pressure transducers
Rotary speed	Max. sensing range = 1 mm	Sick photoelectric sensor
Liquid flowrate	Accuracy ± 0.15 %	Bopp & Reuther magnetic volumetric flowmeter
Air flowrate	Max. pressure hysteresis = 0.25 bar	Festo pneumatic air regulator

*FS BSL= Full scale best straight line

3.3.4 Experimental rig calibration

To establish the accuracy of the results obtained from the multiphase flow loop experimental rig, annuli differential pressure (see Appendix A for the calibration procedure of the pressure transducers used in experimental tests) readings were recorded for experimental tests involving the single-phase flow of water without inner pipe rotation. Experimental results were then compared to the

predicted results using the models suggested Caetano et. al (1992b) (Figure 3.15). A reasonably good match was observed with an average error of 5.5%.

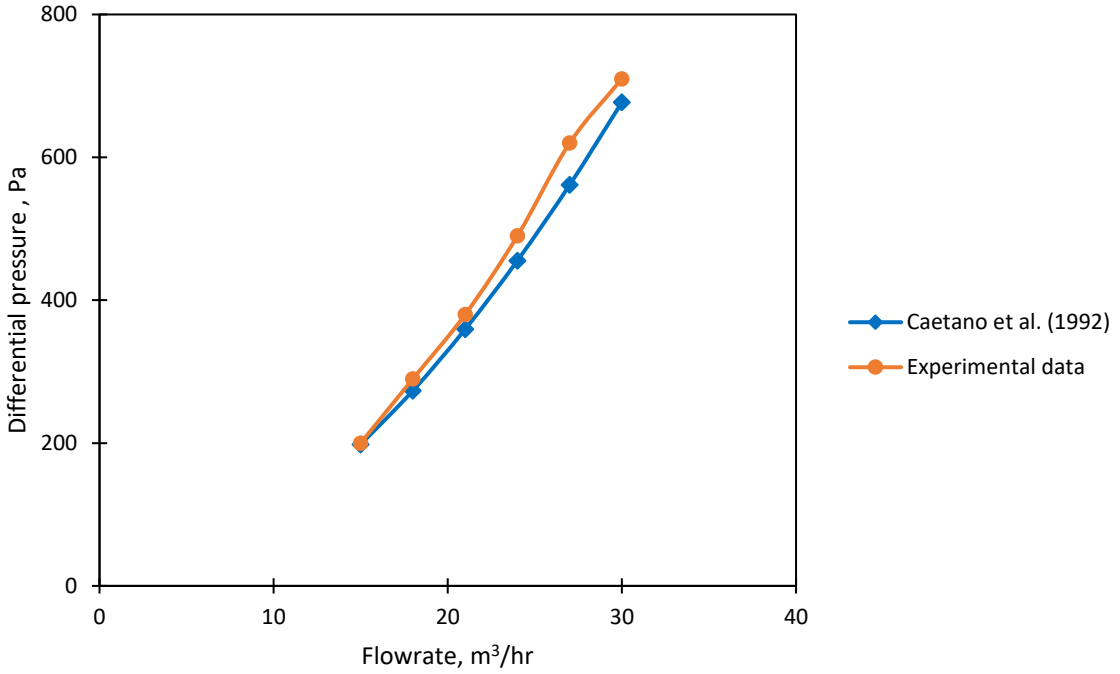

Figure 3.15 Comparison of the differential pressure obtained from the experimental rig to that which is calculated using the model suggested by Caetano et al. (1992b)

After confirming the accuracy of the experimental rig, experimental tests were performed in horizontal and inclined, concentric and eccentric annuli using water, polymer, air-water, and air-polymer, with and without inner pipe rotation.

3.3.5 Multiphase flow loop experimental procedure

The mixing tank A was filled with the desired liquid type (water or polymer solution) to the specified liquid level. For experimental tests involving solid particles, the desired concentration of solid particles were added to the mixing tank and the mechanical agitators were powered on to provide a homogeneous mixture. For experimental tests involving single-phase fluid flow, the centrifugal pump was powered on and set to the desired flowrate using the pump speed controller. For experimental tests involving gas-liquid two-phase flow, air was

introduced into the system using the air flowrate regulator, to the desired air flowrate. Annuli differential pressure data was logged using the data acquisition system (see Appendix B for the block diagram of the LabVIEW program used for all experimental tests), while the gas-liquid two-phase flow pattern, and the particle transport mechanism were observed through the transparent annuli test sections and were captured with a high-definition video camera, for the different operational conditions with and without inner pipe rotation. The rotary speed was then increased using the DC motor speed controller for 60, 90, 120 and 150 rpm. After completing the experimental tests, the valve to the solid separations tank was opened to retrieve and recycle the particles. All steps were repeated for single-phase and two-phase flow experiments at different air and liquid flowrates, inclination angles and pipe eccentricities. All data logged were saved with each experiment repeated to ensure repeatability.

Table 3.4 shows the test matrix based on the operational range (minimum and maximum capacities) of the air and liquid supply and the limits set by the construction of the rig (in terms of health and safety and also vibration minimisation during the operation of the multiphase flow loop).

Table 3.4 Test matrix

Liquid flowrate (m^3/hr)	**Air flowrate (m^3/hr)**	**RPM**	**Hole inclination angle (degrees)**
15	0, 1, 2, 3, 4, 5 and 6	0, 60, 90, 120 and 150	0, 10, 20 and 30
20	0, 1, 2, 3, 4, 5 and 6	0, 60, 90, 120 and 150	0, 10, 20 and 30
25	0, 1, 2, 3, 4, 5 and 6	0, 60, 90, 120 and 150	0, 10, 20 and 30
30	0, 1, 2, 3, 4, 5 and 6	0, 60, 90, 120 and 150	0, 10, 20 and 30
35	0, 1, 2, 3, 4, 5 and 6	0, 60, 90, 120 and 150	0, 10, 20 and 30

3.3.6 Experimental limitations

The research has methodological limits which affects the overall extent to which the components of the Alpha UBD strategy presented in Chapter 2 could be tested through experimental or numerical methods. While the literature identified several integral inputs to the Alpha UBD strategy, due to time and resource limitations, only the relationship between the gas-liquid two-phase flow patterns and the major operational drilling parameters (e.g., gas and liquid flowrates, fluid rheology, inner pipe rotation, pipe inclination angle, pipe eccentricity and solid particle size and density) and their influence and interaction on the fluid flow dynamics and solids transport mechanisms in horizontal and inclined annuli were tested. However, the nature and extent of these relationships are to-date, an important open knowledge gap in literature (Oyeneyin, 2015; Epelle and Gerogiorgis, 2020), making this study's quantification of the above aspects critical. Other limitations to this research study due to time and/or resource constraints are described below:

1. All experiments were conducted under ambient laboratory conditions (22 ^{0}C). Therefore, the complex effect of fluid temperature variations along the wellbore annulus on annular pressure losses was not investigated as part of this study;
2. Due to resource limitations encountered during the experimental research programme, certain areas of the experimental programme, particularly in relation to non-Newtonian fluid flow in eccentric annuli were curtailed impacting the nature of the results originally envisaged;
3. As a result of operational complexities in reconfiguring the multiphase flow loop, only one level of eccentricity was investigated;

4. The gas and liquid flowrates were restricted to 0 to 28 m^3/hr and 0 to 35 m^3/hr respectively, limiting the operational window of the experimental programme and the variation in the observed gas-liquid two-phase flow patterns; and
5. All the solid particles used in experimental tests were spherical in shape. As such, the effect of particle shape was not investigated and its effect on cuttings transport remains unknown.

3.4 Stage 2: Theoretical approach: Multiphase flow modelling

A theoretical approach was used to determine the annuli pressure losses and to evaluate the cuttings transport efficiency, incorporating the multiphase phenomenological physics involved in the wellbore annulus of UBD operations. The theoretical approach is validated with experimental results and can be used as a predictive tool to investigate the mechanism behind Newtonian and non-Newtonian flow with and without cuttings transport within the UBD wellbore annuli. As a result, flow pattern dependent multi-layered models applicable for any level of pipe eccentricity were used for the different cuttings transport mechanisms existing in the different fluid flow patterns (dispersed bubble, bubble and slug), providing a unique method to evaluate cuttings transport efficiency and wellbore hydraulics performance for UBD operations.

The mathematical model takes into consideration the multiphase gas-liquid two-phase flow pattern and the cuttings transport mechanism. The mass, momentum and energy conservation equations are used for the gas-liquid flow patterns (dispersed bubble, bubble, and slug). The model development assumes that the suspension, moving bed and stationary bed layers may be formed individually or simultaneously within the drilling annulus based upon the

operational conditions. Force analysis is used to describe the forces on the cuttings in the wellbore annulus, while dimensional analysis is used to mathematically express the specific cuttings transport mechanism within the wellbore annulus.

3.5 Summary

This chapter discussed the research methodology and methods employed to achieve the research objectives outlined in Chapter 1. The methods employed include physical experiments and theoretical modelling approaches to capture the phenomenological behaviour involved in multiphase flow within annular geometries. The research questions, objectives and contributions addressed and/or made in Chapter 3 are summarised in Table 3.5. The following chapters will discuss the experimental results and findings of this research study.

Table 3.5 Research objective, and output addressed by Chapter 3

AIM	OBJECTIVE	METHOD	OUTPUT
To develop a rigorous integrated strategy for maximising the efficiency of UBD for the transport of cuttings in gas-liquid two-phase flow through wellbore annuli	RO3: To collect experimental data on dispersed bubble, bubble, and slug in horizontal and inclined, concentric and eccentric annuli for Newtonian and non-Newtonian flows, as the occurrence of these flow pattern dominate in UBD operations	Design and construction of multiphase flow loop	Experimental unit is capable of real-time data acquisition and allows for the visualisation and recording of the nature and structure of different gas-liquid two-phase flow patterns and particle transport mechanisms

Chapter 4 : Experimental Results and Discussion

4.1 Introduction

This chapter presents and discusses the experimental results of this research study as outlined in the research methodology of Chapter 3. Due to a lack of published data on the combined effect of inner pipe rotation, pipe eccentricity and pipe inclination angle on Newtonian and non-Newtonian gas-liquid two-phase flow behaviour inside wellbore annuli, laboratory experiments were conducted. This section introduces the chapter. Sections 4.2 to 4.7 present the results of the experimental tests using the multiphase flow loop. Section 4.8 summarises the chapter.

4.2 Fluid flow patterns and cuttings transport mechanisms

The experimental characteristics of the flow patterns observed are given in this section and are used to compare with the flow pattern dependent multiphase flow models presented in Chapter 5 which follows. Figure 4.1 to Figure 4.6 provide examples of the gas-liquid two-phase fluid flow patterns and cuttings transport mechanisms occurring in both single- and two-phase Newtonian and non-Newtonian fluids.

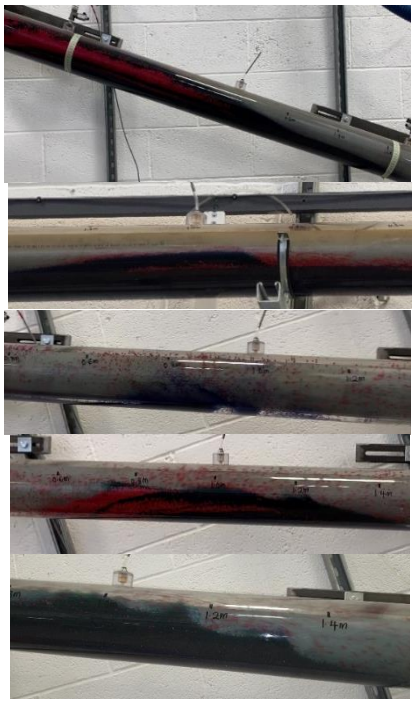

Figure 4.1 Examples of different solid particles transport mechanisms in single-phase (water) flow (a) thick stationary bed ($Q=30m^3/hr$, C_c=4-10% by volume, RPM=0, e=0, $\theta=30^0$), (b) thick stationary bed with a thin moving layer ($Q=25m^3/hr$, C_c=4-10% by volume, RPM=0, e=0, $\theta=0^0$), (c) near homogeneous suspension layer with a moving bed layer ($Q=35m^3/hr$, C_c=4-10% by volume, RPM=0, e=0, $\theta=20^0$), (d) interbedded packed dune with a suspension layer ($Q=28m^3/hr$, C_c=4-10% by volume, RPM=0, e=0, $\theta=20^0$), and (e) waved bed with a suspension layer ($Q=32m^3/hr$, C_c=4-10% by volume, RPM=150, e=0, $\theta=20^0$)

Figure 4.1a shows an inclined annulus in which a thick stationary bed solid configuration exist, representing a significantly large stagnation zone. In this flow condition, the drilling fluid is unable to suspend the solid particles in the wellbore annulus, allowing the solid particles to deposit and accumulate at the lower side of the wellbore, forming a stationary bed. Over time the solids bed continues to grow causing a severe blockage within the wellbore annulus. Figure 4.1b shows a thick stationary bed with a thin moving layer solid configuration in a horizontal annulus. On top of the stationary bed is a moving layer, where the solid particles concentration is not homogeneous. Beneath the moving layer, the solid particles are rolling forward. As the solid particles concentration decreases inside the moving layer, its moving velocity increases. On top of the moving layer, is the drilling fluid layer, where there is nearly to no solid particles.

Figure 4.1c shows a near homogeneous suspension layer with a small moving bed layer, solid configuration in a slightly inclined annulus. Figure 4.1d shows an interbedded packed dune with a suspension layer solid configuration. In this solid configuration, the solid particles flow downward from the rear end of the dune, then move upward in the annulus carried by the drilling fluid, and finally deposit and accumulate at the front end of the dune. Figure 4.1e shows a waved bed with a suspension layer solid configuration. In this solid configuration, the solid particles deposit and accumulate at the lower side of the annulus and form a solid bed when the drilling fluid flowrate is not high enough, with the height of the solid bed changing. Solid particles move downward along the top end of the wave and accumulate at the bottom end of the wave. The waves move forward in the upward direction at a constant speed because of the transfer of solid particles from the top end to the bottom end of the wave.

Generally, the various cuttings transport mechanisms (the geometrical configurations of the liquid and solid phases distribution) experienced during drilling operations using single-phase drilling fluids are a result of the drilling fluid flowrate, annuli size, fluid rheology, solid properties (shape, density, size, volumetric concentration), pipe inclination angle, pipe eccentricity and drillpipe rotary speed. Drilled cuttings are affected by gravity, friction, lift, and drag forces. The gravity force is the major force responsible for the drilled cuttings settling out of the drilling fluid to form a cuttings bed at the lower side of the wellbore annuli and its magnitude is equal to the submerged weight of the drilled cuttings in the drilling fluid. If the drilled cuttings begin to slide or roll on the surface of the annuli wellbore or above the cuttings bed, then the friction force is induced. However, the forces which tend to move the cuttings forward and out of the cuttings bed are the lift and drag forces which act against the

gravitational and frictional forces. The lift force tends to lift the drilled cuttings under strong turbulent into the direction normal to the drilling fluid flow. On the other hand, the drag force tends to drag or roll the drilled cuttings out of the cuttings bed, moving them forward. This occurs due to the viscous flow of the drilling fluid over the upper exposed surface of the drilled cuttings (Luo et al., 1992; Cho et al., 2001).

(a)

(b)

(c)

**Red line indicates the gas-liquid interface

Figure 4.2 Different air-water two-phase flow patterns (a) stratified (Q_m= 32m^3/hr, C_c=0% by volume, RPM=0, e=0, θ=0^0), (b) dispersed bubble flow (Q_m=38m^3/hr, C_c=0% by volume, RPM=0, e=0, θ=20^0), and (c) slug (Q_m=40m^3/hr, C_c=0% by volume, RPM=0, e=0, θ=30^0)

As mentioned in Chapter 2, there are different gas-liquid two-phase fluid flow structures called flow patterns which have been identified in the literature. The experimental conditions considered during experimental tests allowed the visualisation of three main gas-liquid two-phase flow patterns – stratified, slug and dispersed bubble. Figure 4.2a shows a relatively smooth stratified flow pattern in a horizontal annulus, whereby the liquid flows along the bottom of the wellbore annulus and the gas along the top. Figure 4.2b shows the dispersed bubble flow pattern in an inclined annulus in which the gas phase (air) is

suspended as discrete bubbles in an axially continuous liquid phase (drilling fluid) with bubbles uniformly spread in liquid phase without any slippage between the phases. Figure 4.2c shows the slug flow pattern in a horizontal and inclined annulus respectively, characterised by gas flowing in large bubbles known as "Taylor bubbles" while the liquid carries distributed bubbles.

Different gas-liquid two-phase fluid flow patterns exist within wellbore annuli and are strongly affected by the gas and liquid input flowrates, fluid properties (rheology and density), annuli size, pipe inclination angle and pipe eccentricity. Each of these factors are responsible for exerting relative magnitudes of forces – buoyancy, turbulence, inertia, and surface tension, which act on the fluids and result in the different gas-liquid flow patterns (Perez-Tellez, 2003; Eyo and Lao, 2019).

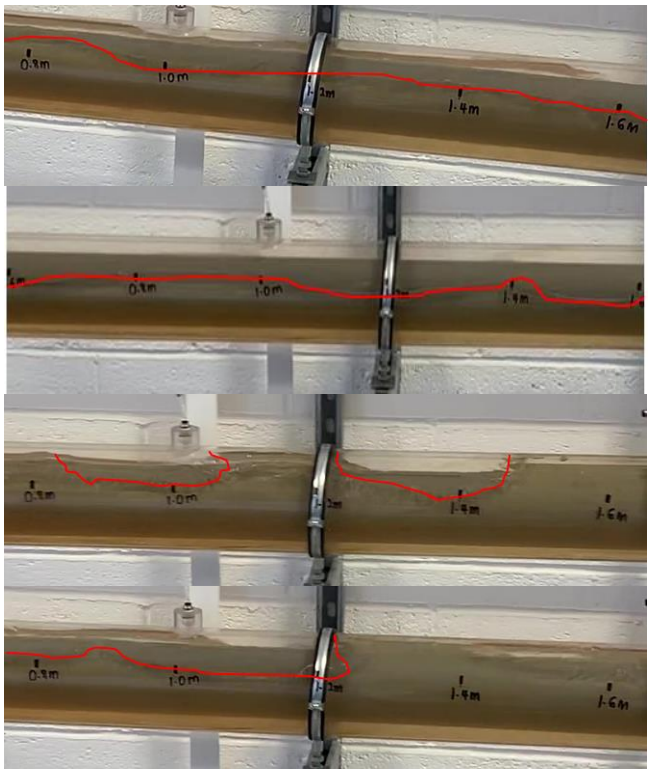

**Red line indicates the gas-liquid interface

Figure 4.3 Slug evolution in a concentric horizontal annulus (Q_m=42m^3/hr, C_c=0% by volume, RPM=0, e=0, θ=30^0) for air-water two-phase flow (a) wavy flow, initial disturbance, (b) disturbance growing, (c) slug initiation (bridging), and (d) slug growth and formation

Figure 4.3 shows an example of slug evolution for an experimental test conducted in a concentric horizontal annulus. Slug flow is highly complex, having highly transient hydrodynamic characteristics due to its inherent unsteady nature. Although the liquid and gas flowrates remain steady, the phase velocities, component mass flowrates, and slug unit pressures, at any annuli cross-section, undergo significant variations with respect to time. Initially, the gas-liquid flow in the annulus is stratified with the liquid layer flowing beneath the gas layer. Within this gas-liquid structure, the liquid layer undergoes shear forces due to the inner pipe and wellbore wall and begins to decelerate (Figure 4.3a). As the liquid velocity decelerates, disturbances begin to initiate and propagate on the gas-liquid interface with varying wavelengths and growth rates (Figure 4.3b). When the amplitude of certain waves increase, bridging occurs within the annulus (Figure 4.3c) which is known as slug initiation. The formation of a blockage is referred to as a slug precursor. This blockage prevents the flow of the gas layer and results in the pressure upstream of the slug precursor to increase. The slug precursor then lifts the slow-moving liquid ahead of it and sheds it behind it, resulting in the formation of the liquid film/gas pocket zone which is terminated by the next precursor. Eventually, the slug precursor increases in volume to form a fully developed slug (Figure 4.3d).

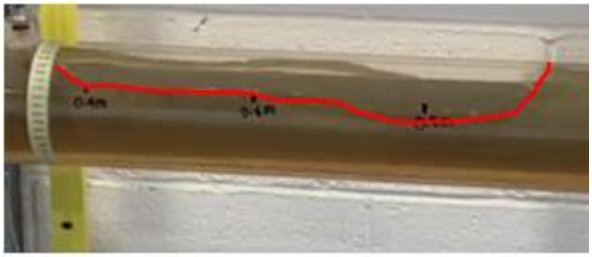

(a)

(b)

**Red line indicates the gas-liquid interface

Figure 4.4 Slug flow in (Q_m=43m^3/hr, C_c=0% by volume, RPM=0, e=0) for air-water two phase flow (a) horizontal concentric annulus ($\theta=0^0$), and (b) inclined concentric annulus ($\theta=30^0$)

Figure 4.4 shows the difference in the slug flow pattern profile in a horizontal and inclined annuli test section under the same test condition. It was observed that the slug flow pattern exhibited different characteristics based upon the gas-liquid phase separation, which is strongly influenced by the pipe inclination angle, leading to differences in the phase variations occurring in either the horizontal or inclined wellbore annuli.

Figure 4.5 Dispersed bubble flow in an inclined annuli (Q_m=38m^3/hr, C_c=0% by volume, RPM=0, e=0, $\theta=20^0$) for air-water two phase flow

Figure 4.5 shows an example of the dispersed bubble flow pattern which is characterised by small discrete gas bubbles being homogeneously distributed in the continuous liquid phase. This is the only flow pattern where no slippage between the phases can be assumed, as the flow is essentially homogeneous.

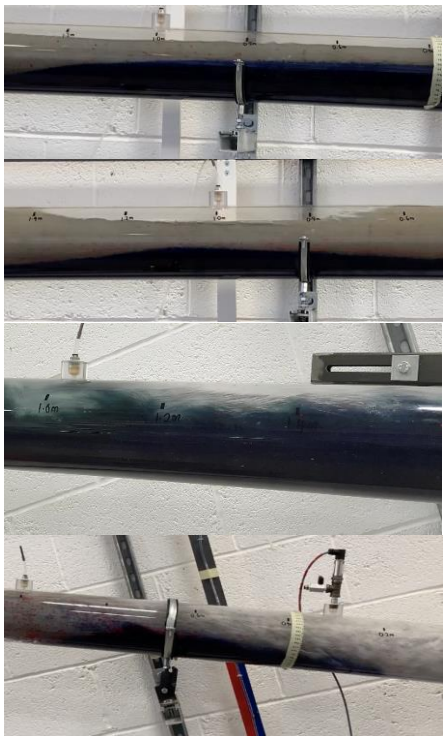

Figure 4.6 Different air-water two-phase fluid flow patterns and solid particles transport mechanisms (a) stratified flow (Q_m=35m^3/hr, C_c=4-10% by volume, RPM=0, e=0, θ=0^0), (b) slug flow (Q_m=40m^3/hr, C_c=4-10% by volume, RPM=0, e=0, θ=0^0), (c) dispersed bubble (Q_m=38m^3/hr, C_c=4-10% by volume, RPM =0, e=0, θ=30^0), and (d) slug flow (Q_m=40m^3/hr, C_c=4-10% by volume, RPM=0, e=0, θ=30^0)

Figure 4.6 shows the different gas-liquid two-phase fluid flow patterns and cutting transport mechanisms. From experimental tests, it was confirmed that that the solid particles are transported only in the liquid phase as there were no solid particles present in the gas phase for gas-liquid two-phase Newtonian and non-Newtonian fluid flows. These results also showed that the effect of the major operational drilling parameters on effective hole cleaning for two-phase flow is strongly influenced by the prevailing gas-liquid two-phase fluid flow pattern and differs significantly from that of the single-phase flow (Figure 4.1). For the flow conditions investigated as part of this study, it was found that the dispersed bubble gas-liquid fluid flow pattern was more effective for hole cleaning whereas the stratified gas-liquid fluid flow pattern was the most ineffective for solids transport.

Thus, to ensure successful UBD operations, effective cuttings transport must be achieved, and it is critical to understand and take into account the effects of the flow pattern variations that may occur during UBD operations and how these flow patterns influence the major operational drilling parameters.

4.3 Effect of gas-liquid fluid flowrate and rheology

While fluid flowrate, hole size, hole inclination angle, fluid rheology and ROP have a strong influence on cuttings transport performance. However, fluid flowrate and rheology are the preferred controllable parameters in field operations. To prevent cuttings transport issues, the drilling wellbore annuli must operate above a critical condition to maintain favourable drilled cuttings movement with this critical condition often referred to as the critical velocity or the minimum transport velocity (MTV). Thus, the wellbore fluid circulation rate needs to be sufficiently high to either prevent the settling of the drilled cuttings or relatively large enough to generate an adequate magnitude of forces (lift and drag) to ensure that the drilled cuttings roll, drag or slide along the bottom of the wellbore annuli. It should be noted however, that an increase in the fluid circulation rate and thereby fluid velocity produces a corresponding increase in the annuli pressure losses.

Additionally, if the fluid mixture velocity falls below the MTV, the drilled cuttings would settle and form a stationary bed. With an increase in the stationary bed height, the annuli flow area for the advancing fluid and drilled cuttings is also decreased, resulting in an increase in the average fluid mixture velocity until the flow condition is met (required MTV) to keep the advancing drilled cuttings moving. At this point, the advancing drilled cuttings are transported above the stationary bed as a moving bed with some drilled cuttings in suspension

depending on the properties of the drilled cuttings. Thus, the annuli pressure losses experienced by the flow of two-phase fluids with drilled cuttings are not only dependent on the fluid flow pattern, but also dependent on the drilled cuttings transport mechanism and are different from that experienced by the flow of the fluids without drilled cuttings.

Experimental results show that the MTV for gas-liquid fluid flow is strongly dependent on the prevailing gas-liquid fluid flow pattern along with other important parameters that influence the solid particle transport efficiency. Figure 4.7 shows the stratified and slug fluid flow patterns formed a stationary bed in the annuli at gas-liquid fluid mixture flowrates of approximately 35 and 42 m^3/hr respectively. It is observed in Figure 4.7 that the stationary bed formed is thick with a very thin moving bed layer whereas in Figure 4.7b the stationary bed is accompanied by a more substantial moving bed layer and considerable amount of solid particles suspended in the turbulent slug body region. Hence, for gas-liquid UBD operations, consideration must be given to the gas-liquid two-phase fluid flow pattern and gas and liquid flowrates to optimise hole cleaning.

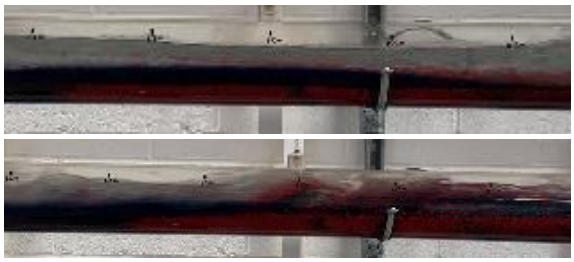

(a)

(b)

Figure 4.7 Flow pattern with different gas-liquid input flowrates (a) stratified flow (Q_m=35m^3/hr, C_c=4-10% by volume, RPM=0, e=0, $\theta=0^0$), and (b) slug flow (Q_m=42m^3/hr, C_c=4-10% by volume, RPM=0, e=0, $\theta=0^0$)

Gas-liquid two-phase fluid rheology significantly influences drilled cuttings transport efficiency in both concentric and eccentric annuli. From experiemental test, it was found that for all fluid flow patterns investigated, the use of a higher

viscosity fluid mixture was more effective for solid particle transport and the prevention of the formation of a stationary bed in the annuli. However, when a stationary bed is already formed, the fluids with a smaller mixture viscosity are more effective in reducing the stationary bed height.

Figure 4.8 shows an example of the comparison of the solid particle transport mechanism for air-water and air-polymer mixtures at the same air-liquid flowrate with the dispersed bubble flow pattern. As the result of the higher mixture viscosity of the air-polymer mixture (non-Newtonian), the solid particles were transported predominantly in suspension (Figure 4.8b) whereas a moving bed mechanism was formed for the air-water mixture.

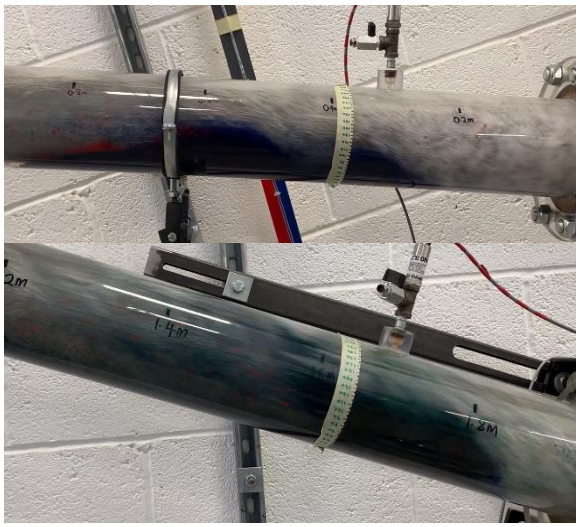

(a)

(b)

Figure 4.8 Dispersed bubble flow pattern at the same air-liquid flowrate (Q_m=42m^3/hr, C_c=4-10% by volume, RPM=0, e=0, θ=30^0) (a) air-water mixture with a moving bed solid particle mechanism, and (b) air-polymer mixture with suspension solid particle mechanism

Experimental results indicate that the fluid mixtures having a higher viscosity value had a lower MTV requirement when compared to the fluids with a smaller viscosity value. However, it should be noted that the properties of the liquid phase are more important than that of the gas phase for solid particle transport as the solid particles are generally transported in the liquid phase.

Figure 4.9 shows the annuli differential pressure data for Newtonian and non-Newtonian gas-liquid two-phase flows with and without particles in the 30^0 inclined annuli. It can be seen that for the two cases without solid particles (air-water and air-polymer), the air-polymer non-Newtonian fluid mixture experienced higher annuli pressure losses than the Newtonian air-water fluid mixture, increasing as the fluid mixture velocity increased. This trend was also observed for the cases with solid particles, with the air-polymer fluid mixture with particles having higher annuli pressure losses than the air-water fluid mixture with particles. Thus, the annuli pressure losses for the cases of fluid flow with solid particles were dependent on the prevailing particle transport mechanism and were noted to be considerably higher than that of the cases without cuttings.

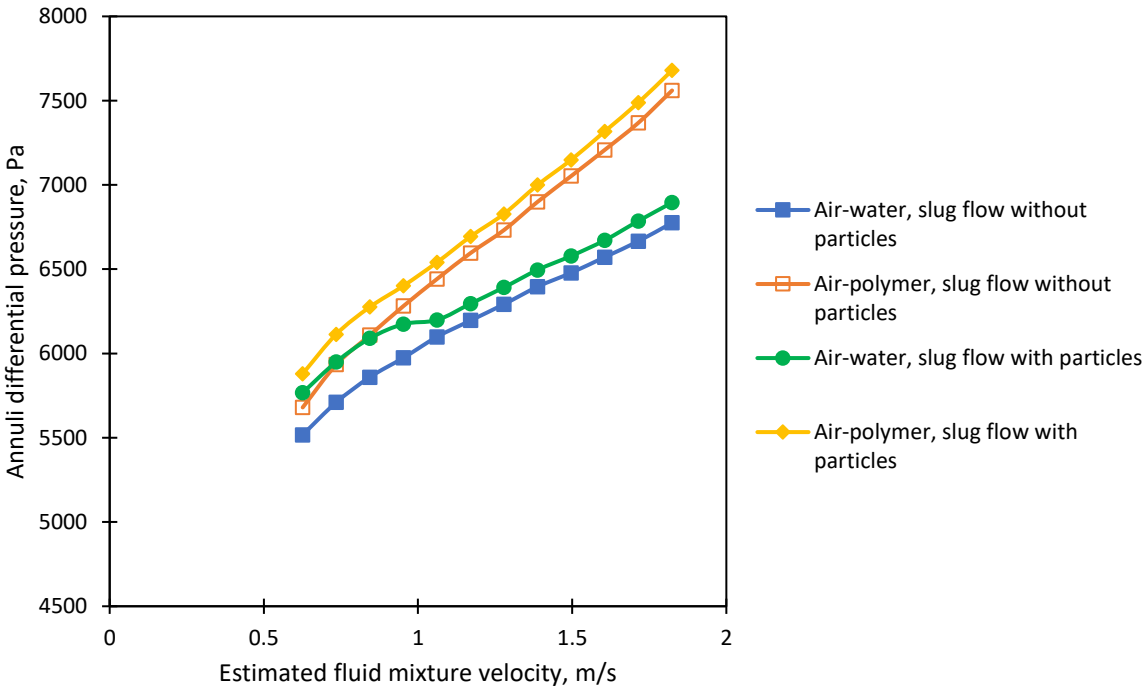

Figure 4.9 Annuli differential pressure vs. fluid mixture velocities for air-water and air-polymer gas-liquid two-phase fluid mixtures with and without solid particles (C_c=0% or 4-10% by volume, RPM=0, e=0, $\theta=30^0$)

At low fluid mixture velocities where the MTV condition was not met, a stationary bed formed which substantially increased the annuli pressure losses for both the Newtonian and non-Newtonian fluid mixtures. Increasing the fluid mixture flowrate reduced the stationary bed height and gradually transformed the stationary bed to a moving bed or suspension mechanism which as a result led to a decrease in the annuli pressure losses. The increase in the fluid flowrate to transport the cuttings influences the fluid flow pattern and produces a corresponding increase in the annuli pressure losses. As such it is necessary to conduct fluid hydraulic calculations and cuttings transport performance analysis to the select the optimal flowrates (both pump and injection) for the UBD operations.

4.4 Effect of pipe inclination angle

Hole inclination angle strongly influences the drilled cuttings tranport efficiency but is also highly dependent on the prevailing fluid flow pattern. It is important to recognise that the prevailing fluid flow pattern is also influenced by the hole inclination angle as its gas and liquid distribution changes as the hole inclination changes. Figure 4.10 shows an example of the gas-liquid flow pattern distibution without solid particles at the same gas-liquid flowrate resulting in a different gas-liquid flow pattern in the horizontal and inclined annuli. In the horizontal annuli, the stratified gas-liquid flow pattern is clearly seen whereas within the inclined annuli a slug flow pattern occurred at the same fluid mixture flowrate.

Figure 4.10 Difference in gas-liquid flow pattern distribution at same air-water flowrate (Q_m=40m^3/hr, C_c=0% by volume, RPM=0, e=0), stratified flow in a horizontal annulus ($\theta=0^0$) (top), and slug flow in an inclined annulus ($\theta=30^0$) (bottom)

Futhermore, Figure 4.11 shows that even when the same fluid flow patten is experienced at the same gas-liquid flowrate in both horizontal and inclined annuli, the gas-liquid fluid distribution still varies. In Figure 4.11a, the horizontal annulus is observed to have a longer liquid film length (L_f = 1.02 m), but as the local mixture properties of the fluid changed with an increase in inclination angle, the liquid film length decreased (L_f = 0.45 m), Figure 4.11b.

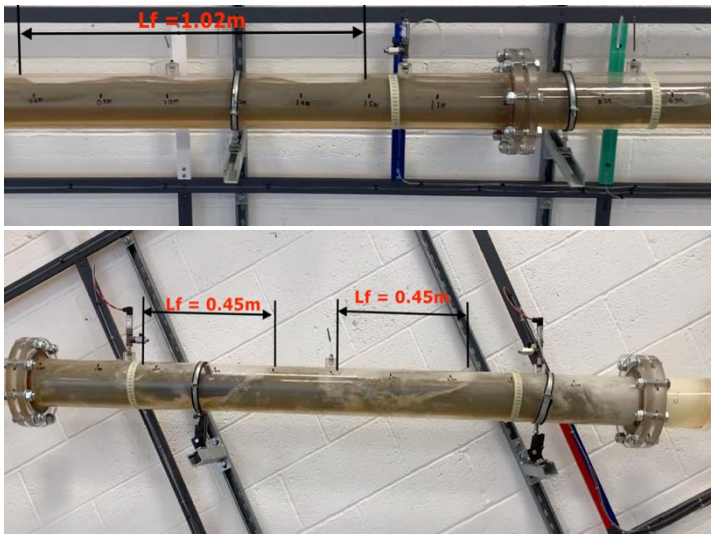

(a) Horizontal

(b) 20^0 Inclined

Figure 4.11 Change in liquid film length for a fully developed slug flow (Q_m=45m^3/hr, C_c=0% by volume, RPM=0, e=0) in a horizontal ($\theta=0^0$) and inclined annulus ($\theta=20^0$) for air-water two-phase flow

Figure 4.12 shows an example of the solids transport mechanism for fully developed slug flow in the horizontal and inclined annuli test sections. It was found that at a specific gas and liquid flowrate, the solid particles in the horizontal test section was being transported primarily as a moving bed whereas a thick stationary bed was formed in the inclined test section and increased with time. The formation of the stationary bed in the inclined annuli test section may be attributed to the change in the local fluid mixture properties in the annuli which changes the forces (gravity, friction, lift and drag) acting on the solid particles, making it difficult to transport the solid particles in an upward inclined direction when the slug flow pattern exists in the annuli.

Figure 4.12 Difference in solid particle transport mechanisms for the same air-water flowrate (Q_m=38m^3/hr, C_c=4-10% by volume, RPM=0, e=0) for slug flow pattern with a moving bed, in a horizontal annulus ($\theta=0^0$) (top), and stationary bed in an inclined annulus ($\theta=30^0$) (bottom)

Figure 4.13 provides experimental results showing the effect of pipe inclination angle on the cuttings transport efficiency in concentric and eccentric annuli. MTV measurements were obtained by adding solid particles at a given concentration into the gas-liquid flow and recording the flowrate at which the solid particles become fully suspended or begin dragging or rolling at the bottom of the annuli. The gas-liquid flowrate required to suspend the solid particles or transport the solid particles in the rolling mechanism was found to increase with an increase

in the pipe inclination angle, with the gradient of this increase being greater for Newtonian gas-liquid two-phase flow than that of non-Newtonian gas-liquid two-phase flow.

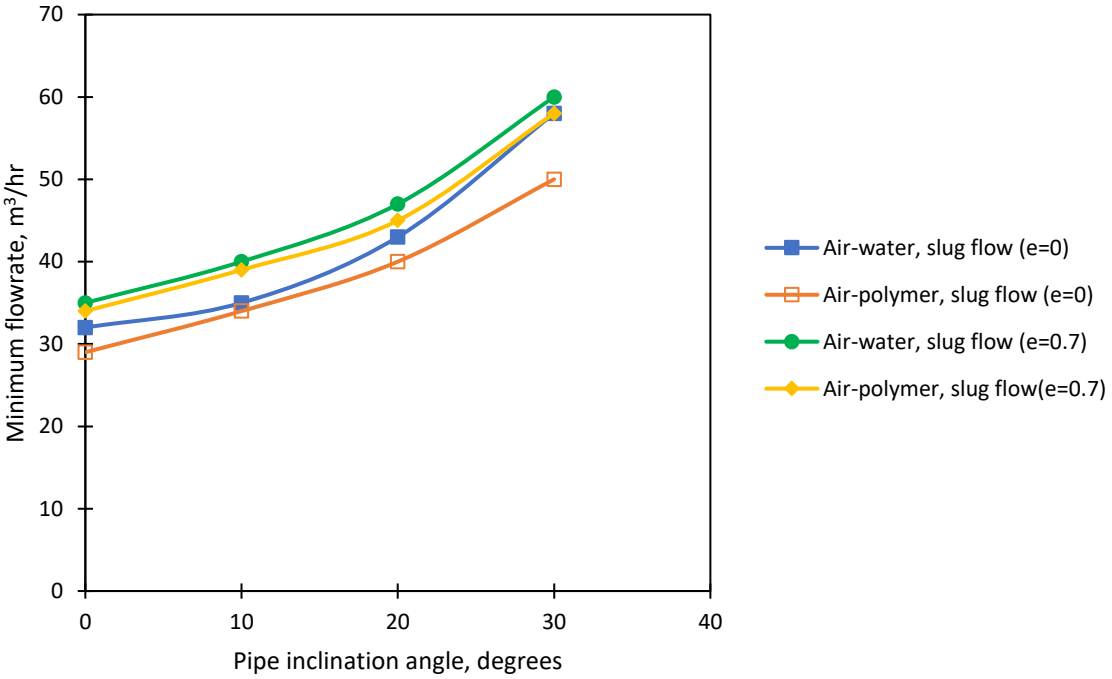

Figure 4.13 Effect of hole inclination angle on solid particle transport for air-water and air-polymer two-phase flows in concentric and eccentric annuli (C_c=4-10% by volume, RPM=0, e=0 or 0.7)

It should be noted that as the hole inclination angle increases, the radial component of the drilled cuttings velocity also increases.

4.5 Effect of solid particles density and size

The magnitude of the gravitional force to the movement of drilled cuttings is strongly dependent on the density and size of the particles. To ensure effective cuttings transport, the gas-liquid two-phase fluid needs to generate a sufficient lift and drag force to overcome the resistance forces acting on the cuttings in the wellbore annuli. The higher the density of the drilled cuttings, the higher the resistance forces and thus, the higher the minimum requirements to ensure effective cuttings transport. Experimental tests showed that solid particle

density exhibited a more pronounced effect than solid particle size and that the effect of the solid particles properties are strongly influenced by the prevailing gas-liquid fluid flow pattern within the annuli. For example, if the stratified fluid flow pattern exists within the annuli, only the liquid properties and velocity would have to be adequate enough to prevent the formation of a stationary bed, as the solid particles will only be transported in the liquid phase of thegas-liquid two-phase fluid mixture. Whereas, for the slug fluid flow pattern, the fluid mixture (gas and liquid) properties and velocity would have to be adequate enough to generate the required forces to prevent the formation of a stationary bed.

Figure 4.14 presents the experimental results of tests performed to determine the MTV to ensure the movement of solid particles, which have different densities and size ranges. It was observed that the MTV required to transport the denser solid particles were significantly higher than that required for the lighter solid particles although the size ranges of the denser solid particles were much less than the lighter solid particles. However, if the density of all the solid particles were effectively the same, the effect of solid particle size on MTV would become more pronounced.

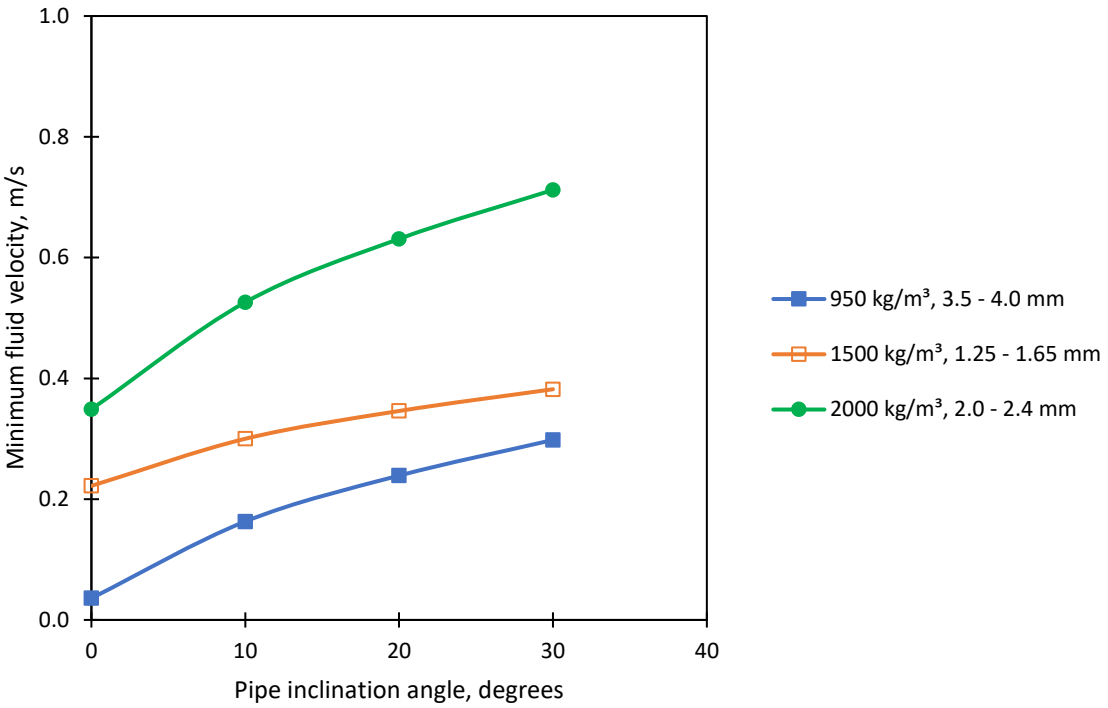

Figure 4.14 Minimum transport velocity of different solid particles vs pipe inclination angle (C_c=4-10% by volume, RPM=0, e=0)

Figure 4.15 shows the lighter red particles having a density of 950 kg/m^3 and size range of 3.5 – 4.0 mm being transported in suspension while the heavier blue solid particles having a density of 1500 kg/m^3 and a size range of 1.25 – 1.65 mm being transported as a moving bed. These two examples highlight the effect of solid particle density on the particle transport mechanism being more influential than its size and as the denser solid particles settle, they in some cases drop out of the moving layer and trap some of the lighter solid particles in the stationary bed.

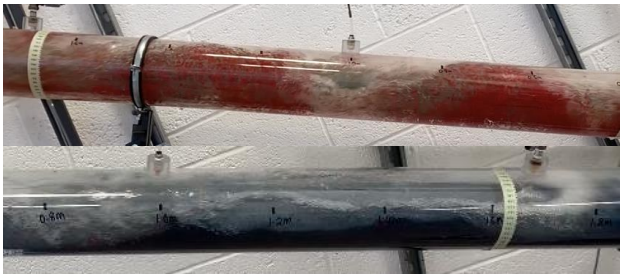

(a)

(b)

Figure 4.15 Effect of the solid particle properties on solid particles transport mechanism (Q_m=38m^3/hr, C_c=4-10% by volume, RPM=0, e=0, θ=20^0) (a) air-water two-phase flow with red solid particles (b) air-water two-phase flow with blue solid particles

4.6 Effect of pipe eccentricity

Pipe position change in wellbore annuli (level of eccentricity or pipe offset from the geometric center of the wellbore annuli) will result in a different fluid mixture velocity profile across the wellbore annuli and affect solid particle transport. The higher the level of eccentricity, the higher the relative reduction of the fluid mixture velocity in the reduced region of the wellbore annuli and higher the relative increase of the velocity in the enlarged region of the wellbore annuli.

The average fluid velocity required to transport the solid particles and prevent the formation of a stationary bed at the bottom of the annuli increases with an increase in pipe eccentricity. Thus, the fluid flow requirement necessary to clean the eccentric annuli is higher than that required for the concentric annuli for gas-liquid flows. In some experimental tests under fluid flowing conditions where no bed or moving bed was formed in the concentric annulus, either a moving bed or a stationary bed was formed in the eccentric annulus.

Figure 4.16 presents the average fluid mixture velocity required to prevent the formation of a stationary bed when solid particles are flowing for both air-water and air-polymer fluid mixtures in concentric (e = 0), and eccentric (e=0.7) annuli. These results clearly show that the MTV required to keep the particles rolling at the bottom of the wellbore annuli increases with eccentricity. It was also observed that in the cases where a stationary bed was formed in both the concentric and eccentri annuli, the height of the stationary bed in the eccentric annuli was higher than that in the concentric annuli.

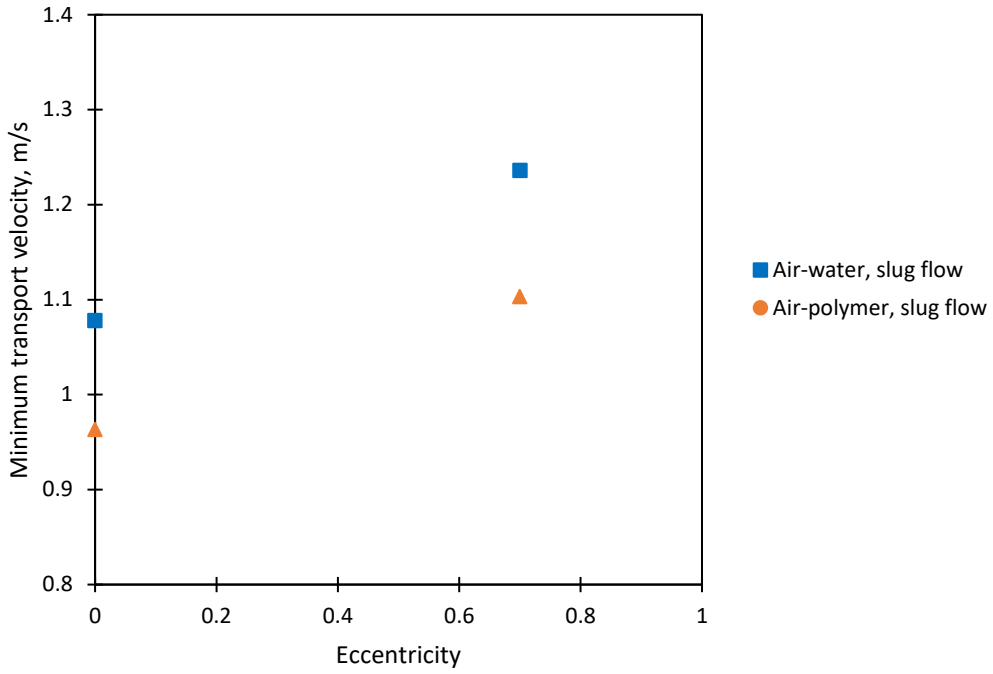

Figure 4.16 Effect of pipe eccentricity (e=0 and e=0.7) on minimum transport velocity (C_c=4-10% by volume, RPM=0, $\theta=0^0$)

4.7 Effect of inner pipe rotation

Inner pipe rotation produces a tangential component of the fluid velocity and annular helical flow be developed in the drilling annuli. It may also induce additional turbulences which can affect solid particle transport in the wellbore annuli. The extent to which inner pipe rotation influences solid particle transport in the annuli is dependent on other influential drilling parameters (e.g., fluid rheology, prevailing gas-liquid fluid flow pattern, pipe inclination angle and pipe eccentricity). From visual observations of different experimental flow conditions, it was seen the prevailing gas-liquid two-phase fluid flow pattern formed in either the concentric or eccentric annuli was mainly governed by drilling fluid rheology and input gas and liquid flowrates. Inner pipe rotation (maximum 150 rpm) did not lead to a transition between one gas-liquid fluid flow pattern to another as gas-liquid fluid flows are typically turbulent in nature. The rotary speed (maximum 150 rpm) could not produce enough tangential force to overcome the axial force of the flow in the annuli. It was found that even though

the inner pipe rotation can improve the solid particle transport, the response of the solid particles to the inner pipe rotation differs and is also governed by the pipe eccentricity and inclination angle. The increase in the inner pipe rotary speed in the horizontal concentric annuli produced little or no effect on the prevention of the formation of a stationary bed in the annuli for both Newtonian and non-Newtonian gas-liquid two-phase fluids.

Figure 4.17 presents the results of the measured stationary bed height formed in both the concentric horizontal and inclined annuli with and without inner pipe rotation. It was observed that the height of the bed formed in the horizontal and inclined concentric annuli with and without inner pipe rotation was more or less the same for all the fluid types (air-water and air-polymer) and gas-liquid two-phase fluid flow patterns.

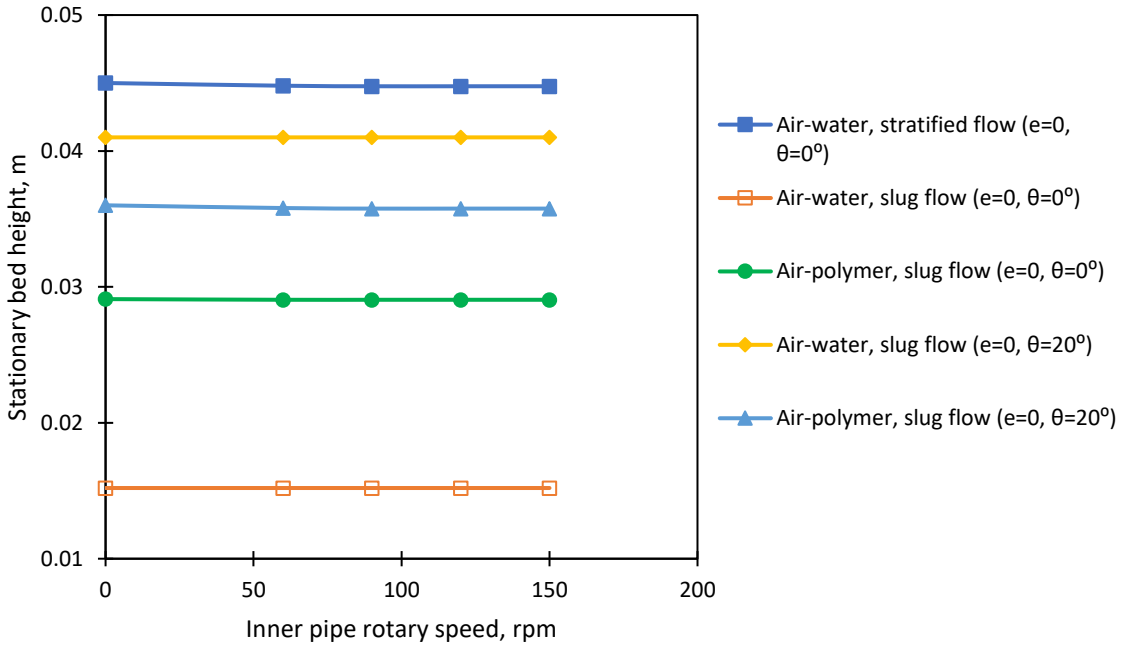

Figure 4.17 Effect of inner pipe rotation on stationary bed height in horizontal and inclined concentric annuli (Cc=4-10% by volume, RPM=0-150, e=0, θ=00 or 200) for air-water and air-polymer two-phase flows

Figure 4.18 shows the solids transport dynamics in the 20° inclined concentric annuli over a finite time interval. It was observed that with an increase in the inner pipe rotational speed, little to no siginificant effect was produced to prevent the formation of a stationary bed or influence the size of the stationary bed once formed.

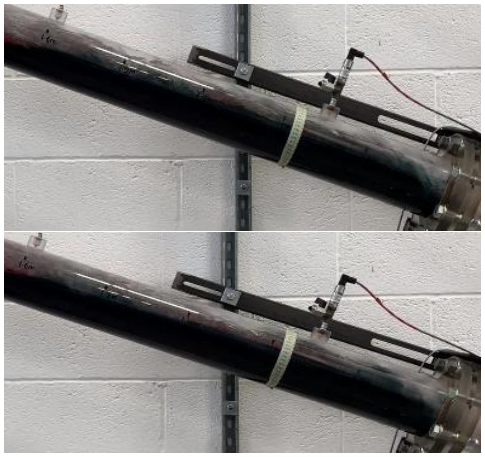

Figure 4.18 Effect of the inner pipe rotation on solid particle stationary bed for air-water two-phase slug flow (Q_m=54m^3/hr, C_c=4-10% by volume, RPM=150, e=0, θ=30^0)

An increase in the inner pipe rotational speed was found to be more beneficial for the transport of the solid particles in the eccentric annuli than that of the concentric annuli. Inner pipe rotation led to a decrease or in some cases the prevention of a stationary bed in eccentric annuli in both horizontal and inclined annuli. Figure 4.19 presents the results of the effect of the inner pipe rotation on the stationary bed height formed in the horizontal and inclined eccentric annuli. For all cases, it was seen that the height of the stationary bed formed in the annuli decreased with an increase in the inner pipe rotational speed in both the horizontal and inclined eccentric annuli. Even though the effect of the inner pipe rotation on the solid particles movement was found to be more significant in the eccentric annuli when compared to the concentric annuli, it should be noted that the magnitude of the effect of inner pipe rotation is strongly influenced by fluid rheology and the pipe inclination angle of the annuli. With

the effect of the inner pipe rotation on gas-liquid two-phase flows being strongly influenced by the gas-liquid two-phase fluid flow pattern. For the experimental conditions investigated in this research, the solid particles in the dispersed bubble flow pattern showed the least response to inner pipe rotation than the other flow patterns. However, for two-phase fluid flows with solid particles through the annuli, the dispersed bubble flow pattern performed better in terms of the solid particle transport than the other flow patterns due to its relatively higher turbulence and gas-liquid in-situ flowrates.

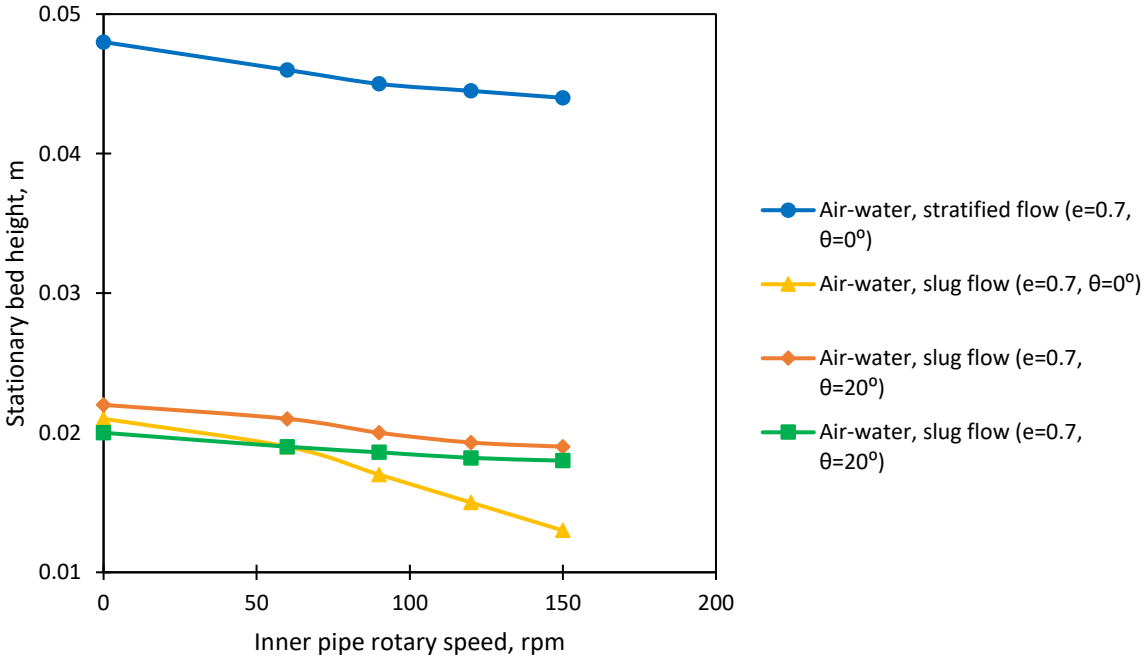

Figure 4.19 Effect of inner pipe rotation on the stationary bed height in the horizontal and inclined eccentric annuli (C_c=4-10% by volume, RPM=0-150, e=0.7, θ=0^0 or 20^0) for air-water and air-polymer two-phase flows

4.8 Annuli pressure gradient

Gas-liquid two-phase flows with solid particles experience a considerably higher annuli pressure gradient than gas-liquid two-phase flows without solid particles. The annuli pressure gradient is strongly dependent on the predominant solids transport mechanism along with the fluid and solid particles properties. If the fluid flowrate produces an average annuli fluid velocity which is lower than the

MTV required to keep the solid particles in suspension, the solid particles would move towards the lower side of the annuli and be transported as a moving bed. However, a stationary bed would be formed if the average annuli fluid velocity drops below the MTV required for the solid particles to slide at the lower side of the annuli. A stationary bed formed in the annuli reduces the fluid flow area and forces the fluid to flow in the reduced flow area above the stationary bed. With the fluid flowrate being constant, this results in an increase in the average annuli fluid velocity, increased wall, and fluid to bed interfacial shear stresses, leading to an increase in the annuli pressure gradient. Figure 4.20 shows an example of the different signals captured by the differential pressure transducers when a stationary bed exist within the annulus and when there is none. The measured real-time differential pressure when a stationary bed exists in the annulus is comparatively higher than that obtained when there is no stationary bed. Although the stationary bed increases the annuli differential pressure gradient, the pressure gradient is still strongly influenced by the gas-liquid two-phase flow pattern, fluid and solid particle properties and the predominant solids transport mechanism in the annuli.

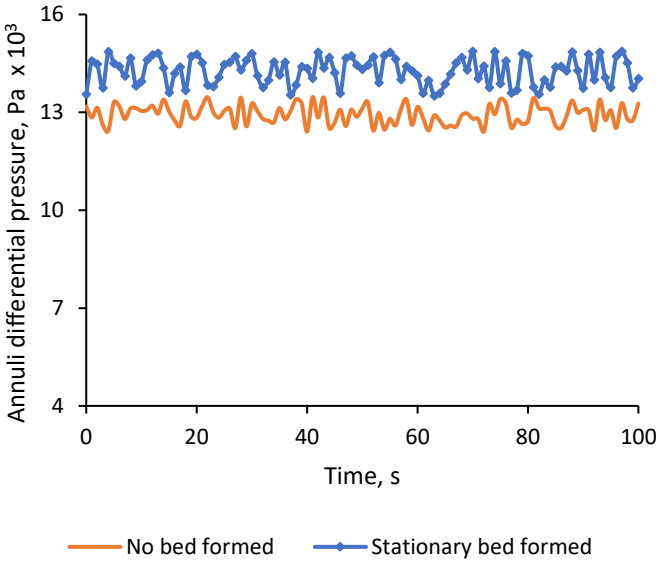

Figure 4.20 Example of the real-time annuli differential pressure data for air-water two-phase slug flow based upon the voltage output from the pressure tranmitters using the data acquistion system

Figure 4.21 and Figure 4.22 present the experimental results of the effect of annuli differential pressure vs fluid mixture velocity for air-water two-phase flow in a horizontal and 30^0 inclined concentric annuli. It is observed that the annuli differential pressure significantly increases with hole inclination angle.

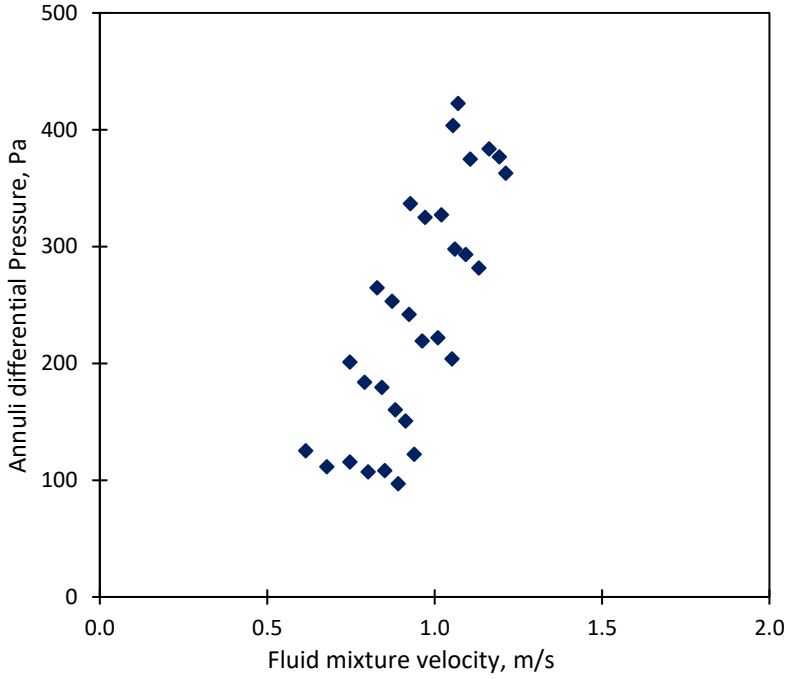

Figure 4.21 Annuli differential pressure vs fluid mixture velocity for air-water two-phase flow (C_c=4-10% by volume, RPM=0, e=0, $\theta=0^0$)

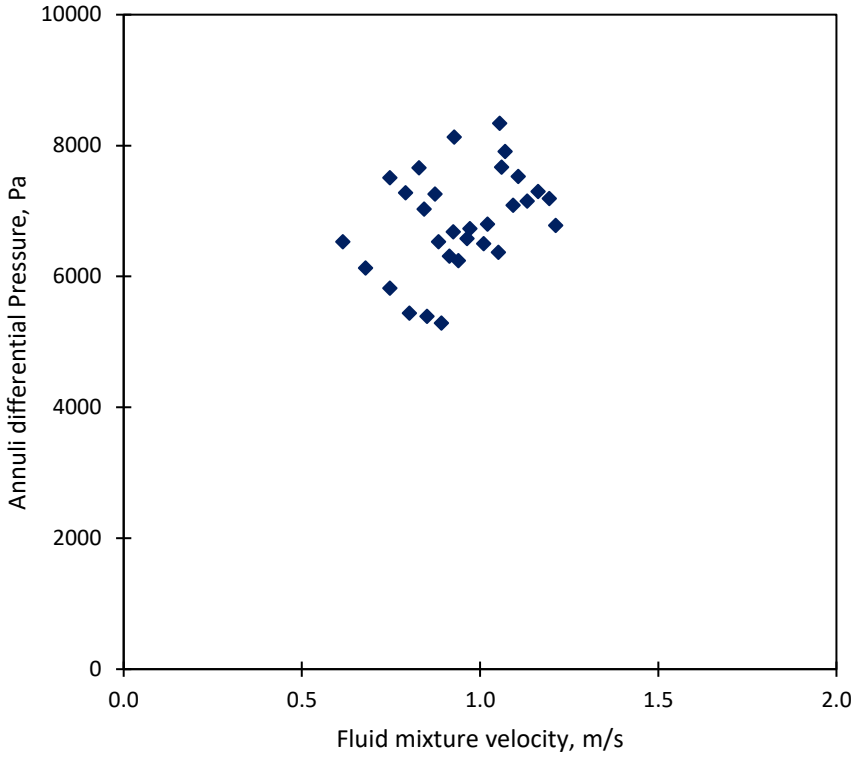

Figure 4.22 Annuli differential pressure vs fluid mixture velocity for air-water two-phase flow (C_c=4-10% by volume, RPM=0, e=0, $\theta=30^0$)

Figure 4.23 and Figure 4.24 present the experimental results of the effect of annuli differential pressure vs fluid mixture velocity for air-polymer two-phase flow in a horizontal and 30^0 inclined concentric annuli. While the difference between the annuli differential pressure of the air-polymer system and the air-water system is marginally less, the annuli pressure difference in the inclined annuli is still substantially greater than the horizontal annuli. This has considerable implications on the pressure management between the toe and the heel lateral section of the well during UBD operations.

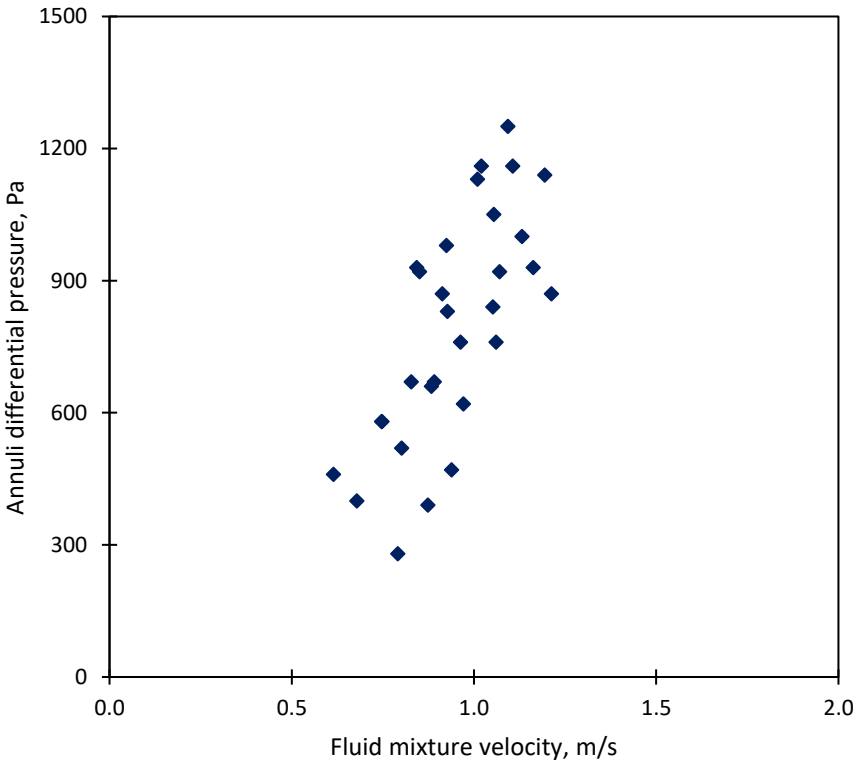

Figure 4.23 Annuli differential pressure vs fluid mixture velocity for air-polymer two-phase flow (C_c=4-10% by volume, RPM=0, e=0, $\theta=0^0$)

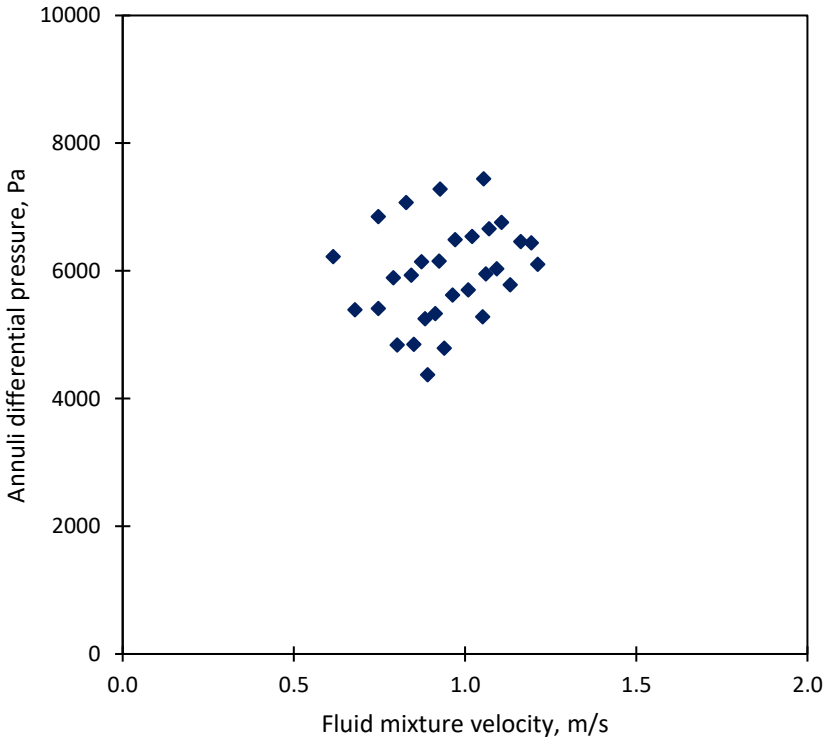

Figure 4.24 Annuli differential pressure vs fluid mixture velocity for air-polymer two-phase flow (C_c=4-10% by volume, RPM=0, e=0, $\theta=30^0$)

4.9 Summary

This chapter presents the results from the multiphase flow loop experiments which were performed to study the effect of gas-liquid two-phase fluid flow patterns on annuli hydraulics and particle transport dynamics in concentric and eccentric horizontal and inclined wellbore annuli. A series of experimental tests were conducted with and without solid particles and the results obtained were compared for various fluid types and flow conditions. Observations and measurements provided the phenomenological effect of gas-liquid two-phase flow patterns on wellbore hydraulics and cuttings transport mechanisms. Experimental results from this study show that the effect of major operational drilling parameters (gas-liquid fluid flowrates, fluid rheology, pipe inclination angle, cuttings size and density, pipe eccentricity, and inner pipe rotation) on cuttings transport efficiency in Newtonian and non-Newtonian gas-liquid two-phase flow is flow pattern dependent. Furthermore, it was found that fluid flow pattern and the prevailing cutting transport mechanism strongly influenced annuli pressure gradient.

The findings of the experimental studies provide the raw data regarding the rheological characteristics of the multiphase fluid system and its hydrodynamic behaviour under specific operating conditions and will be incorporated into the development of the UBD strategy. The research questions, objectives and contributions addressed/made in Chapter 4 are summarised in Table 4.1. Chapter 5 will present the multiphase flow modelling aspect of this research through the integration of both experimental and numerical simulation data.

Table 4.1 Research objectives and outputs addressed/made in Chapter 4

AIM	OBJECTIVES	METHOD	OUTPUT(S)
To develop a rigorous integrated strategy for maximising the efficiency of UBD for the transport of cuttings in gas-liquid two-phase flow through wellbore annuli	RO4: To investigate the effect of the major drilling parameters on the fluid flow dynamics and solids transport mechanisms RO5: To investigate the effect of cuttings transport mechanisms on annuli pressure gradient while identifying areas of preferential flows and stagnation zones	Experimental tests: 1) gas-liquid two-phase fluid flow pattern visualisation, 2) annuli pressure data, 3) cuttings transport mechanisms, and 4) cuttings bed height	Visual observations and measurements on the phenomenological effect of gas-liquid two-phase fluid flow patterns on wellbore hydraulics and cuttings transport mechanisms Evaluation of gas-liquid two-phase fluid flow pattern in identifying areas of preferential flows and stagnation zones since they directly affect the flow of drilling fluid in real well drilling situations

Chapter 5 : Multiphase Flow Modelling Results and Discussion

5.1 Introduction

This chapter presents the multiphase flow modelling aspect of this research work involving a theoretical approach. The theoretical approach is used to determine the annuli pressure losses and to evaluate the cuttings transport efficiency, incorporating the multiphase phenomenological physics involved in the wellbore annulus of UBD operations. The theoretical approach after validation with experimental results can also be used to overcome some limitations with experimental measurements and can be used as a predictive tool to investigate the mechanism behind Newtonian and non-Newtonian flow with and without cuttings transport within the UBD wellbore annuli.

This section introduces the chapter. Section 5.2 presents the theoretical modelling approach for the flow pattern dependent multi-layered models in annular configurations. Section 5.3 provides the particle transport model. Section 5.4 presents the comparison between the experimental data and theoretical model while Section 5.5 presents the model limitations. Section 5.6 summarises this chapter.

5.2 Theoretical approach

As observed from the experimental results presented in Chapter 4, the annuli pressure gradient for gas-liquid two-phase fluid flow depends upon the prevailing gas-liquid fluid flow pattern and the particle transport mechanism. When the velocity of the fluid mixture is greater than the MTV for suspension, the solid particles would be transported by means of a suspension mechanism. However, if the fluid mixture velocity is less than the MTV required to transport

the solid particles by means of a moving mechanism, a stationary bed would be formed in the annuli. As the stationary bed height increases, an increase in the annuli fluid velocity also occurs until the point is reached whereby the advancing solid particles have sufficiently applied forces to keep them in suspension or as part of a moving bed layer. The reduction in fluid flow area and the vertical solid particle concentration gradient have an impact on the hydraulics of the gas-liquid UBD system. As mentioned in Chapter 2, the three particle layers which can be initiated in the drilling annulus are: 1) a suspension layer, 2) a moving bed layer, and 3) a stationary bed layer. Each of these layers can occur individually or simultaneously in the drilling annulus based upon the operational conditions.

Experimental results presented in Chapter 4 also showed that the effect of inner pipe rotation on particle transport was highly influenced on the prevailing gas-liquid two-phase flow pattern. As such, the hydraulics and particle transport evaluation for gas-liquid two-phase fluid flow in the annuli using a multi-layered modelling approach ignores the effect of inner rotation and the validation of the models presented does not include experimental results involving inner pipe rotation. The new multi-layered models presented by Salubi et al. (2022) are flow pattern dependent and can be used to predict the particle transport efficiency, predict the particle transport mechanism, the stationary bed height and annuli pressure gradient for the various gas-liquid two-phase flow patterns for UBD operations. It should be noted that the equations presented here can be applied to any level of pipe eccentricity and are valid for different hole inclination angles (horizontal and inclined). Additionally, as mentioned in Chapter 2, the dispersed bubble, bubble, and slug flow are the dominant gas-liquid two-phase flow patterns in wellbore annuli during gas-liquid UBD

operations. As such, only mathematical models for these flow patterns will be presented.

5.3 Particle transport model

From dimensional analysis, the MTV for rolling, V_{MR} and suspension, V_{MS} can be expressed as:

$$V_{MR} = M_1 \frac{\mu_f}{d_c \rho_f} \left[\frac{{d_c}^3 \rho_f g (\rho_c - \rho_f)[\cos\beta + f_s \sin\beta]}{{\mu_f}^2} \right]^{M_2} \left[\frac{d_x}{d_c} \right]^{M_3} \quad \text{Eq. 5.1}$$

$$V_{MS} = N_1 \frac{\mu_f}{d_c \rho_f} \left[\frac{{d_c}^3 \rho_f g (\rho_c - \rho_f) \sin\beta}{{\mu_f}^2} \right]^{N_2} \left[\frac{d_x}{d_c} \right]^{N_3} \quad \text{Eq. 5.2}$$

where M_1, M_2, M_3, N_1, N_2 and N_3 are coefficients which may be determined experimentally or numerically, μ_f is the drilling fluid viscosity, ρ_f is the drilling fluid density, ρ_c is the cuttings density, d_c is the diameter of the cuttings, d_x is the distance between the drillpipe and the casing wall at the lowest side, g is acceleration due to gravity, f_s is the friction force, and β is the inclination angle between the vertical and wellbore flow axis.

The annuli flow area A_{flow}, is given by:

$$A_{flow} = \frac{Q}{V_f} \quad \text{Eq. 5.3}$$

where Q is the volumetric flowrate and V_f is the average fluid velocity.

Average fluid velocity, V_f

$$V_f = \max(V, V_{MR}) \quad \text{Eq. 5.4}$$

Area of the annuli, A_a

$$A_a = A_b + A_{flow} = \frac{\pi\left({d_2}^2 - {d_1}^2 \right)}{4} \quad \text{Eq. 5.5}$$

where A_b is the area of the stationary cuttings bed, d_1 is the outer diameter of drillpipe and d_2 is the inner diameter of casing or wellbore.

The stationary bed area in either a concentric or eccentric annuli can be determined by taking into account the gradient of the bed area formed in the annuli using geometrical relationships and can be expressed as:

$$A_b = X1(h_b) + X2(h_b) \quad \text{Eq. 5.6}$$

such that,

$$X1(h_b) = \mathbb{R}\left(\frac{{d_2}^2}{4}\sin^{-1}\left(\frac{2h_b - d_2}{d_2}\right) - \frac{{d_1}^2}{4}\left[\sin^{-1}\left(\frac{2h_b - d_2 + 2d_e}{d_1}\right) + \sin^{-1}\left(\frac{d_2 - 2d_e}{d_1}\right)\right]\right) \quad \text{Eq. 5.7}$$

$$X2(h_b) = \mathbb{R}\left(\frac{1}{2}\left[(2h_b - d_2)\left(h_b d_2 - {h_b}^2\right)^{1/2} + (d_2 - 2d_e - 2h_b)\left[\begin{matrix}(d_2 - 2d_e)h_b - {h_b}^2 \\ +\frac{{d_1}^2}{4} - \left(\frac{1}{2}(d_2 - 2d_e)\right)^2\end{matrix}\right]^{1/2} + \frac{\pi {d_2}^2}{4}\right]\right) \quad \text{Eq. 5.8}$$

and where $X1$ and $X2$ are functions for cross-sectional area calculations, h_b is the bed height, $\mathbb{R}$ represent a real number, and d_e is the distance between the centre of the outer pipe and the inner pipe.

And the distance between the inner pipe centre and outer pipe centre d_e can be obtained from:

$$d_e = \frac{1}{2}(d_2 - d_1)e \qquad \text{Eq. 5.9}$$

where e represents the wellbore eccentricity.

The multi-layered mathematical model takes into account the gas-liquid two-phase flow pattern along with the cuttings transport mechanism. The model development assumes that one, two or three layers (suspension, moving bed and stationary bed layers) may occur simultaneously within the drilling annulus based upon the operational conditions. The solid particles can be transported in a homogeneous suspension if $V_f > V_{MS}$, $h_b = 0$, condition is met. Whereas a suspension and moving bed layer can be formed if $V_f < V_{MS}$, $V_f > V_{MR}$, $h_b = 0$. However, if $V_f < V_{MR}$, a stationary bed is formed ($h_b > 0$) and increases until $V_f = V_{MR}$, reducing the flow area in the annuli with advancing solid particles forming a suspension and moving bed layer on top of the stationary bed layer.

5.3.1 Bubble and dispersed bubble flow

Model assumptions are:

1. Steady-state flow,
2. No slip between the solid particles and gas-liquid fluid phase, and
3. No movement of the stationary bed.

The mass balance of the solid particles and the gas-liquid two-phase fluid phase can be expressed as:

Solid particles phase:

$$\rho_c C_1 A_1 V_1 + \rho_c C_2 A_2 V_2 = \rho_c C_c A_a V_a \qquad \text{Eq. 5.10}$$

Drilling fluid phase:

$$\rho_m\,(1-\,C_1)A_1V_1+\;\rho_m\,(1-\,C_2)A_2V_2\;\;=\;\rho_m\,(1-\,C_c)A_aV_a \qquad \text{Eq. 5.11}$$

where A_1 and A_2 is the area of the annulus occupied by layer 1 and layer 2 respectively, V_1 and V_2 is the average velocity of the drilling fluid in layer 1 and layer 2 respectively, C_1 and C_2 is the cuttings concentration of the solids in layer 1 and layer 2 respectively C_c, is the input solid particles (cuttings) concentration, V_a is the average velocity of the drilling fluid in the annulus, and ρ_m is the gas-liquid mixture density.

For bubble and dispersed bubble flow, the momentum equations can be found by considering the sum of the forces acting on each of the three layers as shown in Figure 5.1.

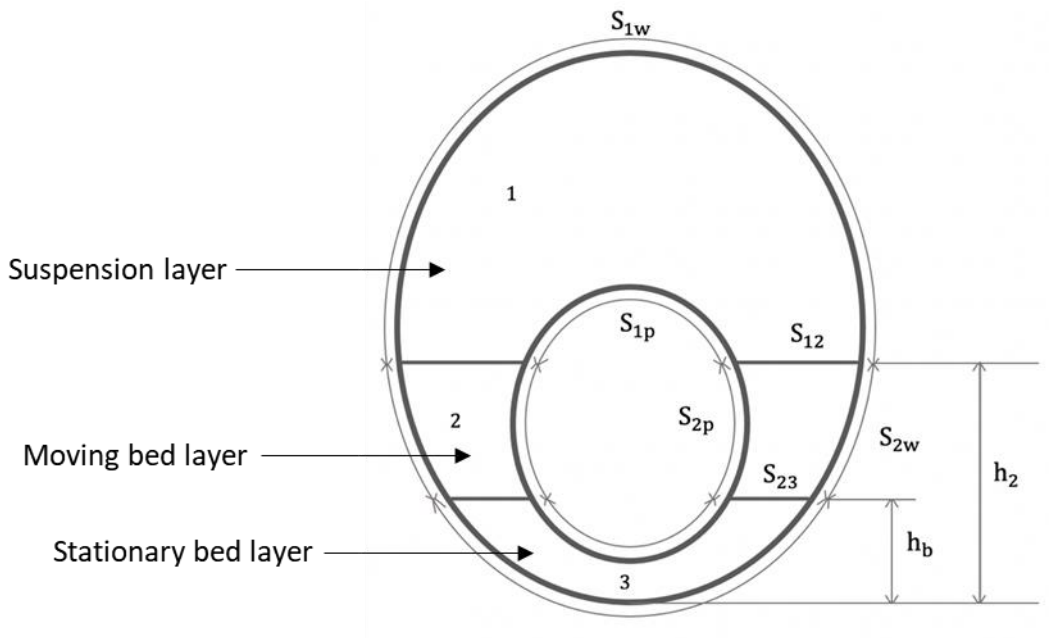

Figure 5.1 Schematic diagram of the three-layer model for dispersed bubble flow (adapted from Salubi et al., 2022)

Suspension layer:

$$-\frac{dP}{\partial L}+\frac{\tau_{1w}S_{1w}}{A_1}+\frac{\tau_{1p}S_{1p}}{A_1}-\frac{\tau_{12}S_{12}}{A_1}+\rho_1 g\sin\theta=0 \qquad \text{Eq. 5.12}$$

Moving bed layer:

$$-\frac{dP}{\partial L}+\frac{\tau_{2w}S_{2w}}{A_2}+\frac{\tau_{2p}S_{2p}}{A_2}+\frac{\tau_{12}S_{12}}{A_2}+\frac{\tau_{23}S_{23}}{A_2}+\rho_2 g\sin\theta=0 \qquad \text{Eq. 5.13}$$

where the wetted perimeters between the various layers and walls are dependent on the height of the suspension-moving bed interface h_2 and the height of the stationary bed h_b (Figure 5.1) and are given by:

$$S_{12}=d_2\sin\left[\cos^{-1}\left(\frac{d_2-2h_2}{d_2}\right)\right]-d_1\sin\left[\cos^{-1}\left(\frac{d_1-2(h_2-d_x)}{d_1}\right)\right] \qquad \text{Eq. 5.14}$$

$$S_{23}=d_2\sin\left[\cos^{-1}\left(\frac{d_2-2h_b}{d_2}\right)\right]-d_1\sin\left[\cos^{-1}\left(\frac{d_1-2(h_b-d_x)}{d_1}\right)\right] \qquad \text{Eq. 5.15}$$

$$S_{1p}=\pi d_1-d_1\cos^{-1}\left(\frac{d_1-2(h_2-d_x)}{d_1}\right) \qquad \text{Eq. 5.16}$$

$$S_{1w}=\pi d_2-d_2\cos^{-1}\left(\frac{d_2-2h_2}{d_2}\right) \qquad \text{Eq. 5.17}$$

$$S_{3w}=d_2\cos^{-1}\left(\frac{d_2-2h_b}{d_2}\right) \qquad \text{Eq. 5.18}$$

$$S_{3p} = d_1 \cos^{-1}\left(\frac{d_1 - 2(h_b - d_x)}{d_1}\right)$$ Eq. 5.19

$$S_{2w} = \pi d_2 - S_{1w} - S_{3w}$$ Eq. 5.20

$$S_{2p} = \pi d_1 - S_{1p} - S_{3p}$$ Eq. 5.21

and

$$d_x = \frac{d_2}{2} - \left(\frac{2d_c + d_1}{2}\right)$$ Eq. 5.22

where $\frac{dP}{\partial L}$ represents the pressure gradient, τ_{1w}, τ_{1p}, τ_{12}, τ_{2w}, τ_{2p}, τ_{12}, τ_{23}, S_{1w}, S_{1p}, S_{12}, S_{2w}, S_{2p}, S_{12},S_{23}, S_{3w}, and S_{3p} represent the various shear stresses and wetted perimeters between layers 1, 2 and 3, the drillpipe wall and annuli wall, ρ_1 and ρ_2 is the gas-liquid mixture density in layers 1 and 2 respectively, and θ is the inclination angle of the annulus.

The density of the mixture for each of the layers can be expressed as:

$$\rho_1 = \rho_m(1 - C_1) + \rho_c C_1$$ Eq. 5.23

$$\rho_2 = \rho_m(1 - C_1) + \rho_c C_2$$ Eq. 5.24

where ρ_m can be expressed as:

$$\rho_m = \rho_L \lambda_L + \rho_G(1 - \lambda_L)$$ Eq. 5.25

where ρ_L and ρ_G are the densities of the liquid and gas respectively, and λ_L is the no-slip liquid holdup.

The cross-sectional area of each of the layers can be calculated using Eq. 5.6 to Eq. 5.9 as a function of the interfacial heights h_2 and h_b:

$$A_1 = A_a - \left(X1(h_2) + X2(h_2)\right) \quad \text{Eq. 5.26}$$

$$A_2 = A_a - A_1 - A_b \quad \text{Eq. 5.27}$$

If a moving bed and suspension layer exist in the annuli with no stationary bed, the interface parameter S_{23} will become zero and S_{1p}, S_{2p}, S_{12}, S_{1w}, and S_{2w} will all have non-zero values. Yet, if there is only a suspension layer in the annuli, only the parameter S_{1w} exists and $S_{1w} = \pi d_2$.

5.3.2 Calculation procedure for bubble and dispersed bubble flow

1. Define fluid, solid particles and wellbore geometry input parameters: Q_L, Q_G, ρ_L, ρ_G, ρ_c, C_c, μ_L, μ_G, σ, θ, d_1, d_2, e.
2. Calculate the MTV for rolling, V_{MR} from Eq. 5.1, where $d_x = 0.5(d_2 - d_1) - d_e$ and $\beta = \pi/2 - \theta$.
3. Obtain the average mixture velocity, V_m using $V_m = (Q_L + Q_G)/A_a$ and compare the value with V_{MR}. If $V_m < V_{MR}$, set $V_m = V_{MR}$.
4. Calculate the annuli flow area, A_{flow} using $A_{flow} = (Q_L + Q_G)/V_m$ and then compute the stationary bed area, A_b where $A_b = A_a - A_{flow}$.
5. Determine the stationary bed height, h_b by computing Eq. 5.5. If $h_b > 0$, proceed to step 7.
6. If $h_b = 0$, obtain V_{MS} from Eq. 5.2. If $V_m \geq V_{MS}$ then move to step 7. It should be noted that the solid particles are in a homogeneous suspension and S_{12}

and S_{23} are zero. Yet, if $V_m < V_{MS}$ then the suspension and moving bed layers exist and S_{23} is zero.

7. Simultaneously compute Eq. 5.10 to Eq. 5.13 to determine the annuli pressure gradient. C_1 , h_2 and V_2 and other output parameters would be available in the final iteration.

5.3.3 Slug flow

Slug flows are typically complex, having highly transient hydrodynamic characteristics making this gas-liquid flow pattern difficult to predict due to its highly unsteady nature and variation of fluid forces or conservation of momentum within the slug body different to those within the liquid film/gas pocket region. In the slug unit, if the annuli fluid velocity of the slug body is less than the MTV required to keep the solid particles moving, the formation of a stationary bed would be initiated, leading to flow of the advancing liquid film/gas pocket region above the stationary bed.

Figure 5.2 shows the gas-liquid two-phase structure and the different particle transport mechanisms which may exist in a fully developed slug flow within an inclined annulus.

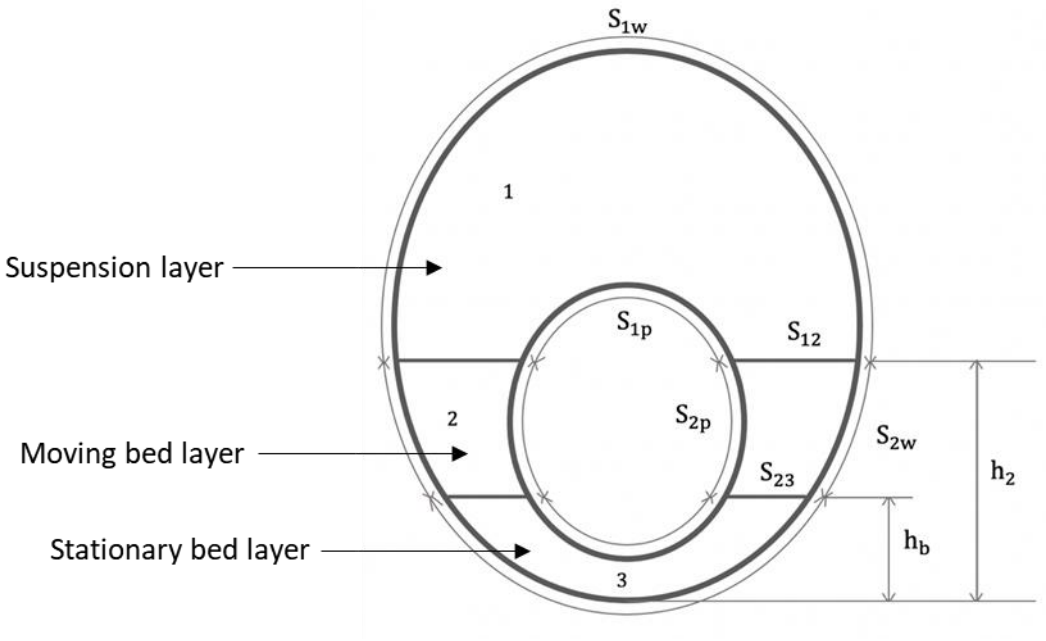

Figure 5.2: Fully developed slug flow with cuttings in an inclined wellbore annulus (Salubi et al., 2022)

The gas and liquid flowrates within a control volume having a liquid slug and liquid film/gas pocket region can be given as:

$$Q_L = V_{Ls}A_{Ls} + V_{Lf}A_{Lf} \quad \text{Eq. 5.28}$$

$$Q_G = V_{Gs}A_{Gs} + V_{Gf}A_{Gf} \quad \text{Eq. 5.29}$$

where Q_L and Q_G are the liquid and gas volumetric flowrate respectively, V_{Ls}, V_{Lf}, V_{Gs}, and V_{Gf} represent the average velocities within the liquid and gas regions of the slug body and liquid-film/gas pocket, and A_{Ls}, A_{Lf}, A_{Gs}, and A_{Gf} represent the area occupied by the liquid and gas within the slug body and liquid-film/gas pocket regions.

The time required for a slug unit t_u, including the liquid slug region t_s, and the liquid film/gas pocket region t_{Lf}, to pass a specified point in the wellbore annulus can be expressed in terms of the translational velocity, V_T:

$$t_u = \frac{L_u}{V_T} \qquad t_s = \frac{L_s}{V_T} \qquad t_{Lf} = \frac{L_{Lf}}{V_T} \qquad \text{Eq. 5.30}$$

where the fully developed slug unit length can be expressed as $L_u = L_s + L_{Lf}$, L_u is the length pf the slug unit, L_s is the length of slug body and L_{Lf} is the length of the liquid in the liquid-film/gas pocket region.

From Eq. 5.28 to Eq. 5.30 the slug unit liquid volume can be expressed as:

$$Q_L t_u = V_{Ls} A_{Ls} t_s + V_{Lf} A_{Lf} t_{Lf} \qquad \text{Eq. 5.31}$$

$$Q_L - V_{Ls} A_{Ls} \frac{L_s}{L_u} - V_{Lf} A_{Lf} \frac{L_{Lf}}{L_u} = 0 \qquad \text{Eq. 5.32}$$

The material balance of the solid particles and fluid (gas-liquid) phase in the fully developed slug unit may be expressed as:

Solid particles phase:

$$\rho_c C_1 A_1 V_1 L_s + \rho_c C_2 A_2 V_2 L_s + \rho_c C_{Lf} A_{flow} \int_0^{L_{Lf}} V_{Lf} H_{Lf} \, \partial L_{Lf} = \rho_c C_c A_a V_a L_u \qquad \text{Eq. 5.33}$$

Drilling fluid phase:

$$\rho_s (1 - C_1) A_1 V_1 L_s + \rho_s (1 - C_2) A_2 V_2 L_s +$$

$$\rho_L (1 - C_{Lf}) A_{flow} \int_0^{L_{Lf}} V_{Lf} H_{Lf} \, \partial L_{Lf} \qquad \text{Eq. 5.34}$$

$$+ \rho_G A_{flow} \int_0^{L_{Lf}} V_{Gf} (1 - H_{Lf}) \, \partial L_{Lf} = \rho_m (1 - C_c) A_a V_a L_u$$

where C_{Lf} is the cuttings concentration in the liquid in the liquid-film/gas pocket region, H_{Lf} is the holdup of the liquid in the liquid-film/gas pocket region, and ρ_s is the density of the slug body.

5.3.3.1 Slug body region

Within the slug body region, the solid particles can be both or either in suspension or in the moving bed layer. Therefore, the momentum equations for the suspension and moving bed layer can be expressed as:

Suspension layer:

$$-\frac{\partial P}{\partial L}\Big)_s + \frac{\tau_{1w}S_{1w}}{A_1} + \frac{\tau_{1p}S_{1p}}{A_1} - \frac{\tau_{12}S_{12}}{A_1} + \rho_1 g \sin\theta = 0 \qquad \text{Eq. 5.35}$$

Moving bed layer:

$$-\frac{\partial P}{\partial L}\Big)_s + \frac{\tau_{2w}S_{2w}}{A_2} + \frac{\tau_{2p}S_{2p}}{A_2} + \frac{\tau_{12}S_{12}}{A_2} + \frac{\tau_{23}S_{23}}{A_2} + \rho_2 g \sin\theta = 0 \qquad \text{Eq. 5.36}$$

where,

$$\tau_{2w} = f_{2w}\frac{\rho_2 V_{Lf}|V_{Lf}|}{2} \qquad \text{Eq. 5.37}$$

$$\tau_{1w} = f_{1w}\frac{\rho_1 V_{Gf}|V_{Gf}|}{2} \qquad \text{Eq. 5.38}$$

$$\tau_{12} = f_{12}\frac{\rho_1 (V_{Gf} - V_{Lf})|V_{Gf} - V_{Lf}|}{2} \qquad \text{Eq. 5.39}$$

$$\tau_{2p} = \frac{f_{2p}\,\rho_2 V_{Lf}|V_{Lf}|}{2} \qquad \text{Eq. 5.40}$$

$$\tau_{1p} = \frac{f_{1p}\,\rho_1 V_{Gf}|V_{Gf}|}{2}$$ Eq. 5.41

where f_{1w}, f_{2w}, f_{12}, f_{2p}, and f_{1p} represent the friction factor between layers 1, 2 and 3, the drillpipe wall and annuli wall.

The mixture density for each of the layers can be expressed as:

$$\rho_1 = \rho_s(1 - C_1) + \rho_c C_1$$ Eq. 5.42

$$\rho_2 = \rho_s(1 - C_2) + \rho_c C_2$$ Eq. 5.43

The slug body fluid density ρ_s is calculated as a function of the liquid holdup in the slug body H_{Ls}.

$$\rho_s = \rho_L H_{Ls} + \rho_G(1 - H_{Ls})$$ Eq. 5.44

where H_{Ls} is the holdup of the liquid in the slug body.

5.3.3.2 Liquid film/gas pocket region

The solid particles flowing in the liquid film/gas pocket zone are only located in the liquid film due to density differences and benefit from the acceleration of the liquid film which keeps them in the suspension. Figure 5.3 shows the geometric configuration of the liquid film/gas pocket zone which contains the gas layer at the top, a liquid region with solid particles in suspension and as a stationary bed.

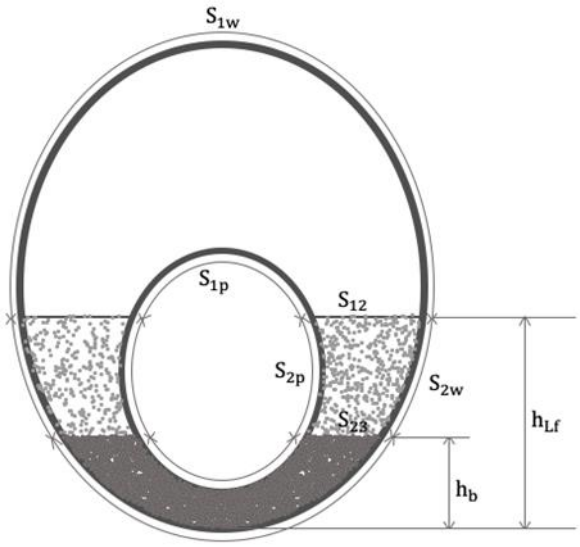

Figure 5.3 Schematic diagram of the mathematical model for liquid film/gas pocket region (Salubi et al., 2022)

The hydrodynamics analysis of the liquid film in the translational velocity coordinate system allows for the conservation of momentum equations for both the gas pocket and the liquid film in the wellbore annulus and is given by:

Layer 1: Gas pocket

$$-\frac{\partial P}{\partial L}+\ \rho_G v_{Gf}\frac{\partial v_{Gf}}{\partial L}+\ \frac{\tau_{1w}S_{1w}}{A_{Gf}}+\ \frac{\tau_{1p}S_{1p}}{A_{Gf}}+\ \frac{\tau_{12}S_{12}}{A_{Gf}}+\ \rho_G g\sin\theta$$

$$-\ \rho_G g\cos\theta\frac{\partial h_{Lf}}{\partial L}=0 \qquad \text{Eq. 5.45}$$

Layer 2: Liquid film and solid particles

$$-\frac{\partial P}{\partial L}+\ \rho_{Lfc}v_{Lf}\frac{\partial v_{Lf}}{\partial L}+\ \frac{\tau_{2w}S_{2w}}{A_{Lf}}+\ \frac{\tau_{2p}S_{2p}}{A_{Lf}}-\ \frac{\tau_{12}S_{12}}{A_{Lf}}+\ \frac{\tau_{23}S_{23}}{A_{Lf}}$$

Eq. 5.46

$$+\ \rho_{Lfc}g\sin\theta-\ \rho_{Lfc}g\cos\theta\frac{\partial h_{Lf}}{\partial L}=0$$

where v_{Gf} and v_{Lf} represent the relative velocities within the gas and liquid regions of the liquid-film/gas pocket respectively, and h_{Lf} is the height of the liquid in the liquid-film/gas pocket region.

The height of the liquid film change in the axial direction can be computed using:

$$\frac{\partial h_{Lf}}{\partial L} = \frac{F1}{F2} \qquad \text{Eq. 5.47}$$

The numerator, F1 and denominator, F2 of the Eq. 74 is given as:

$$F1 = \frac{\tau_{2w}S_{2w}}{A_{Lf}} + \frac{\tau_{2p}S_{2p}}{A_{Lf}} - \frac{\tau_{1w}S_{1w}}{A_{Gf}} - \frac{\tau_{1p}S_{1p}}{A_{Gf}} + \frac{\tau_{23}S_{23}}{A_{Lf}} - \tau_{12}S_{12}\left(\frac{1}{A_{Lf}} + \frac{1}{A_{Gf}}\right) + (\rho_{Lfc} - \rho_G)g\sin\theta \qquad \text{Eq. 5.48}$$

$$F2 = \rho_G v_{Gf}\frac{(V_T - V_{Gs})(1 - H_{Ls})}{(1 - H_{Lf})^2}\frac{\partial H_{Lf}}{\partial h_{Lf}} - \rho_{Lfc}v_{Lf}\frac{(V_T - V_{Ls})H_{Ls}}{{H_{Lf}}^2}\frac{\partial H_{Lf}}{\partial h_{Lf}} + (\rho_{Lfc} - \rho_G)g\cos\theta \qquad \text{Eq. 5.49}$$

$$\frac{\partial H_{Lf}}{\partial h_{Lf}} = 2\frac{\left[\left(\frac{{d_2}^2}{4} - \left(\frac{1}{2}(2h_b - d_2)\right)^2\right)^{1/2} - \left(\frac{{d_1}^2}{4} - \left(\frac{1}{2}(2h_b - d_2 + 2d_e)\right)^2\right)^{1/2}\right]}{A_{flow}} \qquad \text{Eq. 5.50}$$

Eq. 5.47 must be integrated to solve the liquid film profile $h_{Lf}(L)$, and to obtain the liquid film velocity distributions and liquid holdup. The boundary condition for integrating the first-order differential equation is $h_{Lf}(L = 0) = h_{Lf0}$ corresponding to $v_{Lf}(L = 0) = V_T - V_{Ls}$. Before the integration of Eq. 5.47, the

boundary condition needs to be obtained through the computation of Eq. 5.51 obtain the value of h_{Lf0}.

$$f(h_{Lf0}) = H_{Ls} - \frac{X1(h_{Lf0}) + X2(h_{Lf0}) - A_b}{A_{flow}} \quad \text{Eq. 5.51}$$

The total annuli pressure drop within the slug unit can be computed using the global force and momentum balance. The solid particles-fluid mixture average density in the liquid film/gas pocket region can be obtained using the flowing equation:

$$\rho_{LfA} = \frac{\rho_{Lfc}}{L_{Lf}} \int_0^{L_{Lf}} H_{Lf}\, \partial L_{Lf} + \frac{\rho_G}{L_{Lf}} \int_0^{L_{Lf}} (1 - H_{Lf})\, \partial L_{Lf} \quad \text{Eq. 5.52}$$

where ρ_{LfA} and ρ_{Lfc} are the densities of the cuttings-fluid mixture in the liquid-film/gas pocket region and liquid-cuttings mixture in the liquid film respectively. Hence, the total pressure drop throughout the slug unit, ΔP_u, and annuli pressure gradient can be given by:

$$\Delta P_u = \left(\frac{dP}{\partial L}\right)_s L_s + \rho_{LfA} g \sin\theta\, L_{Lf} + \int_0^{L_{Lf}} \frac{\tau_{2w}S_{2w} + \tau_{2p}S_{2p} + \tau_{1w}S_{1w} + \tau_{1p}S_{1p} + \tau_{23}S_{23}}{A_a - A_b}\, dL \quad \text{Eq. 5.53}$$

$$\frac{dP}{dL} = \frac{\Delta P_u}{L_u} \quad \text{Eq. 5.54}$$

It should be noted that the suspension layer concentration profile existing in the different gas-liquid flow patterns can be given by:

$$C(y) = C_{Mb} \exp\left(-\frac{\epsilon_c(y - h_2)}{v_t}\right) \quad \text{Eq. 5.55}$$

where the solid particles (cuttings) concentration within the moving bed layer, C_{Mb} is taken to be 0.52 as a result of cubic packing (Doron and Barnea, 1993), y is the vertical coordinate perpendicular to the annuli axis, ϵ_c is the diffusion coefficient and v_t is the terminal settling velocity of the cuttings.

5.3.4 Calculation procedure for slug flow

1. Define fluid, cuttings, and wellbore geometry input parameters: Q_L, Q_G, ρ_L, ρ_G, ρ_c, C_c, μ_L, μ_G, σ, θ, d_1, d_2, e.
2. Calculate V_{MR} from Eq. 6.1, where $d_x = 0.5(d_2 - d_1) - d_e$ and $\beta = \pi/2 - \theta$.
3. Obtain V_m from $V_m = (Q_L + Q_G)/A_a$ and compare the value with V_{MR}. If $V_m < V_{MR}$, set $V_m = V_{MR}$.
4. Compute the annuli flow area, A_{flow} using $A_{flow} = (Q_L + Q_G)/V_m$ and obtain the stationary bed area, A_b using $A_b = A_a - A_{flow}$.
5. Compute the stationary bed height, h_b by solving Eq. 5.5.
6. Calculate V_T, H_{Ls}, V_{Gs} from closure relationships using Eq. 5.37 to Eq. 41 and solve for V_{Ls} using $V_{Ls} = \left(V_m - V_{Gs}(1 - H_{Ls})\right)/H_{Ls}$.
7. Compute Eq. 5.51 to solve for the liquid film height, h_{Lf0}.
8. Compute the slug body length L_s from Zhang et al. (2003) closure relationship, $L_s = (32\cos^2\theta + 16\sin^2\theta)D_h$.
9. Calculate the liquid film profile $h_{Lf}(L)$, liquid holdup $H_{Lf}(L)$, the axial fluid velocity distributions $V_{Lf}(L)$ and $V_{Gf}(L)$ in the liquid/gas pocket region by integrating Eq. 5.47 from $h_{Lf}(L = 0) = h_{Lf0}$, which gives the length of the liquid

film, $L = L_{Lf}$. The mathematical expressions for the shear stresses in Eq. 5.48 are provided in Eq. 5.37 to Eq. 5.41 It should be noted that if $h_b > 0$, then C_{Lf} is solved using Eq. 5.55. However, if $h_b = 0$, then $C_{Lf} = 0.5$ is assumed.

10. Compute the slug unit length, L_u from $L_u = L_s + L_{Lf}$
11. If $h_b = 0$, determine V_{MS} from Eq. 5.2. If $V_m \geq V_{MS}$ and then proceed to step 12. It should be noted that the solid particles are homogeneously suspended in the slug body region and S_{12} and S_{23} are zero. Yet, if $V_m < V_{MS}$ then the suspension and moving bed layers exist in the slug body region and S_{23} is zero.
12. Simultaneously compute Eq. 5.33 to Eq. 5.36 to calculate the annuli pressure gradient in the slug body region, $\partial P/\partial L)_s$. C_1 , h_2 and V_2 and other output parameters would be available in the final iteration.
13. Solve the fluid mixture average density with solid particles in the liquid film/gas pocket region pf the slug unit using Eq. 5.52.
14. Compute Eq. 5.53 to obtain the total pressure drop across the whole slug unit and determine the annuli pressure gradient using Eq. 5.54.

5.4 Model testing and validation: Annuli pressure gradient

A newly developed 'in-house' computer program was used to solve the mathematical flow pattern dependent multi-layered models. These predicted results were used to compare against experimental results. The performance of the flow pattern dependent multi-layered models was then evaluated by comparison to experimental data. The absolute average percent error, E_{aa}, and the percent standard deviation, E_{sd}, were the comparison parameters used for the evaluation of the model and are given respectively by:

$$E_{aa} = \frac{100}{n}\sum_{i=1}^{n}|e_i| \qquad \text{Eq. 5 .56}$$

$$E_{sd} = 100\sqrt{\sum_{i=1}^{n}\frac{(e_i - E_a)^2}{n-1}} \qquad \text{Eq. 5 .57}$$

where $e_i = (y_{i,meas} - y_{i,pred})/y_{i,meas}$ and y stands for any parameter of interest.

The comparison of the experimental annuli differential pressure and the predicted annuli differential pressure calculated from the flow pattern dependent multi-layered cutting transport models for the investigated gas-liquid two-phase flow patterns (dispersed bubble, bubble and slug), fluid types (air-water and air-polymer), and the different particle transport mechanisms without the effect of inner pipe rotation is presented in Figure 5.4 to Figure 5.7.

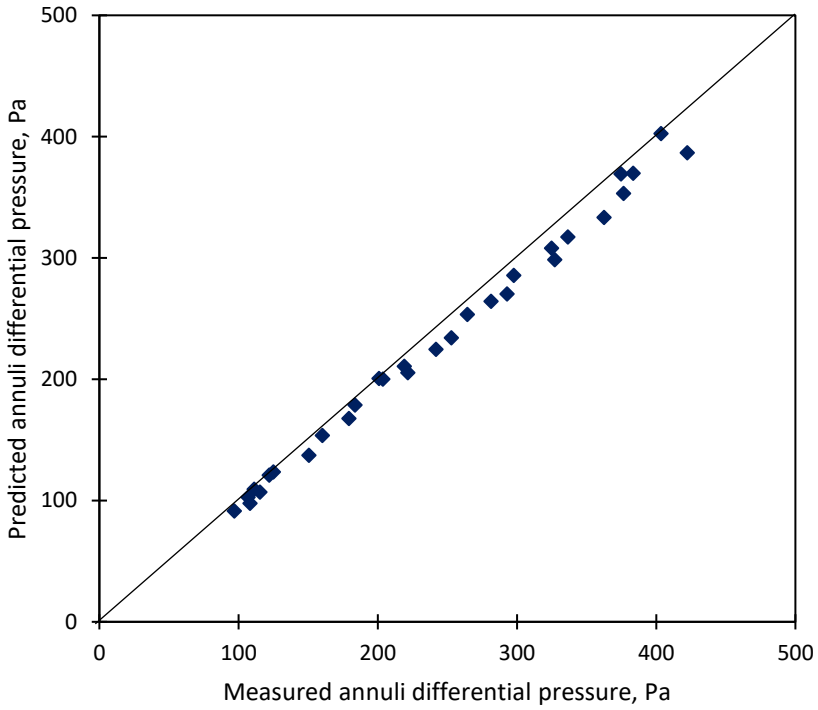

Figure 5.4 Comparison of predicted vs measured annuli differential pressure for air-water two-phase flow in a horizontal concentric annuli

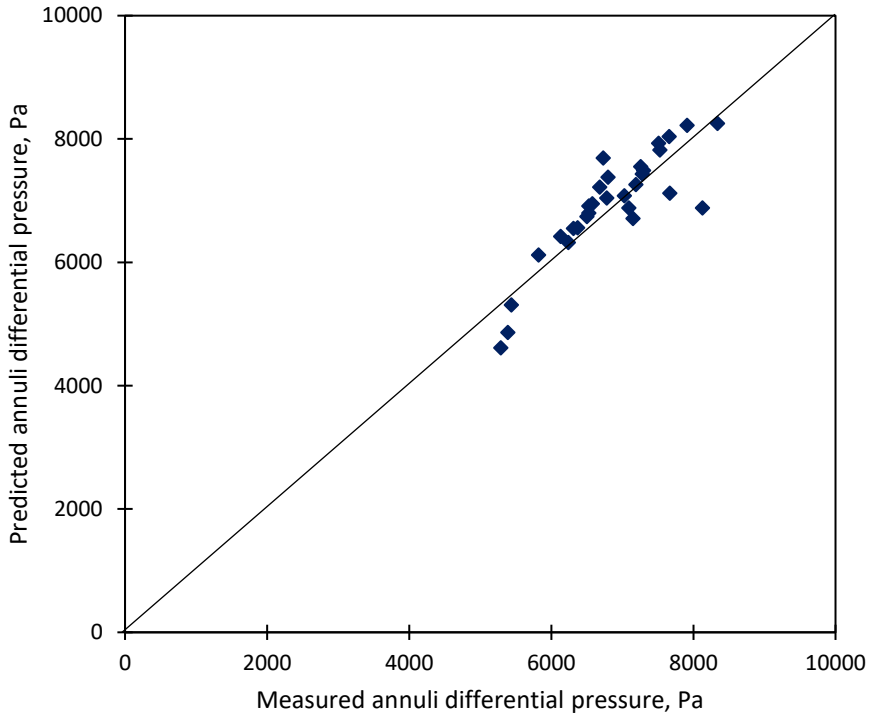

Figure 5.5 Comparison of predicted vs measured annuli differential pressure for air-water two-phase flow in a 30^0 inclination angle concentric annuli

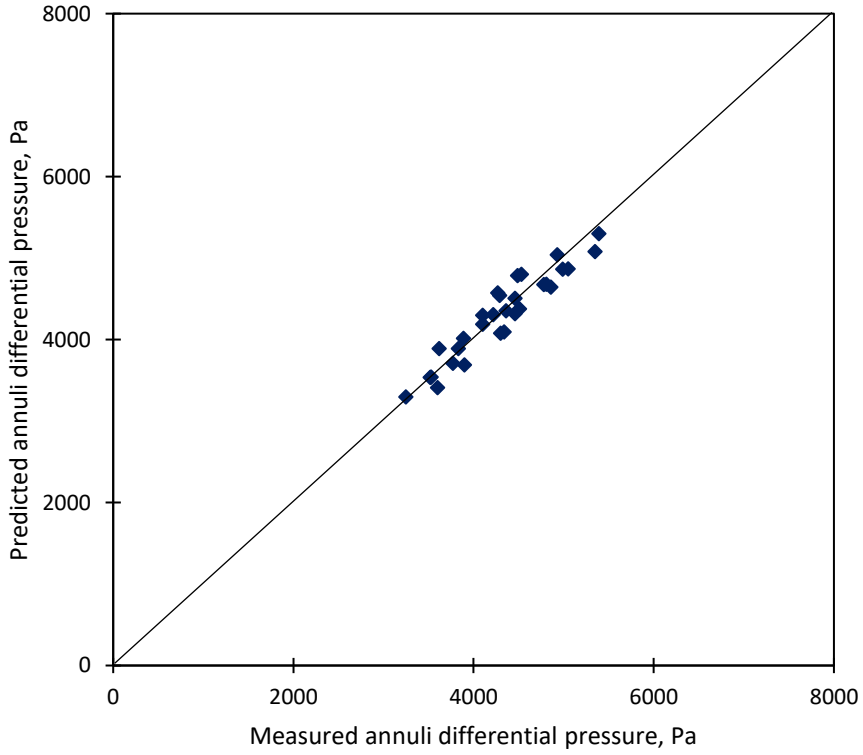

Figure 5.6 Comparison of predicted vs measured annuli differential pressure for air-polymer two-phase flow in a 20^0 inclination angle concentric annuli

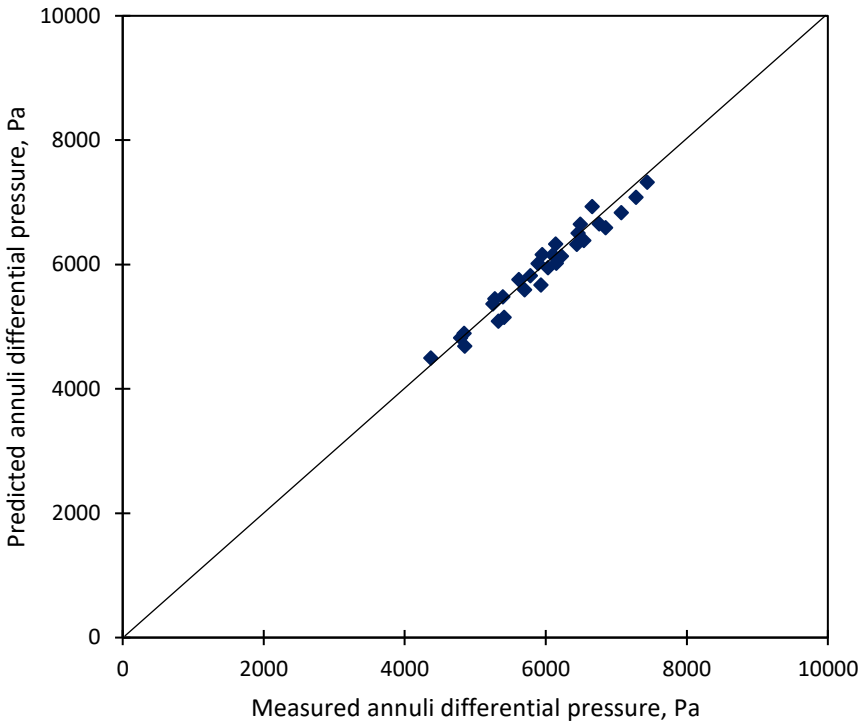

Figure 5.7 Comparison of predicted vs measured annuli differential pressure for air-polymer two-phase flow in a 30^0 inclination angle concentric annuli

The favourable results obtained from the comparison of the measured annuli differential pressure to the predicted annuli differential pressure validates the mathematical models. Overall, for all the air-water two-phase fluid mixtures the average E_{aa} was found to be 5.26% while the E_{sd} was 4.03%. Whereas, for all the air-polymer two-phase fluid mixtures the average E_{aa} was found to be 9.08% while the E_{sd} was 12.59%.

The comparison of the measured and predicted stationary bed height involving air-water and air-polymer gas-liquid two-phase flow with solid particles in the wellbore annuli is shown in Figure 5.8 and Figure 5.9.

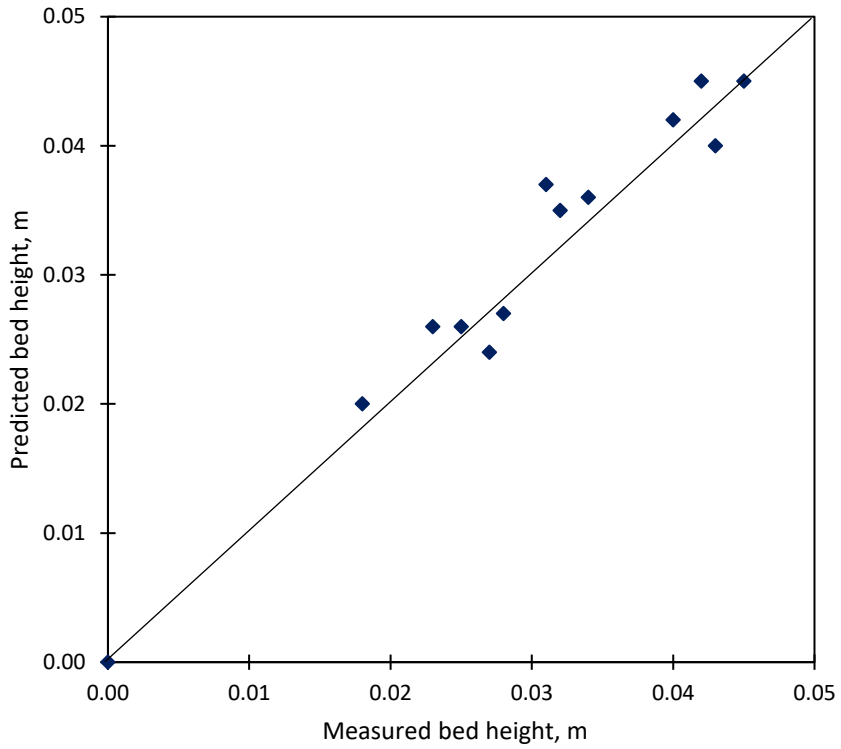

Figure 5.8 Comparison of predicted vs measured stationary bed height for air-water two-phase flow in a horizontal concentric annuli

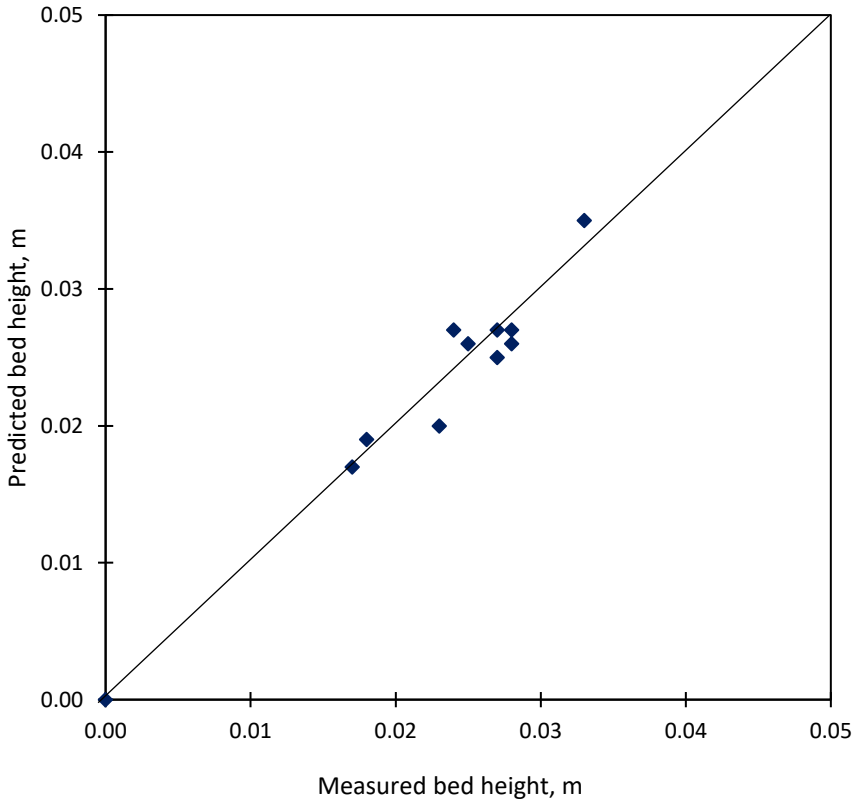

Figure 5.9 Comparison of predicted vs measured stationary bed height for air-polymer two-phase flow in a horizontal concentric annuli

The measured and predicted stationary bed height showed a favourable agreement for both sets of data. For the air-water two-phase fluid mixtures in horizontal concentric annuli the E_{aa} was found to be 8.78% while the E_{sd} was 8.41%. Whereas, for the polymer-water two-phase fluid mixtures in horizontal concentric annuli the E_{aa} was found to be 5.39% while the E_{sd} was 7.26%.

5.5 Model limitations

The flow pattern dependent multi-layered mathematical models do not consider the effect of inner pipe rotation. As such, the validation of the mathematical models did not include the experimental results that involved inner pipe rotation. However, it should be noted that the effect of inner pipe rotation on cuttings transport in gas-liquid two-phase flow is highly dependent on the prevailing gas-liquid fluid flow pattern.

Additionally, the variation between the pressure gradient results obtained experimentally and those predicted using the flow pattern dependent multi-layered mathematical models for the air-polymer two-phase fluid mixture was shown to be significantly higher than the air-water two-phase fluid mixtures. This may be attributed to the polymer solution being a non-Newtonian fluid and the friction factor equation used in this study was for Newtonian annuli fluid flow. Using a friction factor equation developed for non-Newtonian fluid flow in the annuli would result in improved prediction accuracy for non-Newtonian flows.

5.6 Summary

This chapter has presented the multiphase flow modelling aspect of this research through the integration of experimental data. Flow pattern dependent multi-layered models have been used to predict the cuttings transport

mechanism, the stationary bed height and wellbore pressure losses for gas-liquid two-phase fluids in wellbore annuli (Figure 5.10).

These models are applicable for any level of eccentricity and can be used for horizontal and inclined annuli flows. The model testing and validation showed that the models performed favourable against the experimental results.

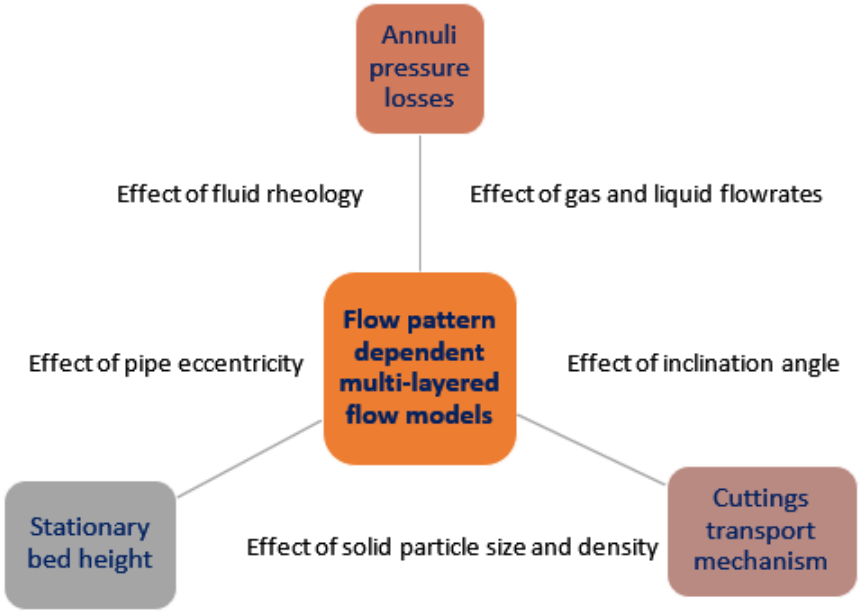

Figure 5.10 Components of the flow pattern dependent multi-layered flow models

The research objectives and contributions addressed/made in Chapter 5 are summarised in Table 5.1. Chapter 6 outlines the conclusions made as part of the research programme and makes recommendations for future investigations within the research framework for the application of the UBD method as an enhanced drilling solution.

Table 5.1 Research objective and output addressed by Chapter 5

AIM	OBJECTIVE	METHOD	OUTPUT
To develop a rigorous integrated strategy for maximising the efficiency of UBD for the transport of cuttings in gas-liquid two-phase flow through wellbore annuli	RO6: To develop and apply a multiphase flow model to evaluate the wellbore hydraulics performance and cuttings transport efficiency and compare with experimental data	Flow pattern dependent multi-layered mathematical modelling	Extension of flow modelling techniques through the testing and validation of fit-for-purpose multi-layered multiphase flow models

Chapter 6 : Conclusions and Recommendations

6.1 Conclusions

Based upon the empirical evidence presented in Chapter 4, for the specified flow conditions investigated as part of this experimental research work, several conclusions have been drawn:

1. Liquid flowrate is the most controllable operational parameter that affects cuttings transport efficiency during gas-liquid UBD operations. However, consideration must be given to the prevailing gas-liquid two-phase flow pattern to accurately establish the optimal liquid and gas flowrate for effective cuttings transport.
2. For flows involving gas-liquid two-phase fluids in annuli, the liquid phase has a more pronounced effect on the movement of the cuttings regardless of the gas-liquid two-phase flow pattern. As such, the liquid properties (fluid rheology) must be considered for the effective transport of cuttings in the wellbore annuli.
3. It is operationally more difficult to clean eccentric annuli than concentric annuli – with no external influence (e.g., inner pipe rotation with or without whirling or orbital motion) for both Newtonian and non-Newtonian gas-liquid two-phase fluid flows.
4. Pipe inclination angle strongly influences cuttings transport efficiency. However, the extent of this effect is strongly influenced by the fluid properties and prevailing gas-liquid two-phase flow pattern.
5. The liquid film length of a fully developed slug flow experiences changes with or without the presence of cuttings. This change in length is dependent on the properties of the fluid mixture and pipe inclination angle.

6. The effect of inner pipe rotation on cuttings transport efficiency for gas-liquid UBD operations is highly influenced by its interdependencies with the prevailing gas-liquid two-phase flow pattern, fluid rheological properties, and wellbore inclination angle.
7. Little to no effect is experienced due to inner pipe rotation on cuttings transport in horizontal concentric annuli under the flow conditions investigated. However, for horizontal and inclined eccentric annuli, inner pipe rotation can improve cuttings transport for Newtonian and non-Newtonian gas-liquid two-phase flows.
8. Annuli pressure losses increase with an increase in the cuttings stationary bed height for both Newtonian and non-Newtonian gas-liquid two-phase flow patterns. Therefore, if the cuttings stationary bed height reduces with inner pipe rotation, this leads to a resultant decrease in the annuli pressure losses.

In summary, the results presented in this study demonstrate that the effect of key drilling parameters on gas-liquid two-phase drilling flows with cuttings are strongly dependent on the prevailing gas-liquid fluid flow pattern and the cuttings transport mechanism. Thus, in order to accurately control wellbore annuli pressures and attain an effective hole cleaning process, the mathematical modelling of the wellbore hydraulics and cuttings transport dynamics for operations with gas-liquid two-phase drilling fluids must take into account the gas-liquid fluid flow pattern and the different cuttings transport mechanism along with the other important drilling parameters.

6.2 Recommendations for future research

This research points to several areas for future work:

1. The synthesis of the technical issues encapsulating the operational method of UBD coupled with the field case study findings (assessing the operational phase and associated outcomes from 25 global UBD field case studies) highlighted the need for more published literature on comprehensive field case studies that document successful and failed UBD implementations. Despite several global UBD based field developments with sufficient drilling records, production history, and cost data available for analysis, the body of published literature lacks thorough, long-term case histories. This study advocates for the need for more published literature on comprehensive field case studies since the capability to learn from past projects and thereafter incorporate this knowledge and experience into future operations directly enhances the oil and gas industry's innovation capability and performance. The availability of such cases would be a substantial step forward in providing the foundational data for reservoir and engineering considerations.
2. Further experimental work should be conducted to gather data over a wider operational (gas and liquid flowrates) and non-Newtonian fluid test property range. Experimental tests should specifically be performed to further investigate the effect of non-Newtonian gas-liquid two-phase fluid flow patterns in horizontal and inclined eccentric, wellbore annuli, with and without solid particles. This investigation will lead to a further phenomenological understanding of the fluid forces, gas-liquid fluid flow patterns, and particle transport mechanisms under consideration.

3. Reliability and accuracy are important requirements for multiphase flow modelling and hole cleaning predictions, to guarantee the successful maintenance of the UBD hydraulic system within a designed underbalanced pressure window. Given the shift towards data-driven models, it is recommended that prediction methods based on hybrid approaches be implemented, whereby phenomenological data-driven models be used for planning UBD operations. Using a hybrid physics data-driven method leverages the strength of each method, with the data-driven approach incorporating an inherent calibration against historical data which may or may not be physics-bound, and the physics-based models which offer explicit insights into the physical phenomenon at work within the multiphase flow drilling annulus with cuttings transport.
4. A more comprehensive understanding of downward gas-liquid two-phase flow patterns in pipe geometry is required. The development of a transient model to perform drillstring predictions is recommended to further improve the UBD/UBHD flow control procedure proposed in this work. This will help to map the factors which influence the pressure variation in pipe geometries and improve the understanding of the mechanisms that govern the various gas-liquid two-phase flow pattern transitions.

References

Abdulrahman, R., 2013. The utilization of underbalanced drilling technology may minimize tight gas reservoir formation damage: A review study. Int. J. Eng. Trends Technol. 5, 10–20.

Adari, R.B., Miska, S., Kuru, E., Bern, P., Saasen, A., 2000. Selecting drilling fluid properties and flow rates for effective hole cleaning in high-angle and horizontal wells, in: SPE Annual Technical Conference and Exhibition. Society of Petroleum Engineers. https://doi.org/10.2118/63050-MS

Ahmed, R.M., Enfis, M.S., El Kheir, H.M., Laget, M., Saasen, A., 2010. The effect of drillstring rotation on equivalent circulation density: Modeling and analysis of field measurements, in: SPE Annual Technical Conference and Exhibition. Society of Petroleum Engineers. https://doi.org/10.2118/135587-MS

Ahmed, R.M., Miska, S.Z., 2008. Experimental study and modeling of yield power-law fluid flow in annuli with drillpipe rotation, in: IADC/SPE Drilling Conference. Society of Petroleum Engineers. https://doi.org/10.2118/112604-MS

Akhshik, S., Behzad, M., Rajabi, M., 2015. CFD–DEM approach to investigate the effect of drill pipe rotation on cuttings transport behavior. J. Pet. Sci. Eng. 127. https://doi.org/10.1016/j.petrol.2015.01.017

Akhshik, S., Rajabi, M., 2018. CFD-DEM modeling of cuttings transport in underbalanced drilling considering aerated mud effects and downhole conditions. J. Pet. Sci. Eng. 160. https://doi.org/10.1016/j.petrol.2017.05.012

Al-Hadhrami, L.M., Shaahid, S.M., Tunde, L.O., Al-Sarkhi, A., 2014. Experimental study on the flow regimes and pressure gradients of air-oil-water three-phase flow in horizontal pipes. Sci. World J. 2014. https://doi.org/10.1155/2014/810527

Al-Saadi, A., Al-Bahlani, S., Al-Mahrooqi, S., Al-Riyamy, M., Carrera, M., Bowling, J., Al-Balushi, A., 2006. Underbalanced drilling experience in PDO, in: International Oil and Gas Conference and Exhibition in China 2006 - Sustainable Growth for Oil and Gas. https://doi.org/10.2523/101776-ms

Al Rubaii, M.M., 2018. A new robust approach for hole cleaning to improve rate of penetration, in: SPE Kingdom of Saudi Arabia Annual Technical Symposium and Exhibition. Society of Petroleum Engineers. https://doi.org/10.2118/192223-MS

Aladwani, F.A., Gray, K.E., 2012. Enhanced model for bottomhole pressure prediction while performing underbalanced drilling operations, in: SPE Kuwait International Petroleum Conference and Exhibition. Society of Petroleum Engineers. https://doi.org/10.2118/163361-MS

Ansari, A.M., Sylvester, N.D., Sarica, C., Shoham, O., Brill, J.P., 1994. A comprehensive mechanistic model for upward two-phase flow in wellbores. SPE Prod. Facil. 9. https://doi.org/10.2118/20630-PA

Ashraf, Q., Khalid, A., Luqman, K., Hadj-Moussa, A., Hussain, M., Hamim, N., 2020. Underbalanced nitrified foam drilling enabled operator to drill without damage and achieve an unprecedented production rate from a depleted and fractured limestone formation in Pakistan, in: International Petroleum Technology Conference 2020, IPTC 2020. International Petroleum Technology Conference. https://doi.org/10.2523/IPTC-20221-MS

Baghernejad, Y., Hajidavalloo, E., Hashem Zadeh, S.M., Behbahani-Nejad, M., 2019. Effect of pipe rotation on flow pattern and pressure drop of horizontal two-phase flow. Int. J. Multiph. Flow 111. https://doi.org/10.1016/j.ijmultiphaseflow.2018.11.012

Bahrami, H., 2012. Evaluating factors controlling damage and productivity in tight gas reservoirs," Curtin University. Curtin University, Curtin, Australia.

Bello, O.O., Falcone, G., Teodoriu, C., 2007. Experimental validation of multiphase flow models and testing of multiphase flow meters: a critical review of flow loops worldwide, in: Computational Methods in Multiphase Flow IV. WIT Press, Southampton, UK. https://doi.org/10.2495/MPF070101

Beltran, J.C., Gabaldon, O., Puerto, G., Alvarado, P., Varon, V., 2006. Case studies - Proactive managed pressure drilling and underbalanced drilling application in San Joaquin wells, Venezuela, in: Proceedings - SPE Annual Technical Conference and Exhibition. https://doi.org/10.2523/100927-ms

Bendlksen, K.H., Malnes, D., Moe, R., Nuland, S., 1991. The dynamic two-fluid model OLGA: Theory and application. SPE Prod. Eng. 6, 171–180. https://doi.org/10.2118/19451-PA

Berg, C., Stakvik, J.Å., Kulikov, S., Badrawi, M., Kaasa, G.O., Dubovstev, A., Korolev, S., Veliyev, G., 2020. Automated pressure control for UBD operations: Case study and field validation, in: SPE Drilling and Completion. https://doi.org/10.2118/194555-PA

Busch, A., Johansen, S.T., 2020. Cuttings transport: On the effect of drill pipe rotation and lateral motion on the cuttings bed. J. Pet. Sci. Eng. 191. https://doi.org/10.1016/j.petrol.2020.107136

Caetano, E.F., Shoham, O., Brill, J.P., 1992a. Upward vertical two-phase flow through an annulus—Part I: Single-phase factor, Taylor bubble rise velocity, and flow pattern prediction. J. Energy Resour. Technol. 114. https://doi.org/10.1115/1.2905917

Caetano, E.F., Shoham, O., Brill, J.P., 1992b. Upward vertical two-phase flow through an annulus—Part II: Modeling bubble, slug, and annular flow. J. Energy Resour. Technol. 114. https://doi.org/10.1115/1.2905916

Capo, J., Yu, M., Miska, S.Z., Takach, N.E., Ahmed, R.M., 2006. Cuttings transport with aqueous foam at intermediate-inclined wells. SPE Drill. Complet. 21. https://doi.org/10.2118/89534-PA

Charlez, P.A., Easton, M., Morrice, G., Tardy, P., 1998. Validation of advanced hydraulic modeling using PWD data, in: All Days. OTC. https://doi.org/10.4043/8804-MS

Chen, Z., Ahmed, R.M., Miska, S.Z., Takach, N.E., Yu, M., Pickell, M.B., Hallman, J.H., 2007. Experimental study on cuttings transport with foam under

simulated horizontal downhole conditions. SPE Drill. Complet. 22. https://doi.org/10.2118/99201-PA

Cho, H., Shah, S.N., Osisanya, S.O., 2002. A three-segment hydraulic model for cuttings transport in coiled tubing horizontal and deviated drilling. J. Can. Pet. Technol. 41. https://doi.org/10.2118/02-06-03

Cho, H., Shah, S.N., Osisanya, S.O., 2001. Effects of fluid flow in a porous cuttings-bed on cuttings transport efficiency and hydraulics, in: SPE Annual Technical Conference and Exhibition. Society of Petroleum Engineers. https://doi.org/10.2118/71374-MS

Cho, H., Shah, S.N., Osisanya, S.O., 2000. A three-layer modeling for cuttings transport with coiled tubing horizontal drilling, in: All Days. SPE. https://doi.org/10.2118/63269-MS

Clark, R.K., Bickham, K.L., 1994. A mechanistic model for cuttings transport, in: SPE Annual Technical Conference and Exhibition. Society of Petroleum Engineers. https://doi.org/10.2118/28306-MS

Cunha, J.C., Rosa, F.S., Santos, H., 2001. Horizontal underbalanced drilling in Northeast Brazil: A field case history, in: SPE Latin American and Caribbean Petroleum Engineering Conference. https://doi.org/10.2118/69490-MS

Das, G., Das, P.K., Purohit, N.K., Mitra, A.K., 1999. Flow pattern transition during gas liquid upflow through vertical concentric annuli—Part I: Experimental investigations. J. Fluids Eng. 121. https://doi.org/10.1115/1.2823552

Davarpanah, A., Mirshekari, B., Razmjoo, A., 2020. A parametric study to numerically analyze the formation damage effect. Energy Explor. Exploit. 38. https://doi.org/10.1177/0144598719873094

Davison, J.M., Leaper, R., Cauley, M.B., Bennett, B., Mackenzie, A., Higgins, C.J., Shuttleworth, N., Wilkinson, D., 2004. Extending the drilling operating window in Brent: Solutions for infill drilling in depleting reservoirs, in: Proceedings of the Drilling Conference. https://doi.org/10.2118/87174-ms

Delwiche, R.A., Lejeune, M.W.D., Mawet, P.F.B.N., Vighetto, R., 1992. Slimhole drilling hydraulics, in: SPE Annual Technical Conference and Exhibition. Society of Petroleum Engineers. https://doi.org/10.2118/24596-MS

Doron, P., Barnea, D., 1993. A three-layer model for solid-liquid flow in horizontal pipes. Int. J. Multiph. Flow 19. https://doi.org/10.1016/0301-9322(93)90076-7

Duan, M., Miska, S., Yu, M., Takach, N., Ahmed, R., Hallman, J., 2010. Experimental study and modeling of cuttings transport using foam with drillpipe rotation. SPE Drill. Complet. 25. https://doi.org/10.2118/116300-PA

Eck-Olsen, J., Vollen, E., Tønnessen, T., 2004. Challenges in implementing UBD technology, in: SPE/IADC Underbalanced Technology Conference and Exhibition - Proceedings. https://doi.org/10.2523/91239-ms

Eissa, W., Al-Harthi, S., 2003. Underbalanced drilling building the future for PDO, in: Proceedings of the Drilling Conference.

https://doi.org/10.2118/85317-ms

Epelle, E.I., Gerogiorgis, D.I., 2018. Transient and steady state analysis of drill cuttings transport phenomena under turbulent conditions. Chem. Eng. Res. Des. 131. https://doi.org/10.1016/j.cherd.2017.11.023

Erge, O., Karimi Vajargah, A., Ozbayoglu, M.E., van Oort, E., 2015. Frictional pressure loss of drilling fluids in a fully eccentric annulus. J. Nat. Gas Sci. Eng. 26. https://doi.org/10.1016/j.jngse.2015.07.030

Erge, O., Ozbayoglu, M.E., Miska, S.Z., Yu, M., Takach, N., Saasen, A., May, R., 2014. Effect of drillstring deflection and rotary speed on annular frictional pressure losses. J. Energy Resour. Technol. 136. https://doi.org/10.1115/1.4027565

Escudier, M.P., Gouldson, I.W., Oliveira, P.J., Pinho, F.T., 2000. Effects of inner cylinder rotation on laminar flow of a Newtonian fluid through an eccentric annulus. Int. J. Heat Fluid Flow 21. https://doi.org/10.1016/S0142-727X(99)00059-4

Escudier, M.P., Oliveira, P.J., Pinho, F.T., 2002. Fully developed laminar flow of purely viscous non-Newtonian liquids through annuli, including the effects of eccentricity and inner-cylinder rotation. Int. J. Heat Fluid Flow 23. https://doi.org/10.1016/S0142-727X(01)00135-7

Eyo, E.N., Lao, L., 2019. Gas-liquid flow regimes in horizontal annulus. J. Pet. Sci. Eng. 175. https://doi.org/10.1016/j.petrol.2018.12.056

Falcone, G., Hewitt, G., Alimonti, C., 2009. Multiphase Flow Metering: Principles and Applications, 1st ed. Elsevier Science.

Fan, J., Wang, X., Han, S., Yu, Z., 2009. A novel approach to modeling and simulating of underbalanced drilling process in oil and gas wells. https://doi.org/10.1007/978-3-642-03664-4_45

Fattah, K.A.A., El-Katatney, S.M.M., Dahab, A.A.A., 2011. Potential implementation of underbalanced drilling technique in Egyptian oil fields. J. King Saud Univ. - Eng. Sci. 23. https://doi.org/10.1016/j.jksues.2010.02.001

Ferroudji, H., Hadjadj, A., Haddad, A., Ofei, T.N., 2019. Numerical study of parameters affecting pressure drop of power-law fluid in horizontal annulus for laminar and turbulent flows. J. Pet. Explor. Prod. Technol. 9. https://doi.org/10.1007/s13202-019-0706-x

Gao, E., Young, A.C., 1995. Hole cleaning in extended reach wells: Field experience and theoretical analysis using a pseudo-oil (acetal) based mud, in: SPE/IADC Drilling Conference. Society of Petroleum Engineers. https://doi.org/10.2118/29425-MS

Garcia-Hernandez, A.J., Miska, S.Z., Yu, M., Takach, N.E., Zettner, C.M., 2007. Determination of cuttings lag in horizontal and deviated wells, in: SPE Annual Technical Conference and Exhibition. Society of Petroleum Engineers. https://doi.org/10.2118/109630-MS

Gavignet, A.A., Sobey, I.J., 1989. Model aids cuttings transport prediction. J. Pet. Technol. 41. https://doi.org/10.2118/15417-PA

Guimerans, R., Curtis, F., Urbanowski, R., Wilson, B., Ruiz, S., 2001. Fluid selection for underbalanced drilling operations, in: UB Technology Conference.

Guo, B., Feng, Y., Ghalambor, A., 2008. Prediction of influx rate and volume for planning UBD horizontal wells to reduce formation damage, in: Proceedings - SPE International Symposium on Formation Damage Control. Society of Petroleum Engineers. https://doi.org/10.2118/111346-ms

Guo, B., Ghalambor, A., 2004. Pressure stability analysis for aerated mud drilling using an analytical hydraulics model, in: All Days. SPE. https://doi.org/10.2118/91356-MS

Guo, B., Shi, X., 2007. A rigorous reservoir-wellbore cross-flow equation for predicting liquid inflow rate during underbalanced horizontal drilling, in: Asia Pacific Oil and Gas Conference and Exhibition. Society of Petroleum Engineers. https://doi.org/10.2523/108363-ms

Haciislamoglu, M., Langlinais, J., 1990. Non-Newtonian flow in eccentric annuli. J. Energy Resour. Technol. 112. https://doi.org/10.1115/1.2905753

Halliburton, 2019. Optimize pressure drilling, minimize damage to the reservoir [WWW Document]. F. Product. URL https://www.halliburton.com/en-US/ps/solutions/mature-fields/challenges-solutions/field-productivity/default.html (accessed 6.19.20).

Hansen, S.A., Sterri, N., 1995. Drill pipe rotation effects on frictional pressure losses in slim annuli, in: SPE Annual Technical Conference and Exhibition. Society of Petroleum Engineers. https://doi.org/10.2118/30488-MS

Hasan, A.R., Kabir, C.S., 1992. Two-phase flow in vertical and inclined annuli. Int. J. Multiph. Flow 18. https://doi.org/10.1016/0301-9322(92)90089-Y

Hemphill, T., Bern, P.A., Rojas, J., Ravi, K., 2007. Field validation of drillpipe rotation effects on equivalent circulating density, in: SPE Annual Technical Conference and Exhibition. Society of Petroleum Engineers. https://doi.org/10.2118/110470-MS

Heydari, O., Sahraei, E., Skalle, P., 2017. Investigating the impact of drillpipe's rotation and eccentricity on cuttings transport phenomenon in various horizontal annuluses using computational fluid dynamics (CFD). J. Pet. Sci. Eng. 156. https://doi.org/10.1016/j.petrol.2017.06.059

Hoekstra, T., Hopkins, C., Fleck, A., Bell, G., 2000. Technical challenges encountered during coiled tubing underbalanced drilling in Oman, in: Society of Petroleum Engineers - Abu Dhabi International Petroleum Exhibition and Conference 2000, ADIPEC 2000. https://doi.org/10.2118/87240-ms

Huaizhong, S., Heqian, Z., Zhaosheng, J., Jingbin, L., Xinxu, H., Shijie, Z., 2019. Numerical simulation and experimental study of cuttings transport in narrow annulus. J. Energy Resour. Technol. 141. https://doi.org/10.1115/1.4042448

Isambourg, P., Bertin, D.L., Brangetto, M., 1999. Field hydraulic tests improve HPHT drilling safety and performance. SPE Drill. Complet. 14. https://doi.org/10.2118/59527-PA

Jacobs, T., 2015. The new pathways of multiphase flow modeling. J. Pet. Technol. 67. https://doi.org/10.2118/0215-0062-JPT

Jahanandish, I., Salimifard, B., Jalalifar, H., 2011. Predicting bottomhole pressure in vertical multiphase flowing wells using artificial neural networks. J. Pet. Sci. Eng. 75. https://doi.org/10.1016/j.petrol.2010.11.019

Jeong, J.J., Ozar, B., Dixit, A., Juliá, J.E., Hibiki, T., Ishii, M., 2008. Interfacial area transport of vertical upward air–water two-phase flow in an annulus channel. Int. J. Heat Fluid Flow 29. https://doi.org/10.1016/j.ijheatfluidflow.2007.07.007

Kamp, A.M., Rivero, M., 1999. Layer modeling for cuttings transport in highly inclined wellbores, in: All Days. SPE. https://doi.org/10.2118/53942-MS

Kelessidis, V., Bandelis, G., 2004. Flow patterns and minimum suspension velocity for efficient cuttings transport in horizontal and deviated wells in coiled-tubing drilling. SPE Drill. Complet. 19, 213–227. https://doi.org/10.2118/81746-PA

Kelessidis, V.C., Bandelis, G.E., 2004. Flow patterns and minimum suspension velocity for efficient cuttings transport in horizontal and deviated wells in coiled-tubing drilling. SPE Drill. Complet. 19. https://doi.org/10.2118/81746-PA

Kelessidis, V.C., Dalamarinis, P., Maglione, R., 2011. Experimental study and predictions of pressure losses of fluids modeled as Herschel–Bulkley in concentric and eccentric annuli in laminar, transitional and turbulent flows. J. Pet. Sci. Eng. 77. https://doi.org/10.1016/j.petrol.2011.04.004

Kelessidis, V.C., Dukler, A.E., 1989. Modeling flow pattern transitions for upward gas-liquid flow in vertical concentric and eccentric annuli. Int. J. Multiph. Flow 15. https://doi.org/10.1016/0301-9322(89)90069-4

Kimery, D., McCaffrey, M., 2004. Underbalanced drilling in Canada: Tracking the long-term performance of underbalanced drilling projects in Canada, in: All Days. SPE. https://doi.org/10.2118/91593-MS

Kimery, D., Van Der Werken, T., 2004. Damage interpretation of properly and improperly drilled underbalanced horizontals in the fractured Jean Marie reservoir using novel modeling and methodology, in: SPE/IADC Underbalanced Technology Conference and Exhibition - Proceedings. https://doi.org/10.2523/91607-ms

Lage, A.C.V.M., Fjelde, K.K., Time, R.W., 2003. Underbalanced drilling dynamics: Two-phase flow modeling and experiments. SPE J. 8. https://doi.org/10.2118/83607-PA

Lage, A.C.V.M., Time, R.W., 2002. An experimental and theoretical investigation of upward two-phase flow in annuli. SPE J. 7. https://doi.org/10.2118/79512-PA

Lage, A.C.V.M., Time, R.W., 2000. Mechanistic model for upward two-phase flow in annuli, in: All Days. SPE. https://doi.org/10.2118/63127-MS

Li, Y., Kuru, E., 2003. Numerical modelling of cuttings transport with foam in horizontal wells. J. Can. Pet. Technol. 42, 54–61.

https://doi.org/10.2118/03-10-06

Lim, S.N., Khalil, M., Mohamed Jan, B., Si Ali, B., 2015. Lightweight biopolymer drilling fluid for underbalanced drilling: An optimization study. J. Pet. Sci. Eng. 129. https://doi.org/10.1016/j.petrol.2015.03.006

Luo, Y., Bern, P.A., Chambers, B.D., 1992. Flow-rate predictions for cleaning deviated wells, in: IADC/SPE Drilling Conference. Society of Petroleum Engineers. https://doi.org/10.2118/23884-MS

Mahmoud, A.A., Elzenary, M., Elkatatny, S., 2020. New hybrid hole cleaning model for vertical and deviated wells. J. Energy Resour. Technol. 142. https://doi.org/10.1115/1.4045169

Mahmoud, H., Hamza, A., Nasser, M.S., Hussein, I.A., Ahmed, R., Karami, H., 2020. Hole cleaning and drilling fluid sweeps in horizontal and deviated wells: Comprehensive review. J. Pet. Sci. Eng. 186. https://doi.org/10.1016/j.petrol.2019.106748

Marbun, B.T.H., Arliyando, L., Sinaga, S.Z., Arimbawa, G.V.I., 2013. Feasibility study of underbalanced drilling using coiled tubing (CT-UBD): A case study Field A, Indonesia, in: Society of Petroleum Engineers - Coiled Tubing and Well Intervention Conference and Exhibition 2013.

Marken, C.D., He, X., Saasen, A., 1992. The influence of drilling conditions on annular pressure losses, in: All Days. SPE. https://doi.org/10.2118/24598-MS

Martins, A.L., Lourenço, A.M.F., de Sa, C.H.M., 2001. Foam property requirements for proper hole cleaning while drilling horizontal wells in underbalanced conditions. SPE Drill. Complet. 16. https://doi.org/10.2118/74333-PA

Martins, A.L., Santana, C.C., 1992. Evaluation of cuttings transport in horizontal and near horizontal wells -A dimensionless approach, in: SPE Latin America Petroleum Engineering Conference. Society of Petroleum Engineers. https://doi.org/10.2118/23643-MS

Masuda, Y., Doan, Q., Oguztoreli, M., Naganawa, S., Yonezawa, T., Kbayashi, A., Kamp, A., 2000. Critical cuttings transport velocity in inclined annulus: Experimental studies and numerical simulation, in: SPE/CIM International Conference on Horizontal Well Technology. Society of Petroleum Engineers. https://doi.org/10.2118/65502-MS

McCann, R.C., Quigley, M.S., Zamora, M., Slater, K.S., 1995. Effects of high-speed pipe rotation on pressures in narrow annuli. SPE Drill. Complet. 10. https://doi.org/10.2118/26343-PA

Merlo, A., Maglione, R., Piatti, C., 1995. An innovative model for drilling fluid hydraulics, in: All Days. SPE. https://doi.org/10.2118/29259-MS

Metin, C.O., Ozbayoglu, M.E., 2007. Two-phase fluid flow through fully eccentric horizontal annuli: A mechanistic approach, in: All Days. SPE. https://doi.org/10.2118/107076-MS

Miszewski, A., Miszewski, T., Hatgelakas, P., 2018. Underbalanced drilling with coiled tubing: A case study in marginal shallow wells, in: Society of

Petroleum Engineers - SPE/ICoTA Coiled Tubing and Well Intervention Conference and Exhibition 2018. https://doi.org/10.2118/189904-ms

Moore, D.D., Bencheikh, A., Chopty, J.R., 2004. Drilling underbalanced in Hassi Messaoud, in: SPE/IADC Underbalanced Technology Conference and Exhibition - Proceedings. https://doi.org/10.2118/91519-ms

Motghare, P., Musale, A., Desai, A.B., Parmar, A.D., 2019. Underbalanced drilling: Experience in India, in: Society of Petroleum Engineers - SPE Oil and Gas India Conference and Exhibition 2019, OGIC 2019. https://doi.org/10.2118/194664-ms

Muqeem, M.A., Jarrett, C.M., Abdul, H.J., 2008. Underbalanced drilling of oil wells in Saudi Arabia: Case history and lessons learned, in: Society of Petroleum Engineers - SPE/IADC Managed Pressure Drilling and Underbalanced Operations Conference and Exhibition 2008. https://doi.org/10.2118/114258-ms

Mykytiw, C., Suryanarayana, P.V., Brand, P.R., 2004. Practical use of a multiphase flow simulator for underbalanced drilling applications design - The tricks of the trade, in: All Days. SPE. https://doi.org/10.2118/91598-MS

Naganawa, S., Nomura, T., 2006. Simulating transient behavior of cuttings transport over whole trajectory of extended reach well, in: All Days. SPE. https://doi.org/10.2118/103923-MS

Nakoryakov, V.E., Kuznetsov, V.V., Vitovsky, O.V., 1992. Experimental investigation of upward gas-liquid flow in a vertical narrow annulus. Int. J. Multiph. Flow 18. https://doi.org/10.1016/0301-9322(92)90019-D

Nguyen, D., Rahman, S.S., 1998. A three-layer hydraulic program for effective cuttings transport and hole cleaning in highly deviated and horizontal wells. SPE Drill. Complet. 13. https://doi.org/10.2118/51186-PA

Nossen, J., Liu, L., Skjaeraasen, O., Tutkun, M., Amundsen, J.E., Sleipnaes, H.G., Popovici, N., Hald, K., Langsholt, M., Ibarra, R., 2017. An experimental study of two-phase in horizontal and inclined annuli, in: 18th International Conference on Multiphase Production Technology, MPT 2017, 7-9 June. Cannes, France.

Nouri, J.M., Whitelaw, J.H., 1997. Flow of Newtonian and non-Newtonian fluids in an eccentric annulus with rotation of the inner cylinder. Int. J. Heat Fluid Flow 18. https://doi.org/10.1016/S0142-727X(96)00086-0

Ooms, G., Kampman-Reinhartz, B.E., 2000. Influence of drillpipe rotation and eccentricity on pressure drop over borehole with Newtonian liquid during drilling. SPE Drill. Complet. 15. https://doi.org/10.2118/67618-PA

Osgouei, R.E., Ozbayoglu, M.E., Ozbayoglu, A.M., Eren, T., 2013. Three phase flow characteristics in inclined eccentric annuli, in: SPE/IADC Middle East Drilling Technology Conference & Exhibition. SPE. https://doi.org/10.2118/166687-MS

Oyeneyin, B., 2015. Integrated Sand Management For Effective Hydrocarbon Flow Assurance, 1st ed, Developments in Petroleum Science. Elsevier.

Oyeneyin, B.M., Kelessidis, V.C., Bandelis, G., Dalamarinis, P., 2009. Developing a managed pressure drilling strategy for casing drilling operations. Adv. Mater. Res. 62–64. https://doi.org/10.4028/www.scientific.net/AMR.62-64.456

Oyeneyin, M.B., 2003. Challenges of underbalanced drilling for West Africa, in: Nigeria Annual International Conference and Exhibition, Abuja, Nigeria. SPE. https://doi.org/10.2118/85662-MS

Ozar, B., Jeong, J.J., Dixit, A., Juliá, J.E., Hibiki, T., Ishii, M., 2008. Flow structure of gas–liquid two-phase flow in an annulus. Chem. Eng. Sci. 63. https://doi.org/10.1016/j.ces.2008.04.042

Ozbayoglu, A.M., Yuksel, H.E., 2012. Analysis of gas–liquid behavior in eccentric horizontal annuli with image processing and artificial intelligence techniques. J. Pet. Sci. Eng. 81. https://doi.org/10.1016/j.petrol.2011.12.008

Ozbayoglu, E.M., Sorgun, M., 2010. Frictional pressure loss estimation of non-Newtonian fluids in realistic annulus with pipe rotation. J. Can. Pet. Technol. 49. https://doi.org/10.2118/141518-PA

Ozbayoglu, M.E., Ozbayoglu, M.A., 2007. Flow pattern and frictional-pressure-loss estimation using neural networks for UBD operations, in: IADC/SPE Managed Pressure Drilling & Underbalanced Operations. Society of Petroleum Engineers. https://doi.org/10.2118/108340-MS

Papadimitriou, D.A., Shoham, O., 1991. A mechanistic model for predicting annulus bottomhole pressures in pumping wells, in: All Days. SPE. https://doi.org/10.2118/21669-MS

Patel, D., 2006. Modification of Generalized Hydraulic Calculation Method for Non-Newtonian Fluids in Eccentric Annuli. Texas A&M University-Kingsville, Kingsville, Texas.

Perez-Tellez, C., 2003. Improved bottomhole pressure control for underbalanced drilling operations. Louisiana State University and Agricultural and Mechanical College, Louisiana, USA.

Pérez-Téllez, C., Smith, J.R., Edwards, J.K., 2004. Improved bottomhole pressure control for underbalanced drilling operations, in: Proceedings of the Drilling Conference. https://doi.org/10.2523/87225-ms

Pérez-Téllez, C., Smith, J.R., Edwards, J.K., 2003. A new comprehensive, mechanistic model for underbalanced drilling improves wellbore pressure predictions. SPE Drill. Complet. 18, 199–208. https://doi.org/10.2118/85110-PA

Piroozian, A., Ismail, I., Yaacob, Z., Babakhani, P., Ismail, A.S.I., 2012. Impact of drilling fluid viscosity, velocity and hole inclination on cuttings transport in horizontal and highly deviated wells. J. Pet. Explor. Prod. Technol. 2. https://doi.org/10.1007/s13202-012-0031-0

Prasun, S., Ghalambor, A., 2018. Transient cuttings transport with foam in horizontal wells-A numerical simulation study for applications in depleted reservoirs, in: SPE International Conference and Exhibition on Formation Damage Control. Society of Petroleum Engineers.

https://doi.org/10.2118/189472-MS

Qutob, H.H., Ferreira, H., 2005. The SURE way to underbalanced drilling, in: SPE Middle East Oil and Gas Show and Conference, MEOS, Proceedings. Society of Petroleum Engineers. https://doi.org/10.2118/93346-MS

Raeiszadeh, F., Hajidavalloo, E., Behbahaninejad, M., Hanafizadeh, P., 2016. Effect of pipe rotation on downward co-current air–water flow in a vertical pipe. Int. J. Multiph. Flow 81. https://doi.org/10.1016/j.ijmultiphaseflow.2016.01.002

Rashidi, M., Sedaghat, A., Misbah, B., Sabati, M., Vaidyan, K., Mostafaeipour, A., Dehshiri, S.S.H., Almutairi, K., Issakhov, A., 2021. Introducing a rheology model for non-Newtonian drilling fluids. Geofluids 2021. https://doi.org/10.1155/2021/1344776

Rooki, R., Doulati Ardejani, F., Moradzadeh, A., Norouzi, M., 2014. Simulation of cuttings transport with foam in deviated wellbores using computational fluid dynamics. J. Pet. Explor. Prod. Technol. 4. https://doi.org/10.1007/s13202-013-0077-7

Rooki, R., Rakhshkhorshid, M., 2017. Cuttings transport modeling in underbalanced oil drilling operation using radial basis neural network. Egypt. J. Pet. 26. https://doi.org/10.1016/j.ejpe.2016.08.001

Saasen, A., 2014. Annular frictional pressure losses during drilling—Predicting the effect of drillstring rotation. J. Energy Resour. Technol. 136. https://doi.org/10.1115/1.4026205

Sadatomi, M., Sato, Y., Saruwatari, S., 1982. Two-phase flow in vertical noncircular channels. Int. J. Multiph. Flow 8. https://doi.org/10.1016/0301-9322(82)90068-4

Safar, H., Azhary, S., Hljazl, A., Qutob, H., Chopty, J., Pham, C., 2007. Underbalanced drilling successfully implemented on first dual lateral well in Libya, in: SPE Middle East Oil and Gas Show and Conference, MEOS, Proceedings. https://doi.org/10.2523/104620-ms

Salubi, V., Mahon, R., Oluyemi, G., Oyeneyin, B., 2022. Effect of two-phase gas-liquid flow patterns on cuttings transport efficiency. J. Pet. Sci. Eng. 208. https://doi.org/10.1016/j.petrol.2021.109281

Shadravan, A., Khodadadian, M., Roohi, A., Amani, M., 2009. Underbalanced drilling in depleted formation achieves great success: Case study, in: 71st European Association of Geoscientists and Engineers Conference and Exhibition 2009: Balancing Global Resources. Incorporating SPE EUROPEC 2009. https://doi.org/10.2118/119211-ms

Shatwan, M., Qutob, H., Vieira, P., 2011. Horizontal underbalanced drilling technology successfully applied in Field AA-Libya: Case study, in: Proceedings of the SPE/IADC Middle East Drilling Technology Conference and Exhibition. https://doi.org/10.2118/148521-ms

Shiddiq, A.M.I., Christiantoro, B., Syafri, I., Abdurrokhim, A., Marbun, B.T.H., Wattimury, P., Resesiyanto, H., 2017. A comprehensive comparison study of empirical cutting transport models in inclined and horizontal wells. J. Eng. Technol. Sci. 49. https://doi.org/10.5614/j.eng.technol.sci.2017.49.2.9

Shiomi, Y., Kutsuna, H., Akagawa, K., Ozawa, M., 1993. Two-phase flow in an annulus with a rotating inner cylinder (flow pattern in bubbly flow region). Nucl. Eng. Des. 141. https://doi.org/10.1016/0029-5493(93)90089-R

Skalle, P., 2011. Drilling Fluid Engineering. Pal Skalle & Ventus Publishing ApS.

Sorgun, M., 2013. Simple correlations and analysis of cuttings transport with Newtonian and non-Newtonian fluids in horizontal and deviated wells. J. Energy Resour. Technol. 135. https://doi.org/10.1115/1.4023740

Sorgun, M., Schubert, J.J., Aydin, I., Ozbayoglu, M.E., 2010. Modeling of Newtonian fluids in annular geometries with inner pipe rotation, in: ASME 2010 3rd Joint US-European Fluids Engineering Summer Meeting: Volume 1, Symposia – Parts A, B, and C. ASMEDC. https://doi.org/10.1115/FEDSM-ICNMM2010-31176

Sun, B., 2016. Multiphase Flow in Oil and Gas Well Drilling. John Wiley & Sons Singapore Pte. Ltd, Singapore. https://doi.org/10.1002/9781118720288

Sun, X., Kuran, S., Ishii, M., 2004. Cap bubbly-to-slug flow regime transition in a vertical annulus. Exp. Fluids 37. https://doi.org/10.1007/s00348-004-0809-z

Sun, X., Wang, K., Yan, T., Shao, S., Jiao, J., 2014. Effect of drillpipe rotation on cuttings transport using computational fluid dynamics (CFD) in complex structure wells. J. Pet. Explor. Prod. Technol. 4. https://doi.org/10.1007/s13202-014-0118-x

Sunthankar, A.A., Kuru, E., Miska, S., Kamp, A., 2003. New developments in aerated mud hydraulics for drilling in inclined wells. SPE Drill. Complet. 18. https://doi.org/10.2118/83638-PA

Suradi, S.R., Mamat, N.S., Jaafar, M.Z., Sulaiman, W.R.W., Ismail, A.R., 2015. Study of cuttings transport using stable foam based mud in inclined wellbore. J. Appl. Sci. 15. https://doi.org/10.3923/jas.2015.808.814

Taghipour, A., Lund, B., David Ytrehus, J., Skalle, P., Saasen, A., Reyes, A., Abdollahi, J., 2014. Experimental study of hydraulics and cuttings transport in circular and noncircular wellbores. J. Energy Resour. Technol. 136. https://doi.org/10.1115/1.4027452

Tariq, Z., Mahmoud, M., Abdulraheem, A., 2020. Real-time prognosis of flowing bottom-hole pressure in a vertical well for a multiphase flow using computational intelligence techniques. J. Pet. Explor. Prod. Technol. 10. https://doi.org/10.1007/s13202-019-0728-4

Urbieta, A., Tellez, C.P., Lupo, C.P.M., Castellanos, J.M., Ramirez, O., Puerto, G.C., Bedoya, J.I., Perez Tellez, C., Lupo, C.P.M., Castellanos De La Fuente, J.M., Puerto, G.C., Bedoya, J.I., Ramirez Lamus, O.E., 2009. First application of concentric nitrogen injection technique for a managed pressure drilling depleted well in Southern Mexico, in: Society of Petroleum Engineers - IADC/SPE Managed Pressure Drilling and Underbalanced Operations Conference and Exhibition 2009 - Drilling in India: Challenges and Opportunities. SPE. https://doi.org/10.2118/122198-ms

Veeken, C.A.M., Van Velzen, J.F.G., Van Den Beukel, J., Lee, H.M., Hakvoort, R.G., Hollman, F.J., Evans, C., Okkerman, J.A., 2007. Underbalanced

drilling and completion of sand-prone tight gas reservoirs in Southern North Sea, in: SPE - European Formation Damage Conference, Proceedings, EFDC. https://doi.org/10.2523/107673-ms

Vieira Neto, J.L., Martins, A.L., Ataíde, C.H., Barrozo, M.A.S., 2014. The effect of the inner cylinder rotation on the fluid dynamics of non-Newtonian fluids in concentric and eccentric annuli. Brazilian J. Chem. Eng. 31. https://doi.org/10.1590/0104-6632.20140314s00002871

Villasmil, R., Segovia, G.J., Valera, R.E., Lopez, C., Fernandez, A., Hinestroza, D., 2003. Evolution of drilling technology in mature reservoirs of Lake Maracaibo: Short-radius reentries, horizontal wells, and highly deviated wells, in: Proceedings of the SPE Latin American and Caribbean Petroleum Engineering Conference. https://doi.org/10.2118/81030-ms

Vonthethoff, M.L., Schoemaker, S., Telesford, A.L., 2009. Underbalanced drilling in a highly depleted reservoir, onshore South Australia: Technical and operational challenges, in: 8th European Formation Damage Conference. https://doi.org/10.2118/121632-ms

Wan, S., Morrison, D., Bryden, I., 2000. The flow of Newtonian and inelastic non-Newtonian fluids in eccentric annuli with inner-cylinder rotation. Theor. Comput. Fluid Dyn. 13, 349–359.

Wang, Z., Zhai, Y., Hao, X., Guo, X., Sun, L., 2010. Numerical simulation on three layer dynamic cutting transport model and its application on extended reach drilling, in: IADC/SPE Asia Pacific Drilling Technology Conference and Exhibition. Society of Petroleum Engineers. https://doi.org/10.2118/134306-MS

Ward, C., Andreassen, E., 1998. Pressure-while-drilling data improve reservoir drilling performance. SPE Drill. Complet. 13. https://doi.org/10.2118/37588-PA

Wei, N., Meng, Y., Li, G., Wan, L., Xu, Z., Xu, X., Zhang, Y., 2013. Cuttings transport models and experimental visualization of underbalanced horizontal drilling. Math. Probl. Eng. 2013. https://doi.org/10.1155/2013/764782

Wei, X., 1997. Effects of drillpipe rotation on annular frictional pressure loss in laminar, helical flow of power-law fluids in concentric and eccentric annuli. The University of Tulsa, Tulsa, Oklahoma, USA.

Wongwises, S., Pipathattakul, M., 2006. Flow pattern, pressure drop and void fraction of two-phase gas–liquid flow in an inclined narrow annular channel. Exp. Therm. Fluid Sci. 30. https://doi.org/10.1016/j.expthermflusci.2005.08.002

Woodrow, C.K., Elliot, D., Pickles, R., Cox, D.B., 2008. One company's first exploration UBD well for characterizing low permeability reservoirs, in: SPE North Africa Technical Conference & Exhibition. Society of Petroleum Engineers. https://doi.org/10.2118/112907-MS

Xu, J., Ozbayoglu, E., Miska, S.Z., Yu, M., Takach, N., 2013. Cuttings transport with foam in highly inclined wells at simulated downhole conditions. Arch. Min. Sci. 58. https://doi.org/10.2478/amsc-2013-0032

Yeu, W.J., Katende, A., Sagala, F., Ismail, I., 2019. Improving hole cleaning using low density polyethylene beads at different mud circulation rates in different hole angles. J. Nat. Gas Sci. Eng. 61. https://doi.org/10.1016/j.jngse.2018.11.012

Zhang, H.-Q., Wang, Q., Sarica, C., Brill, J.P., 2003. A unified mechanistic model for slug liquid holdup and transition between slug and dispersed bubble flows. Int. J. Multiph. Flow 29. https://doi.org/10.1016/S0301-9322(02)00111-8

Zhou, L., Ahmed, R.M., Miska, S.Z., Takach, N.E., Yu, M., Pickell, M.B., 2004a. Experimental study and modeling of cuttings transport with aerated mud in horizontal wellbore at simulated downhole conditions, in: All Days. SPE. https://doi.org/10.2118/90038-MS

Zhou, L., Ahmed, R.M., Miska, S.Z., Takach, N.E., Yu, M., Pickell, M.B., 2004b. Experimental study of aerated mud flows under horizontal borehole conditions, in: All Days. SPE. https://doi.org/10.2118/89531-MS

Appendix A: Pressure Transducer Calibration

Calibration of the Pressure Transducer Used for Multiphase Flow Loop Experiments

To develop calibration charts for the pressure transducers used on the multiphase flow loop, calibration tests were performed using a certified Druck pressure calibrator. As shown in Fig. A.1 the gauge pressure transducer was coupled to a power supply, the Druck pressure calibrator and National Instruments Compact Reconfigurable Input/Output console which was then connected to LabVIEW to determine the output voltage.

Figure. A.1 Pressure transducer calibration setup

These output voltage readings were used in the calibration charts to calculate the corresponding pressure values and error margin, accurately scaling the output readings so that 1 V measured by the pressure transducer will produce an output reading in LabVIEW of 1 bar.

Test Procedure for the Calibration of the Pressure Transducers

The following outlines the test procedure utilised to calibrate the pressure transducers.

1. Pressure transducers were electrically wired according to the pin configuration of the connectors as outlined in the calibration certificate of each transducer:
    - Pin 1 (+ Excitation) wired to the + port of the 30 V DC power supply;
    - Pin 2 (- Excitation) wired to the - port of the 30 V DC power supply;
    - Pin 3 (+ Output) wired to the CompactRIO, NI 9219 C series module.
2. The – port of the 30V DC power supply was connected to Channel 0 of the NI 9219 C series module through an electrical wire along with the Pin 3, + Output wire of the gauge pressure transducer.
3. The CompactRIO was connected to the laptop which had LabVIEW on it using an Ethernet cable.
4. The Druck pressure calibrator was connected to the gauge pressure transducer via a cable tubing.

Calibration Test Result Example for a Gauge Pressure Transducer

Table A.1 provide the calibration test result of a gauge pressure transducer using the Druck pressure calibrator.

Table A.1 Calibration test 1 measurement for gauge pressure transducer SN 457091

Pressure transducer: S/N 457091		
Calibration Test: 1		
Pressure (bar)	**Voltage (V)**	**Error**
0	0.01	0.01
1	1.011	0.011
2	2.012	0.012
3	3.014	0.014
4	4.016	0.016
5	5.019	0.019
6	6.02	0.02
7	7.023	0.023
8	8.023	0.023
9	9.024	0.024
10	10.024	0.024

Figure. A.2 highlights the almost linear relationship between the measured voltages across the gauge transducer when an applied pressure is used and the error difference between the measured and expected voltage. This result was used for the multiphase flow loop calibration tests as an error parameter that was factored into the LabVIEW program using a mathematical operational so that 1 V measured across the gauge pressure transducer will result in a 1 bar of pressure.

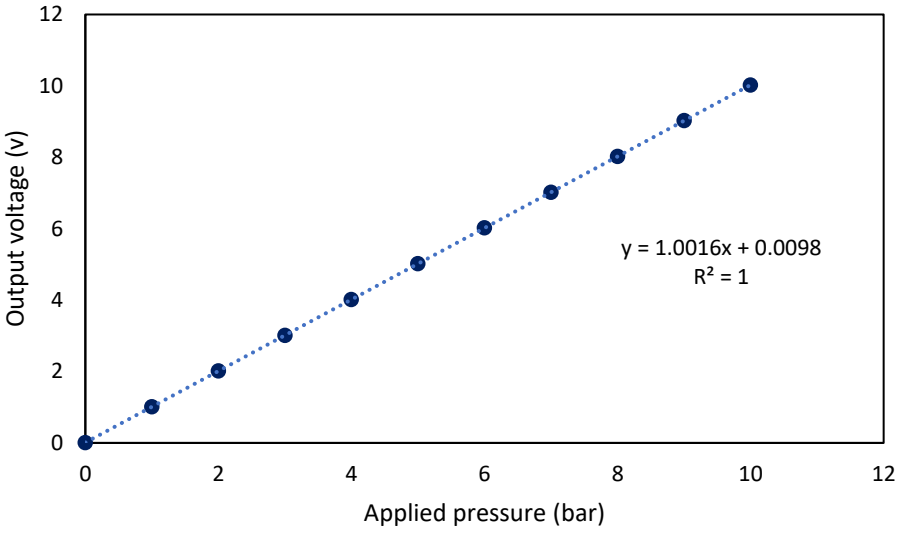

Figure A.2 Output voltage vs applied pressure for pressure transducer S/N 457091 calibration test 1

Appendix B: LabVIEW Program Used for Data Acquisition

Laboratory Virtual Instrument Engineering Workbench (LabVIEW) is a versatile graphical programming environment used for data acquisition purposes developed by National Instruments. LabVIEW was used to evaluate and log the measured data. The NI SCB-68 E series and USB-6009 pressure logging devices were coupled to the computer workstation using appropriate electronic interfaces for data logging and monitoring. The fluid flowrate, pressure, and rotary speed were the parameters logged and monitored. Fig. A.1 below show the block diagram of the LabVIEW program used to for all experimental tests.

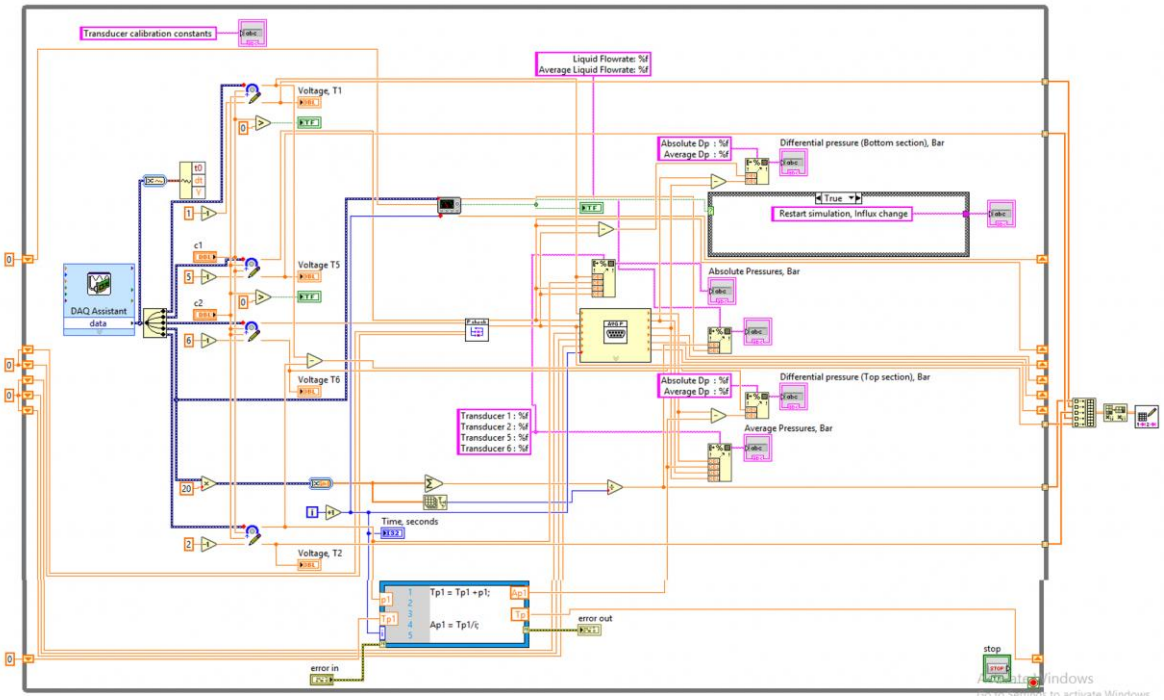

Fig. B.1 Block diagram of the LabVIEW program used for all experimental tests

Appendix C: Fluid Properties Measurement

Viscosity

After an adequate hydrate period, the xanthan gum polymer solution was measured using a 12-speed fann-35SA viscometer capable of providing a relationship between shear stress and stress rate, thereby providing viscosity data which was used to determine the rheological properties of the polymer solution. The polymer solution viscosity was measured at approximately 22 ºC.

Procedure Used for Viscosity Measurements

The rotor and bob were connected to the spring. The test xanthan gum polymer was then poured into the sample cup which was then securely fixed onto the base of the fann-35SA viscometer. Thereafter, the spindle was placed inside the xanthan gum polymer sample up to the designated point by raising the base.

With the test xanthan gum polymer sample and equipment properly setup, the gearbox was adjusted to the low mode and the motor started to the lowest RPM. Readings were recorded when the dial stabilised, and the process repeated for the other low mode RPMs. Thereafter, the motor was switched off and the gearbox adjusted to the high mode. The motor was restarted, and the procedure repeated for all the high mode RPMs with the dial readings being recorded. All viscosity measurement tests were conducted thrice for repeatability and the average value taken to perform the rheological characterisation. Fig. C.1 shows a photo of the fann-35SA viscometer which was used in determining the

rheological characteristics of the polymer solution used in the experimental tests.

Fig. C.1 fann-35SA 12 speed viscometer

Mud Balance

The fann mud balance model 140 is made up of a liquid sample cup and counterweight attached to a fixed graduated beam. The density of the xanthan gum polymer sample was read at the point where the slider-weight sat on the beam at a level point.

Procedure Used for Density Measurements

The liquid sample cup was filled with the test xanthan gum polymer and then firmly covered with the lid. Thereafter, the lid was rotated to allow some of the xanthan gum polymer sample to squeeze through the vent hole to ensure that there were no air bubbles within the liquid sample cup. The excess xanthan gum polymer sample was then cleaned off the outer surface of the liquid sample cup. Later, the mud balance was placed with its knife-edge on the stand and balanced until level by shifting the rider. The xanthan gum polymer sample density was read from the edge of the slider as shown by the indicator on the rider.

Fig. C.2 shows a photo of the fann mud balance model 140 which was used in measuring density of the polymer solution used in the experimental tests.

Fig. C.2 fann mud balance model 140

Appendix D: Viscosity Data for Polymer Solution from fann 35SA Viscometer

Run 1				
RPM	**Shear rate, γ (s^{-1})**	**Dial reading θ**	**Shear stress, τ (dynes/cm^2)**	**Viscosity, μ (cP)**
600	1020	13	66.43	6.51
300	510	10	51.10	10.02
200	340	9	45.99	13.53
180	306	8	40.88	13.36
100	170	7	35.77	21.04
90	153	7	35.77	23.38
60	102	6	30.66	30.06
30	51	5	25.55	50.10
6	10.2	3	15.33	150.29
3	5.1	3	15.33	300.59
1.8	3.06	2.5	12.78	417.48
0.9	1.53	2	10.22	667.97

Run 2				
RPM	**Shear rate, γ (s^{-1})**	**Dial reading θ**	**Shear stress, τ (dynes/cm^2)**	**Viscosity, μ (cP)**
600	1020	13	66.43	6.51
300	510	13	66.43	13.03
200	340	9	45.99	13.53
180	306	8	40.88	13.36
100	170	7	35.77	21.04
90	153	7	35.77	23.38
60	102	6	30.66	30.06
30	51	5	25.55	50.10
6	10.2	3	15.33	150.29
3	5.1	3	15.33	300.59
1.8	3.06	2.5	12.78	417.48
0.9	1.53	2	10.22	667.97

Run 3				
RPM	**Shear rate, γ (s^{-1})**	**Dial reading θ**	**Shear stress, τ (dynes/cm^2)**	**Viscosity, μ (cP)**
600	1020	13	66.43	6.51
300	510	10	51.10	10.02
200	340	8.5	43.44	12.78
180	306	8	40.88	13.36
100	170	7	35.77	21.04
90	153	7	35.77	23.38
60	102	6	30.66	30.06
30	51	5	25.55	50.10
6	10.2	3	15.33	150.29
3	5.1	3	15.33	300.59
1.8	3.06	2.5	12.78	417.48
0.9	1.53	2	10.22	667.97

Average				
RPM	**Shear rate, γ (s^{-1})**	**Dial reading θ**	**Shear stress, τ (dynes/cm^2)**	**Viscosity, μ (cP)**
600	1020	13.0	66.43	6.51
300	510	11.0	56.21	11.02
200	340	8.8	45.14	13.28
180	306	8.0	40.88	13.36
100	170	7.0	35.77	21.04
90	153	7.0	35.77	23.38
60	102	6.0	30.66	30.06
30	51	5.0	25.55	50.10
6	10	3.0	15.33	150.29
3	5	3.0	15.33	300.59
2	3	2.5	12.78	417.48
1	2	2.0	10.22	667.97